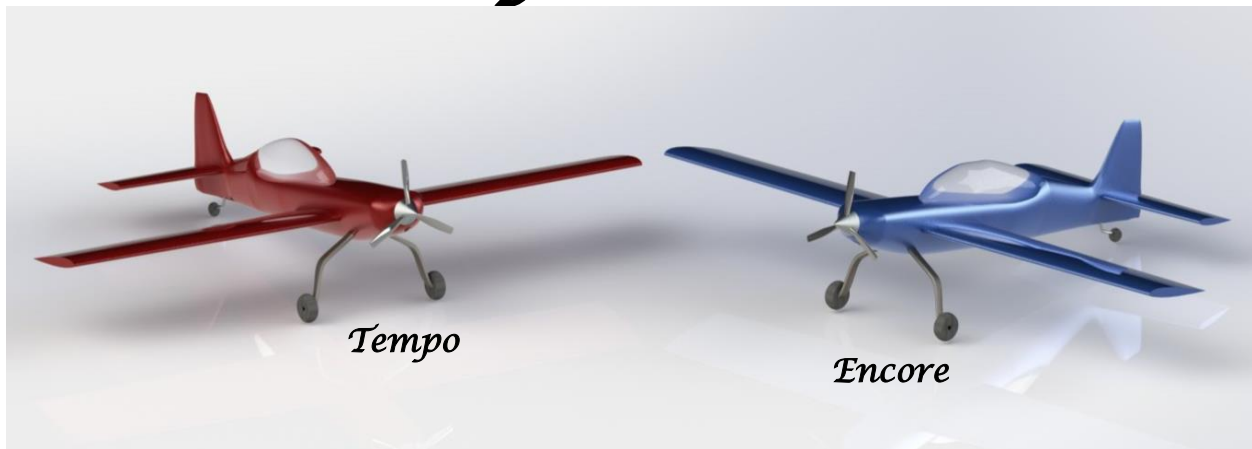


*Avem Dynamics presents*



# *Tempo and Encore*

**RESPONSE TO THE 2015-2016 AIAA  
UNDERGRADUATE TEAM AIRCRAFT DESIGN COMPETITION**

CALIFORNIA POLYTECHNIC STATE UNIVERSITY, SAN LUIS OBISPO

AEROSPACE ENGINEERING DEPARTMENT

AIRCRAFT DESIGN 2015-2016


## Executive Summary

Avem Dynamics is proud to present Tempo and Encore, the newest innovation in Light Sport Aircraft (LSA), a family of aerobatic aircraft in response to the 2016 Request for Proposal<sup>1</sup> from the American Institute of Aeronautics and Astronautics (AIAA) for the Undergraduate Team Aircraft Design Competition. As the LSA market continues to grow, the demand for high performing, aerobatic aircraft will skyrocket, creating the perfect market for a new company to enter. Avem Dynamics has designed a family of aerobatic aircraft that will be the newest sensation in LSA.

Aerobatic performance is of the utmost importance to Avem Dynamics. Tempo provides the aerobatic performance that LSA pilots desire with a sleek, modern design that will catch the eye. With superior aerodynamic performance, an easily maintainable structure, and lowered manufacturing costs, Tempo is accessible to all different types of pilots. Encore is a two-seat trainer variant of Tempo, maintaining the same high performance aerodynamics as Tempo, while allowing for superior training capabilities. Due to the high level of commonality and similar handling qualities between Tempo and Encore, pilots will be able to use Encore as a trainer version of Tempo.

Avem Dynamics is confident that this family of aerobatic aircraft will be profitable and desirable in the growing LSA market.

Avem Dynamics Team

**Brandon Baldwin**  
Aerodynamics  
AIAA: 513616



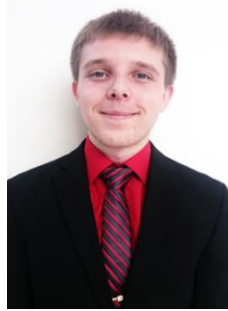
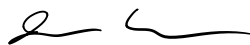

**Conner Brown**  
Performance  
AIAA: 688244




**Dana Clarke**  
Aerodynamics  
AIAA: 688327



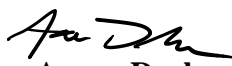

**Matthew Teare**  
Propulsion  
AIAA: 688324

**James Walker**  
Mass Properties  
AIAA: 688414




**Alex Ziebart**  
Configuration  
AIAA: 688325



**Aaron Drake**  
Faculty Advisor  
AIAA: 99736




**Kelsey Belmont**  
Co-Lead, Controls  
AIAA: 492250




**Dan Baifus**  
Co-Lead, Configuration  
AIAA: 688228



**Robert McDonald**  
Faculty Advisor  
AIAA: 171269

## Table of Contents

1	Introduction.....	10
1.1	Requirements .....	10
1.1.1	RFP Requirements .....	10
1.1.2	Derived Requirements .....	12
1.2	Design Objectives .....	12
2	Market Analysis .....	13
3	Aerobatic Competition.....	16
3.1	IAC Intermediate Category .....	17
3.2	Aerobatic Mission Profile .....	18
4	Aircraft Sizing.....	19
4.1	Constraint Diagram .....	19
4.2	Derived Maximum Lift Coefficient .....	23
5	Configuration .....	24
5.1	Aesthetics .....	24
5.2	Seating Configuration .....	25
5.3	Landing Gear.....	26
5.3.1	Landing Gear Type .....	26
5.3.2	Landing Gear Placement.....	27
5.4	Inboard Profile .....	28
6	Aerodynamics .....	30
6.1	Airfoil Selection.....	31
6.2	Wing Design .....	32
6.2.1	Wing Span .....	33
6.2.2	Wing Taper .....	35
6.3	Drag Estimation .....	38
6.3.1	Drag Buildup Comparison .....	39
6.3.2	Drag Polar.....	40
7	Propulsion.....	40
7.1	Methodology .....	40
7.1.1	Fixed Pitch Propellers.....	41
7.2	Engine Trade Methodology.....	41
7.3	Engine Selection .....	41
7.4	Propeller Matching.....	42
7.4.1	Propeller Characteristics .....	42
7.4.2	Propeller Design Process .....	42
7.4.3	Propeller Performance .....	43
8	Structures .....	47
8.1	V-n Diagram .....	47

8.2	Spar Sizing .....	49
8.3	Materials and Manufacturing .....	50
8.3.1	Material Selection .....	50
8.3.2	Manufacturing.....	51
9	Mass Properties.....	52
9.1	Methodology .....	52
9.1.1	Wing .....	53
9.1.2	Empennage .....	54
9.1.3	Fuselage .....	55
9.1.4	Systems .....	57
9.1.5	Furnishing.....	57
9.1.6	Landing Gear .....	57
9.2	Weight Summary .....	57
9.3	Commonality.....	57
10	Stability and Controls .....	59
10.1	Center of Gravity .....	59
10.2	Longitudinal Stability.....	61
10.3	Trim Analysis.....	62
10.3.1	Elevator Sizing .....	65
10.4	Directional Stability .....	65
10.4.1	Vertical tail sizing .....	65
10.4.1	Rudder Sizing .....	66
10.4.2	Spin Recovery .....	67
10.5	Aileron Sizing .....	70
10.6	Empennage Summary .....	71
11	Performance .....	72
11.1	Flight Envelope .....	73
11.2	Takeoff And Landing.....	74
11.2.1	Takeoff .....	74
11.2.2	Landing.....	76
11.3	Maximum Rate of Climb .....	77
11.4	Cruise Performance.....	78
11.5	Payload Range.....	80
11.6	Turn Performance .....	81
12	Cost Estimate .....	82
12.1	Development Cost.....	82
12.2	Flyaway Cost.....	83
12.3	Sellinllg Price .....	84
12.4	Operating Cost .....	85

13	Conclusion .....	85
14	References.....	86

## List of Figures

Figure 1: Piston Aircraft Sold and New LSA Registrations .....	14
Figure 2: 2016 Known Compulsory for Intermediate Category .....	17
Figure 3: Tempo Competition Mission Profile .....	19
Figure 4: Constraint Diagram for Tempo .....	21
Figure 5: Constraint Diagram for Tempo .....	22
Figure 6: $C_{L,max}$ Constraint Diagram for Tempo .....	23
Figure 7: $C_{L,max}$ Constraint Diagram for Encore .....	24
Figure 8: Aesthetics Survey Results .....	25
Figure 9: Side-by-Side versus Tandem Seating .....	25
Figure 10: Landing Gear Placement with Main Track 25-35% of Wingspan .....	27
Figure 11: Landing Gear Placement .....	28
Figure 12: Inboard Profiles .....	29
Figure 13: Location of Fuel in Wings .....	30
Figure 14: Root bending moment for a given load limits and wingspans .....	33
Figure 15: Wing weight verses wingspan .....	34
Figure 16: Variation of root bending moment in roll with wingspan .....	35
Figure 17: Lift Distributions for NACA 23012 Airfoil .....	36
Figure 18: Comparison of Various Taper Ratios .....	37
Figure 19: Inverted Lift Distribution .....	38
Figure 20: Drag Polar for Tempo and Encore .....	40
Figure 21: Propeller design process .....	43
Figure 22: Optimal Propeller Load Curve .....	44
Figure 23: Thrust and Power at Varying Advance Ratios .....	44
Figure 24: Maximum Thrust Performance .....	45
Figure 25: Engine Performance .....	46
Figure 26: Overall Propulsion System Efficiency .....	46
Figure 27: V-n Diagram for Tempo .....	47
Figure 28: V-n Diagram for Encore .....	48
Figure 29: Spar Location in Wing .....	49
Figure 30: Tempo Shares Geometric Similarities with P-51 .....	51
Figure 31: Wing Weight Linear Fit to Cessna Dataset .....	54
Figure 32: Horizontal Tail Linear Fit to Cessna Dataset .....	55
Figure 33: Vertical Tail Linear Fit to Cessna Dataset .....	55
Figure 34: Fuselage Linear Fit to Cessna Dataset .....	56
Figure 36: Loading Diagram for Tempo .....	60
Figure 35: Loading Diagram for Encore .....	60
Figure 37: X-Plot for Encore .....	62
Figure 38: X-Plot for Tempo .....	62
Figure 39: Trim Diagram for Tempo at Forward CG Limit .....	63
Figure 40: Trim Diagram for Tempo Aft CG Limit .....	63
Figure 41: Trim Diagram for Encore at Aft CG Limit .....	64
Figure 42: Trim Diagram for Encore at Forward CG Limit .....	64
Figure 43: Directional Stability X-plot .....	65
Figure 44: Constraint Diagram for Rudder Sizing .....	67
Figure 45: Part of the rudder unshielded by horizontal tail. ....	68
Figure 46: Necessary Components to find TDPF .....	68
Figure 47: Determination of Satisfactory Spin Recovery .....	69
Figure 48: Ranging Velocities for Aileron Sizing .....	70
Figure 49: Sized Ailerons on Wing .....	71
Figure 50: The horizontal and vertical tail .....	71
Figure 51: Flight Envelope for Tempo .....	73
Figure 52: Flight Envelope for Encore .....	74
Figure 53: Takeoff Field Length for Tempo .....	75
Figure 54: Takeoff Field Length for Encore .....	76

Figure 55: Landing Field Length for Tempo .....	77
Figure 56: Landing Field Length for Encore .....	77
Figure 57: Maximum Rate of Climb for Tempo and Encore.....	78
Figure 58: Tempo Fuel Consumption .....	78
Figure 59: Fuel Consumption for Encore .....	79
Figure 60: Tempo Engine RPM and Speed .....	79
Figure 61: Encore Engine RPM and Speed .....	79
Figure 62: Payload Range Diagram for Tempo and Encore .....	80
Figure 63: Turn Performance for Tempo.....	81
Figure 64: Turn Performance for Encore.....	82



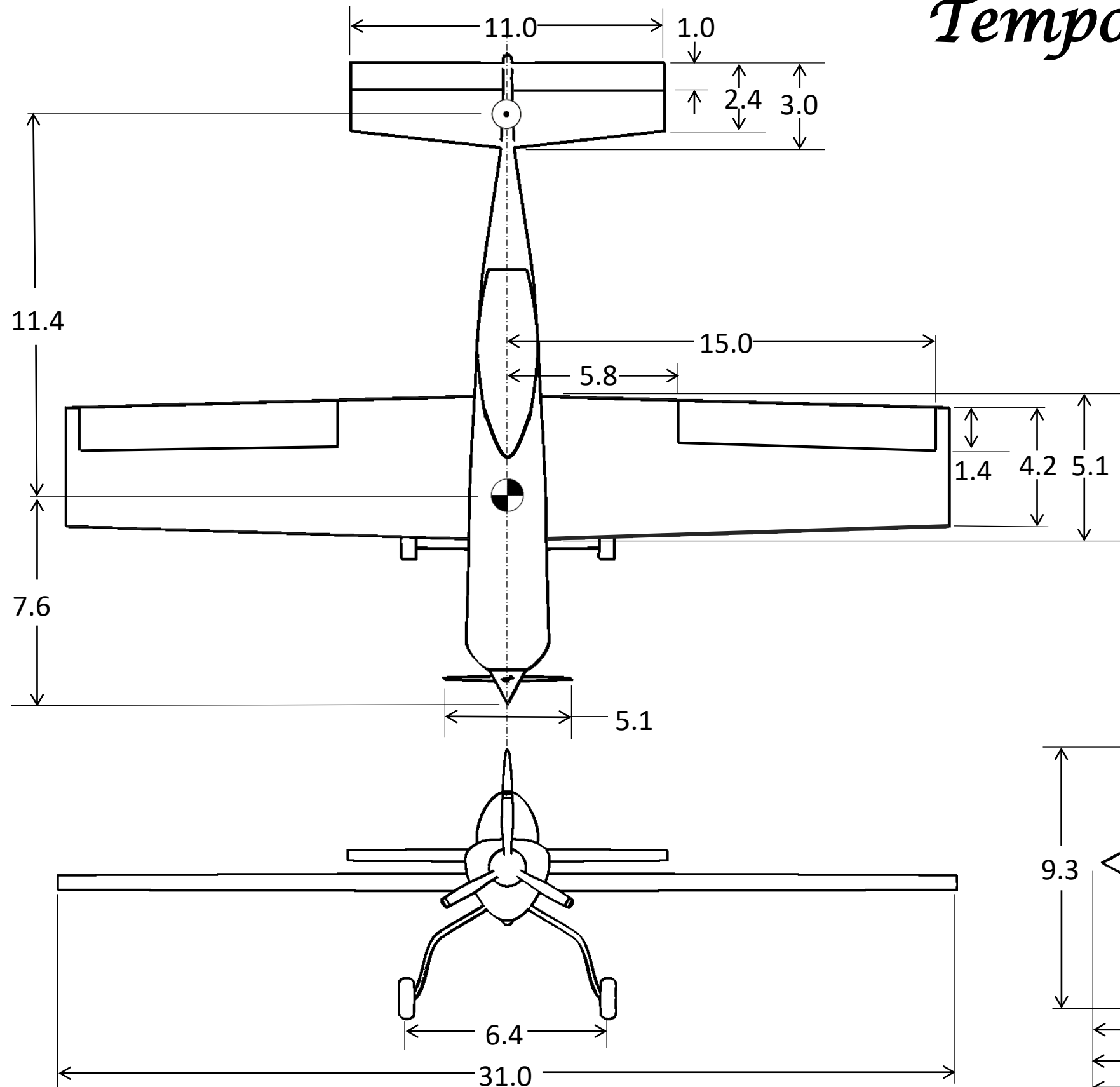
## List of Tables

Table 1: Requirements for Tempo and Encore .....	11
Table 2: Top Selling LSA Sold in 2014 .....	15
Table 3: Top-selling Aerobatic Aircraft Sold in 2014 .....	16
Table 4: Governing Constraints .....	20
Table 5: Comparison of Seating Configuration .....	26
Table 6: Airfoil Trade Study.....	32
Table 7: Varying Taper Ratios .....	37
Table 8: Drag Component Build-up for Tempo .....	39
Table 9: Engine Comparison .....	42
Table 10: Propeller Characteristics .....	43
Table 11: Component Weight Breakdown .....	58
Table 12: Varying Payload Weights for Tempo and Encore .....	59
Table 13: Comparison of Volume Coefficients .....	72

## Nomenclature

AR	= aspect ratio
AF	= activity factor
B	= aircraft weight fraction
D	= drag force
$C_D$	= drag coefficient
$C_{D,0}$	= zero-lift drag coefficient
$C_{D,i}$	= induced drag coefficient
$C_f$	= skin friction coefficient
$C_L$	= lift coefficient
$C_{L,cruise}$	= lift coefficient at cruise conditions
$C_{L,max}$	= max lift coefficient of the vehicle
$C_{L,min}$	= max negative lift coefficient of the vehicle
$C_{L,i}$	= integrated design lift coefficient
$C_{n\beta}$	= directional stability
ISA	= international standard atmosphere
L	= lift force
LDFL	= landing field length
$L_{\delta_a}$	= non-dimensional variation of the airplane rolling moment coefficient with aileron deflection
$L_p$	= non-dimensional variation of airplane rolling moment
g	= gravitational acceleration
I	= inertia
$N_{blade}$	= number of propeller blades
$P_s$	= specific excess power
P	= power provided by the engine
q	= dynamic pressure
S	= wing area
$S_{wet}$	= wetted area
$S_h$	= horizontal tail area
$S_v$	= vertical tail area
t/c	= thickness to chord ratio
v	= velocity
$v_T$	= velocity at touchdown
W	= weight
$W_{Propulsion}$	= weight of the propulsion unit
$W_{Engine}$	= weight of the engine unit
$W_{Propeller}$	= weight of the propeller
$X_{CG}$	= center of gravity location
$X_{ac}$	= aerodynamic center location
$\alpha$	= power lapse
$\beta_{3/4}$	= angle of each blade at $\frac{3}{4}$ the length
$\delta_a$	= aileron deflection
$\delta_{r,max}$	= maximum rudder deflection
$\varepsilon$	= Oswald efficiency
$\lambda$	= taper ratio
$\eta_p$	= propeller efficiency
$\Phi$	= steady state roll
$\rho$	= density
$\mu_r$	= coefficient of rolling friction

# Tempo



### General Characteristics:

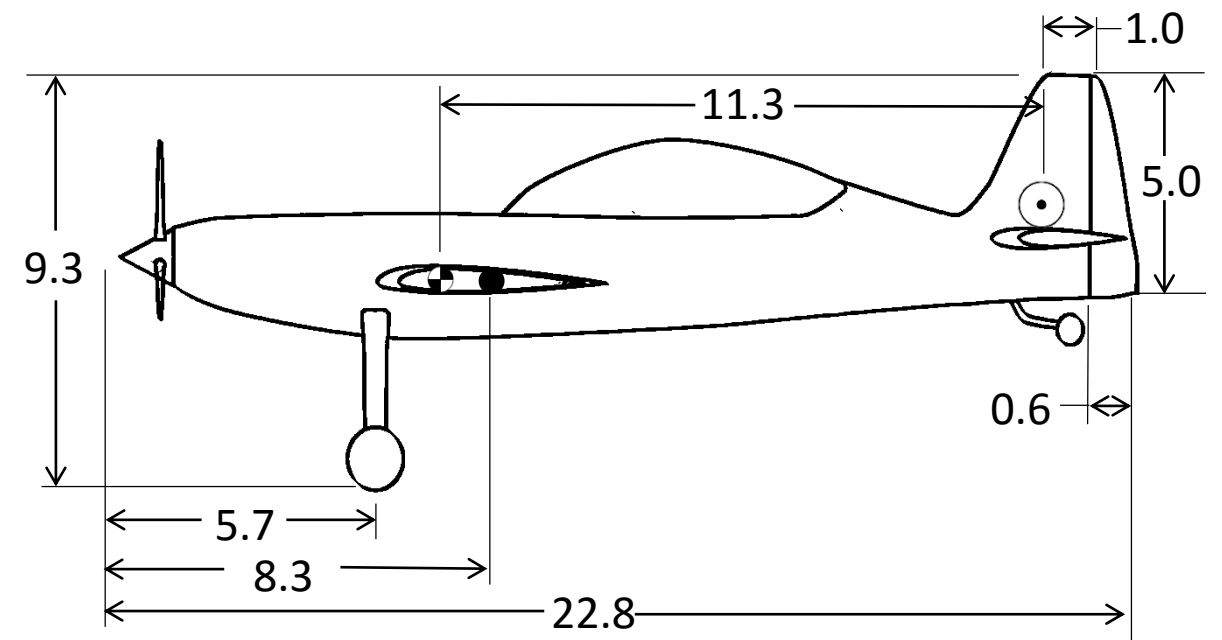
Capacity: One pilot  
 Wing Area: 143 ft<sup>2</sup>  
 Max Takeoff Weight: 1087 lbs  
 Empty Weight: 738 lbs  
 Powerplant: 1 x Lycoming AEIO 230, 116 HP  
 Fuel Capacity: 12 US Gallons

### Performance:

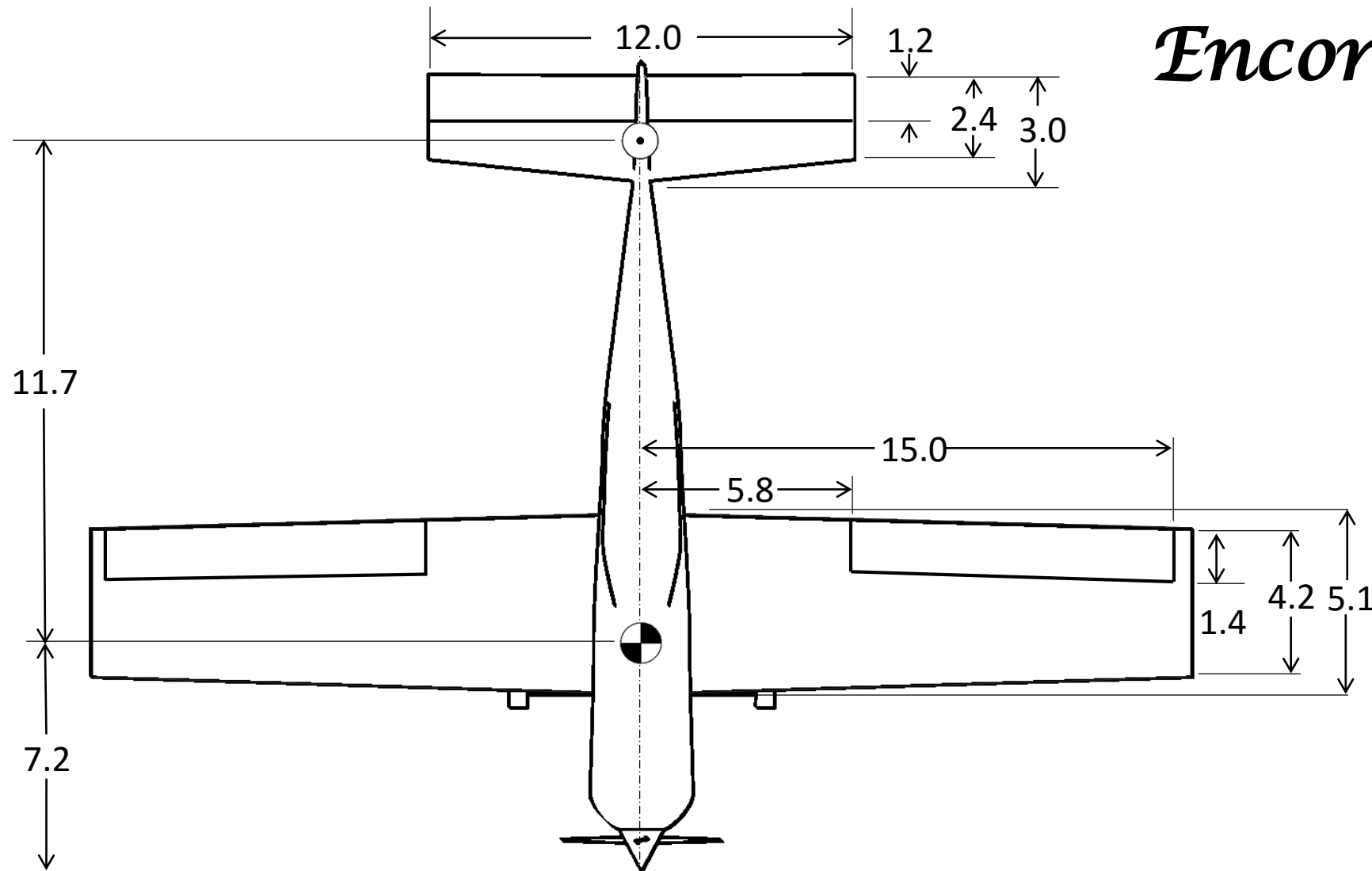
Climb Rate: 1980 fpm  
 Roll Rate: 360 deg/sec  
 Never Exceed Speed: 139 KCAS  
 Cruise Speed: 82 KCAS  
 Stall Speed: 39 KCAS  
 Max Range: 355 nm

### Legend:

- ⊕ Center of Gravity
- Aerodynamic Center
- Center of Pressure



# Encore



**General Characteristics:**

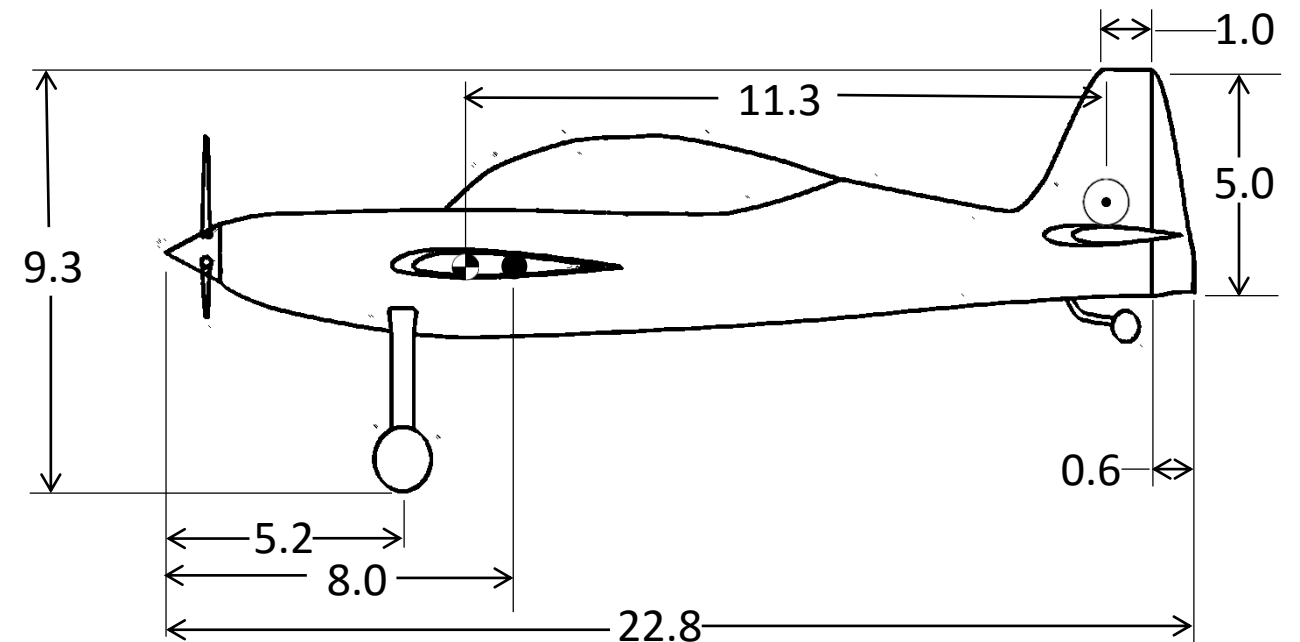
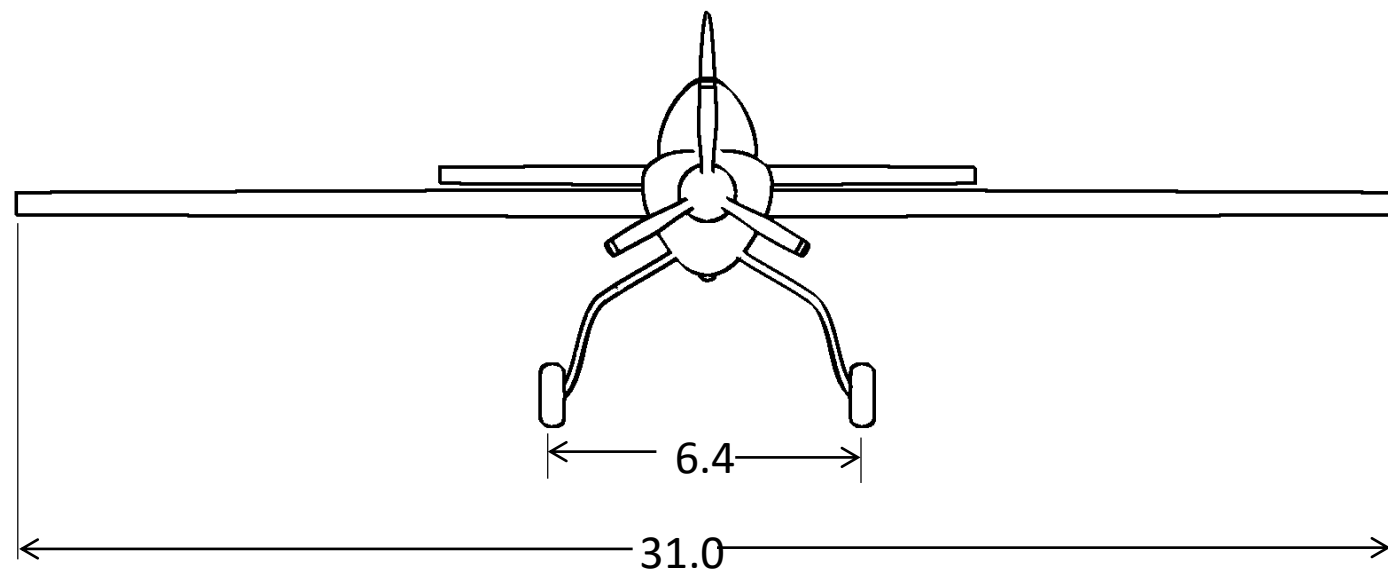
Capacity: One pilot  
 Wing Area: 143 ft<sup>2</sup>  
 Max Takeoff Weight: 1297 lbs  
 Empty Weight: 767 lbs  
 Powerplant: 1 x Lycoming AEIO 230, 116 HP  
 Fuel Capacity: 12 US Gallons

**Performance:**

Climb Rate: 1590 fpm  
 Roll Rate: 360 deg/sec  
 Never Exceed Speed: 150 KCAS  
 Cruise Speed: 82 KCAS  
 Stall Speed: 42 KCAS  
 Max Range: 355 nm

**Legend:**

- ⊕ Center of Gravity
- Aerodynamic Center
- ⊙ Center of Pressure



## 1 Introduction

The 2015-2016 AIAA Undergraduate Team Design Competition Request for Proposal (RFP) <sup>1</sup> calls for an aerobatic light sport aircraft family. This two-member family will have both single and two seat variants. The single-seat variant will be competitive in the International Aerobatic Club (IAC) intermediate category, while the two seat model serves as a general sport and aerobatic trainer. The entry into service (EIS) for the first model is 2020 and the second model is in 2021. For LSA, The Federal Aviation Administration (FAA) and ASTM International<sup>2</sup> require the unique constraint of a maximum speed of 120 knots calibrated airspeed, limiting the upper end of the flight envelope. This maximum speed requirement coupled with the RFP specific requirement of a 1500fpm climb rate creates an interesting design problem. Avem has designed a unique propulsion system that will achieve the desired performance throughout the entire flight envelope, discussed further in Section 7. The key objective of the aircraft family is to have a high level of commonality between the two variants that will help minimize development and production costs. In order to meet this objective, Avem has chosen a specific configuration that will allow for a high degree of commonality between the two aircraft, discussed in Section 9.3. Aerobatic performance is of the utmost importance to Avem so an in-depth performance analysis has been completed to demonstrate superior qualities of the aircraft family, discussed in Section 11. A detailed weight breakdown ensures compliance with the ASTM International requirement of a maximum weight of 1320lbs, tabulated in Section 9. Avem Dynamics presents Tempo and Encore, the single-seat and two seat aircraft respectively, as the solution to the new, modern aerobatic LSA. To begin the discussion of the aircraft family, the requirements and objectives are further outlined in Section 1.1.

### 1.1 REQUIREMENTS

Both variants must comply with ASTM International, FAA, and RFP specific requirements, which are shown in Table 1. Important design objectives from the RFP, dealing with commonality, aesthetics, and manufacturing as also discussed. More requirements were derived throughout the design process.

#### 1.1.1 RFP REQUIREMENTS

The RFP states that both aircraft must meet the FAA LSA definition and ASTM International Standards for an LSA, which are described in Table 1 as Requirements 1.0 – 8.0. Requirement 3.0 is unique to LSA since most aircraft have a minimum speed requirement and not a maximum speed requirement. This requirement, in conjunction with the desired climb rate, are key when deciding what propulsion system to incorporate, Requirements

RBS	Requirement
1.0	The aircraft shall have a gross takeoff weight less than or equal to 1,320 lbs (1,430 lbs for seaplanes).
2.0	The aircraft shall have a maximum stall speed of 45 knots CAS in clean configuration.
3.0	The aircraft shall have a maximum speed in level flight of 120 knots CAS.
4.0	The aircraft shall have a maximum capacity of two people.
5.0	The aircraft shall have only one single piston engine that meets the LSA ASTM standards presently or plans to meet them by EIS.
6.0	The aircraft shall have either a fixed-pitch or ground adjustable propeller.
7.0	The aircraft's cabin shall be unpressurized.
8.0	The aircraft shall have fixed landing gear, except for seaplanes.
9.0	The avionics shall meet LSA ASTM standards presently or plans to meet them by EIS.
10.0	The single seat aircraft shall have a payload of a 230 lb pilot, a 15 lb parachute, and 1.5 hours of fuel.
10.1	The single seat aircraft shall withstand +6/-5 G limit loads with the payload capacity described in 10.1
10.2	The single seat aircraft shall have a minimum ferry range of 300 nmi with a 30 minute fuel reserve.
10.3	The single seat aircraft shall have a climb rate of at least 1,500 fpm at sea level (International Standard Atmosphere (ISA) + 10° C )
10.4	The single seat aircraft shall have a maximum takeoff and landing field length of 1,200 ft over a 50 ft obstacle to a dry pavement runway (sea level ISA + 10° C).
10.5.1	The single seat aircraft takeoff and landing performance shall be shown at ISA + 10° C at 5,000 ft Mean Sea Level (MSL).
10.5.2	The single seat aircraft takeoff and landing performance shall be shown for a grass field at sea level (ISA + 0° C).
10.6	The single seat aircraft shall have a minimum roll rate of 180 degrees per second at either the maximum level cruise speed or the maximum speed of 120 knots CAS, whichever is slower.
10.7	The single seat aircraft must have space for 30 lb and 4 cubic feet of baggage for the ferry missions.
10.8	The single seat aircraft's performance shall be competitive in Internal Aerobatic Club intermediate category competition.
11.0	The two seat aircraft shall have a payload of two 200 lb pilots, two 15 lb parachutes, and 1.5 hours of fuel.
11.1	The two seat aircraft shall withstand +6/-3 G limit loads with the payload capacity described in 11.1
11.2	The two seat aircraft shall have a minimum ferry range of 250 nmi with a 30 minute fuel reserve.
11.3	The two seat aircraft shall have a climb rate of at least 800 fpm at sea level ( ISA + 10° C )
11.4	The two seat aircraft shall have a maximum takeoff and landing field length of 1,500 ft over a 50 ft obstacle to a dry pavement runway (sea level ISA + 10° C).
11.5.1	The two seat aircraft takeoff and landing performance shall be shown at ISA + 10° C at 5,000 ft MSL.
11.5.2	The two seat aircraft takeoff and landing performance shall be shown for a grass field at sea level (ISA + 0° C).
11.6	The two seat aircraft must have space for at least 30 lb and 6 cubic feet of baggage for the ferry missions.
12.0	The aircraft family shall accommodate a pilot (and passenger) at most 6 ft tall.
13.0	The aircraft family shall be capable of flying inverted (-1G) for at least 5 minutes.

*Table 1: Requirements for Tempo and Encore*

10.3 and 11.3 respectively. An interesting tradeoff occurs between the high climb rate requirement and the low maximum speed requirement, and this tradeoff is a main driving factor during the design process. The single-seat variant has a climb rate of 1,500fpm at sea level, while the two seat variant is slightly more relaxed at 800fpm. These requirements pertain most directly to selecting an engine and sizing an appropriate propeller.

Requirement 10.8, which requires the single-seat variant to have competitive aerobatic performance, sets this aircraft apart from the two seat variant. The single-seat variant must be competitive in the intermediate category of the IAC competitions, implying that it should be able to perform basic maneuvers such as spins, loops, turns, and rolls as well as snap rolls and inverted maneuvers, discussed further in Section 3. The two seat variant serves as an aerobatic trainer and general sport aircraft and must be able to perform the same maneuvers as the single-seat for training purposes, but not at a competitive level.

### 1.1.2 DERIVED REQUIREMENTS

Certain requirements, not specified by ASTM International, FAA, or RFP, arise from the previously stated requirements. The first of these derived requirements is the maximum lift coefficient for the aircraft,  $C_{L,max}$ . This derived requirement is taken from the requirements for landing field length for Tempo and stall speed for Encore. Because  $C_{L,max}$  depends on wing loading, all point performance constraints were considered for the mentioned requirements and  $C_{L,max}$  was derived, as described in Section 4.2. Another derived requirement is the type of airfoil used for the wing. The inverted flight requirement from the RFP influences the airfoil choice to a more symmetric design for the better performance characteristics at negative values of lift, examined more closely in Section 6.1. A third derived requirement to improve aerobatic performance includes a desire for sharp stall characteristics from the planform of the wing. To perform sharp stall induced maneuvers commonly experienced in intermediate category competition, like a snap roll, it is necessary for the aircraft to stall all at once to accurately execute the maneuver.

## 1.2 DESIGN OBJECTIVES

While not requirements, the design objectives are criteria desirable in the aircraft. The first design objective stated in the RFP is for the re-use of at least 75% of the airframe and systems by weight for both the single and two seat variants. This commonality between the two aircraft does not include the propulsion system, engine or propeller. This objective is interpreted as the main structure and systems of Encore should be 75% common with the main structure and systems of Tempo. In this way, Tempo will come first in the design process and Encore will

follow. Tempo was chosen as the comparison aircraft in order to prioritize the aerobatic performance and achieve the desired commonality with a lower total weight to normalize the aircraft.

The second design objective is to have visually appealing aircraft. Since Avem Dynamics is entering the market as a new company, it is the plan that the company will established itself as a stylish option to the LSA market. The more aircraft that are sold, the more money Avem Dynamics will make and be able to turn a profit. Because "visually appealing" is somewhat arbitrary, small scale market research is performed to decide what constitutes a "pretty" aircraft to the public. This research takes into account non-customers, such as students, to achieve a rudimentary study on what makes an aircraft appealing. In addition, an interview with Dan Rhin,<sup>4</sup> designer of the DR-107 and DR-109 (aerobatic, LSA aircraft) was conducted to determine desirable aesthetics for competitive aircraft, further discussed in Section 5.1.

The next design objective is to minimize maintenance cost of the aircraft. This objective will make the aircraft more marketable since maintaining the aircraft is what the customer will spend the most money on. This objective is closely tied to how the aircraft is manufactured and is thus closely tied to the next design objective.

The last design objective is to minimize production costs of the aircraft. Once again, Avem Dynamics is new to the market and so most of the startup capital will go into deciding where and how the aircraft will be manufactured. The facilities, expertise on manufacturing, laborers, and materials will all have to be established before production can begin on the aircraft, regardless of the materials chosen or manufacturing techniques chosen. Thus, throughout the design process, manufacturing techniques and materials play a role in the decision process. The materials will affect the manufacturing technique needed and is looked at more closely in Section 8.3.

## 2 Market Analysis

As a new company entering the LSA market, it is crucial to gain a better understanding of the competition; therefore, a market analysis was conducted in order to gain more knowledge of the LSA and aerobatic markets and to ultimately to develop reasonable sales goals. Certain characteristics were determined: how many LSA are sold per year, the number of LSA sold per company, and which companies are successful and why. These characteristics were examined using data from the General Aviation Manufacturers Association<sup>3</sup> and Johnson's LSA market information website.<sup>5</sup> Once the overall climate is determined, the company can evaluate if there is a demand for a new aerobatic LSA.



A good place to start in a market analysis is determining how many LSA are sold per year to gain an understanding of the size of the LSA market. Figure 1 plots the number of LSA registered with the FAA each year along with the number of piston engine aircraft sold each

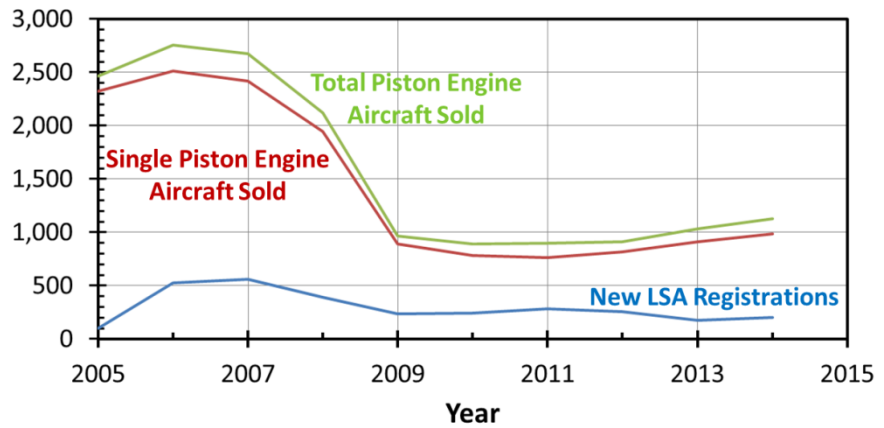


Figure 1: Piston Aircraft Sold and New LSA Registrations

year. New LSA registrations are a representation of how many LSA are manufactured, and thus sold in a given year. The plot shows that 199 new LSA were registered in 2014. The number of total and single piston engine aircraft sold per year are presented alongside the new LSA registrations. Since LSA are single piston aircraft, this comparison gives an idea of the overall success rate of this type of aircraft to a more general market. It can be seen from the figure that both the LSA and piston engine markets took large hits due to the recession in 2007-2009 and still have not fully recovered. Taking a closer look at the results of the recession, from the year 2007 to the year 2009, the total and single piston engine aircraft markets decreased by nearly 70%, while new LSA registrations only went down by about 50%. These numbers infer that although the overall piston engine market took a massive hit during the recession, LSA did not suffer as much. This observation is interesting because LSA are bought primarily for leisure purposes, and during a financial crisis the first expenses people cut out are leisure expenses; however, the LSA market did not decrease as significantly as might be expected. One possibility for this difference is that due to the recession, aircraft customers decided to buy the cheaper LSA over a larger piston engine aircraft. This decision could be an indication that although the LSA market is small and relatively new, people are still interested in buying them even in economic struggles.

Now that an understanding of the overall trend of the LSA market has been formulated, the likelihood of company success within this market can be evaluated. Table 2 shows a list of companies that registered the most LSA with the FAA in 2014. In addition to the number of aircraft registered, the table also presents the year of the companies' founding, the most common model of each company, and the base price of each of the models. There are a number of important takeaways from this table. First, it should be noted that the RFP states that an aerobatic LSA

Table 2: Top Selling LSA Sold in 2014<sup>4,5</sup>

Manufacturer	Year Founded	Main Model	Cost of Main Model	Aircraft Registered
CubCrafters	1980	Carbon Cub SS	\$172,990	50
Van's	1973	RV-12	\$123,000	26
Progressive Aerodyne	1991	SeaRey	\$125,000	19
Flight Design	1988	CTLSi	\$156,500	16
Tecnam	1986	P92	\$130,999	14
Aeropro (Aerotek)	1983	A240/220	\$88,950	11
American Legend	2005	Legend Cub	\$136,900	10
Czech Sport Aircraft	1934	SportCruiser	\$119,000	9

must be designed, yet none of the leading LSA in the market are aerobatic LSA. Therefore, it can be concluded that this specific type of aircraft is underrepresented within the market, and Avem Dynamics can take advantage of this and become a leader with unique class of aircraft.

Also, all the aircraft in Table 2 are two seat LSA which gives the indication that single-seat variants are also underrepresented in the market. CubCrafters only registered 50 aircraft in 2014 and the majority of companies registered between 10 and 20 in 2014. This data demonstrates that Avem Dynamics will need to be profitable selling 10-20 aircraft per year. However, the minimum production rate in the RFP is 4 aircraft per month (48 per year). Therefore, Avem Dynamics will aim to be profitable selling 48 aircraft per year. Looking at the cost of the main models of each company, most aircraft are sold for \$100,000 to \$200,000. These prices give an indication for an approximate range in which the designed aircraft should be sold in order to be competitive in this market.

Many of the companies listed in Table 2 are well established and have existed for a number of decades. As a new company, it would be beneficial to investigate how new companies attempting to enter this market have fared. An example of a new company attempting to enter this market is Icon Aircraft. Icon has recently certified their new LSA, the A5. Although they have not sold any aircraft yet, they have recently entered production and already have a backlog of over 1,000 orders. This success demonstrates that LSA customers are not deterred by a new and unproven company as long as the product is intriguing and worth buying. As a result, it can be concluded that with a strong product a new company can have great success in the LSA market.

Since Tempo and Encore are aerobatic aircraft, it is important to also research the aerobatic market. Table 3 lists the most successful aerobatic aircraft companies from 2014. Note that none of the bestselling aerobatic aircraft

qualify as LSA. Therefore, once again, it can be concluded that the market of aerobatic LSA is underrepresented within both the LSA and aerobatic markets. Looking at Table 3 there are some key highlights to notice. First, aerobatic aircraft sell significantly more than LSA. All of the aerobatic aircraft listed sell for more than \$200,000. This increase in price indicates that if an aerobatic LSA is sold around the average price of other LSA, it will be a relatively inexpensive competitor in the aerobatic market. Another interesting fact is that the most successful aerobatic aircraft companies sell less product than the leading LSA companies; but, the moderately successful companies sell in the range of 10 to 20 aircraft each year so it is reasonable to assume that aerobatic LSA will sell in that same range.

*Table 3: Top-selling Aerobatic Aircraft Sold in 2014<sup>3,4</sup>*

Manufacturer	Main Model	Cost of Main Model	Number Sold
Extra	EA-300	\$350,000	31
American Champion	Super Decathlon	\$238,900	30
WACO Classic Aircraft	2T-1A-2 (Great Lakes)	\$245,000	11
XtremeAir	XA42	\$240,000	9

There are a number of conclusions that can be drawn after conducting the market analysis. First, the LSA market was not hit as hard during the recession, which indicates that people are still willing to buy LSA even during financial struggles. Additionally, Avem Dynamics can aim to sell 4 aircraft per month – achieving the RFP objective, while still falling within the range of yearly sales of existing LSA companies. Using Icon Aircraft’s new A5 as an example, a new company can have great success in the LSA market with a strong enough product. Finally, after investigating the LSA and aerobatic markets, it was determined that the specific category of aerobatic LSA was not strongly represented in either market. Therefore, by designing aerobatic LSA, Avem Dynamics can hopefully have great success, and become a leader in a unique class of aircraft by simply providing a product that was previously underappreciated in both LSA and aerobatic markets.

### 3 Aerobatic Competition

The RFP states that Tempo must be competitive within the International Aerobatic Club’s intermediate category. This section describes this competition level and gives an expected competition mission profile.

### 3.1 IAC INTERMEDIATE CATEGORY

Within the International Aerobatic Club (IAC) there are five categories of competition: primary, sportsman, intermediate, advanced, and unlimited. The intermediate category falls within the mid-range of difficulty where the pilots are beginning to be tested on more complex maneuvers and combinations of maneuvers within a sequence. From this it can be inferred that Tempo and Encore will be flown by experienced pilots or at least accompanied by one. This category includes maneuvers consisting of the basic maneuvers such as spins, loops, rolls, and turns with the addition of the snap roll and inverted figures. A snap roll is a rapid horizontal spin that is induced by a rapid pitch input followed by a rapid yaw input. Thus, the aircraft must be able to fly inverted and have competitive roll rates which are requirements stated in the RFP.

During the competition, an intermediate category pilot is expected to perform a known, unknown, and free program. The known program is published each year by either the international or national aerobatic club before any of the competitions. The 2016 known compulsory<sup>6</sup> for the intermediate category is shown in Figure 2 in Aresti symbols, where the triangles represents a positive g snap roll, the red lines represented inverted flight, and the arrows represent aileron roll. The sequence illustrates a typical intermediate category routine that includes various loops, snap rolls, inverted flight, and other basic maneuvers. The unknown program is revealed to the pilot the day of the competition. This program is meant to test the pilot's ability to fly a sequence that they have never flown. A free program is designed for the pilot to demonstrate style, creativity, and flying skills through a

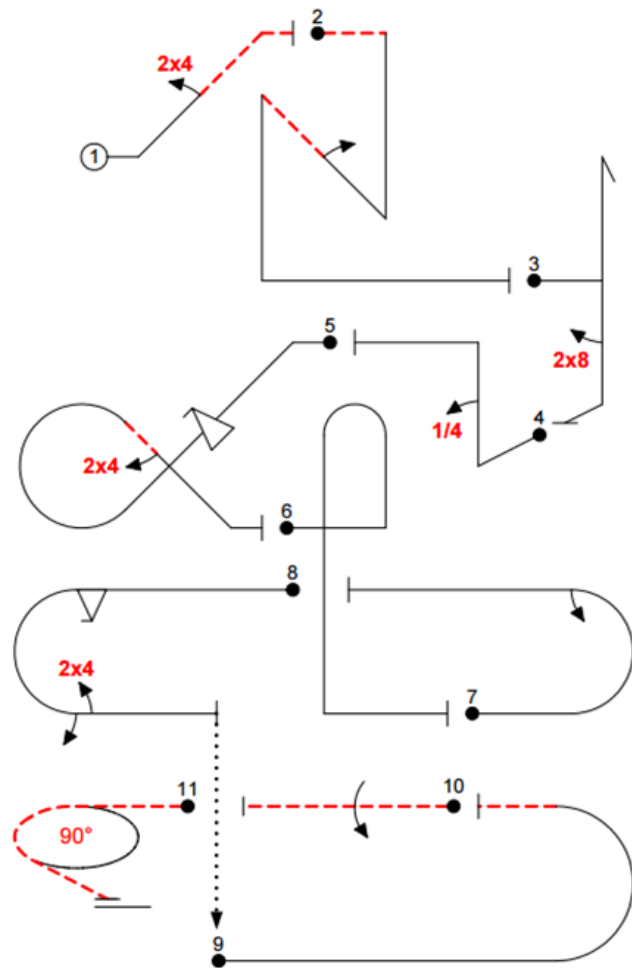


Figure 2: 2016 Known Compulsory for Intermediate Category

sequenced designed by the pilot. However, this sequence is limited to the maneuvers allowed in the intermediate category. Therefore, the aircraft must not only have enough fuel and power to perform the required maneuvers, but also adequately sized control surfaces and proper structure. These characteristics will be assessed in further detail throughout this document.

During a competition, all the programs must be performed within the aerobatic box to insure safety and to allow the aircraft to always remain in the judges' eyesight. The box is 3,280ft long and 3,280ft wide.<sup>7</sup> The height of the box varies based on level of competition. For the intermediate category the lower limit of the box is 1,200 feet above the ground and the upper limit is 3,500ft above the ground. White markers are placed on the ground to mark the corners of the box, but if the pilot exceeds these boundaries they are penalized and points are deducted from the final score. Therefore, it is important that the pilot is able to see the markers during the entire sequence. There is a buffer zone of 164ft along each axis beyond the marked aerobatic box boundaries. Each excursion into the buffer zone is penalized. One nautical mile beyond the buffer zone is the deadline line, or safety buffer zone. A greater penalty is applied if the pilot crosses this line. If any of the figures are flown entirely outside the box, then the pilot receives an automatic zero score.

There are between 3 and 9 grading judges at any competition. The grading judges assess the quality of each figure flown and assign a score between zero and ten to the pilots, with 10 being flawless. A zero can be given if a figure is flown incorrectly. A presentation score is given at the end of a sequence to reflect the placement of the sequences throughout the aerobatic box. The pilot's skills mostly determine the quality of the aerobatic maneuvers, but the shape and aesthetics of the aircraft enhance the overall appearance of the maneuvers. Thus, the aircraft must aid the pilot in executing the maneuvers.

## 3.2 AEROBATIC MISSION PROFILE

The single seat is expected to be used primarily as a competitive aerobatic aircraft. For this reason, an aerobatic mission profile has been developed to depict a typical mission of Tempo. Figure 3 shows what the mission for an aerobatic competition would look like, specifically in the intermediate category of the IAC. The aircraft will most likely takeoff at the airport at which the competition is being held and loiter for approximately one minute until it is that pilot's turn to compete. The pilot will fly over to the competition area and into the aerobatic box. The routine will last about four minutes and then the pilot will exit the aerobatic box and land. When flying during the competition, the engine will be at maximum continuous power almost the entire time, this leads to a cruise speed of

120 KCAS for competition. Tempo is expected to have a competition weight of 1005 pounds, based on needing fuel for about 40 minutes of flight time (including the 30 minute fuel reserve) as well as having a pilot that is the maximum weight the RFP requires which is 230 pounds.

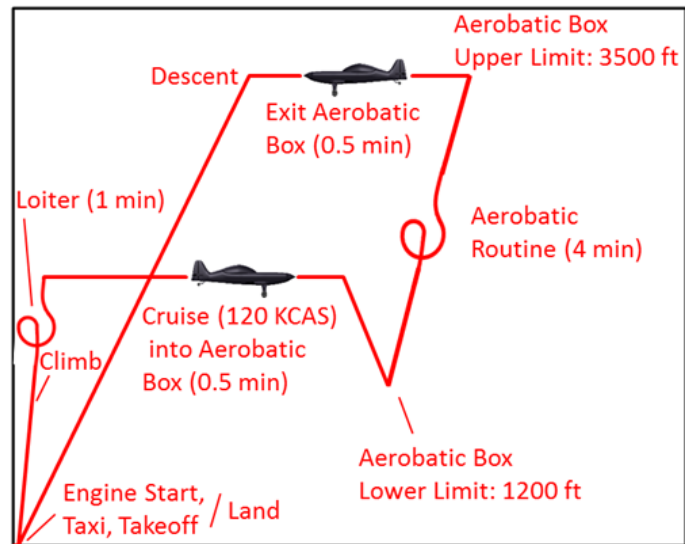


Figure 3: Tempo Competition Mission Profile

## 4 Aircraft Sizing

This section describes the sizing choices for Tempo and Encore, which are determined by plotting the major constraints with respect to wing loading and power-to-weight. Then from the constraint diagrams the wing loading and power-to-weight for each aircraft are selected. In order to maintain commonality between aircraft, it is desired to select design points for each aircraft that yield the same wing area and propulsion system for the aircraft. The power-to-weight selected is based on the power output of the selected engine, the Lycoming AEIO-233 and the weight estimates of the aircraft.

### 4.1 CONSTRAINT DIAGRAM

The objective of the constraint diagram is to determine a design point that yields the power-to-weight ratio and wing loading (weight-to-wing area ratio) of the aircraft. The specific excess power equation is used since it involves both power-to-weight and wing loading. This equation incorporates the requirements and constraints from the RFP, which are listed in Table 4. The requirements are expressed by creating contours of either specific excess power (for maximum speed and climb rate), simplified takeoff and landing integrals for the takeoff and landing

requirements, or  $C_{L,max}$  conditions for the stall speed. Then the constraints are plotted along the contour related to its specific excess power for each requirement on a graph of wing loading versus power-to-weight.

The requirements in Table 4 indicate that the constraint diagram for Tempo and Encore will be slightly different. Due to the commonality design objective, it is preferable to have constraint diagrams that yield the same wing area for both aircraft. Additionally, it would be beneficial for both aircraft to utilize the same propulsion system, allowing the company to order the same engine in greater quantity, possibly leading to a discount on the price per engine. The constraint diagrams for Tempo and Encore are shown in Figure 4 and Figure 5 respectively.

Table 4: Governing Constraints

Constraint	Tempo	Encore
Maximum Speed	120 KCAS	120 KCAS
Climb Rate	1,500fpm	800fpm
Takeoff Length      Field	1,200ft over 50ft obstacle	1,500ft over 50ft obstacle
Landing Length      Field	1,200ft over 50ft obstacle	1,500ft over 50ft obstacle
Stall Speed	45 KCAS	45 KCAS

The maximum speed constraint for the Tempo, indicated by the blue line in Figure 4, is 120 knots calibrated in level flight. This constraint is created with a specific excess power of zero since the aircraft is in steady level flight and thrust equals drag. The next constraint that is restricting the design space for Tempo is the 1,500fpm climb rate, indicated by the red line in Figure 4. This constraint occurs at sea level in ISA + 10°C. The first step to calculating the specific excess power for this constraint is determining the velocity. The velocity that yields the maximum specific excess power is used for each power-to-weight and wing loading. Then for the various velocities, power-to-weights, and wing loadings, the contour associated with a specific excess power of 1,500fpm is plotted. The remaining three lines – stall speed, landing and takeoff field lengths – are functions of  $C_{L,max}$ . A  $C_{L,max}$  of 1.45 was used for these three constraints. This value will allow the aircraft to perform without using a high lift system, allowing for a simpler configuration and potentially lowering the manufacturing costs. Tempo has to take off and land in no more than 1,200ft over a 50-foot obstacle. The maximum allowable stall speed for Tempo and Encore is 45 knots calibrated in a clean configuration.

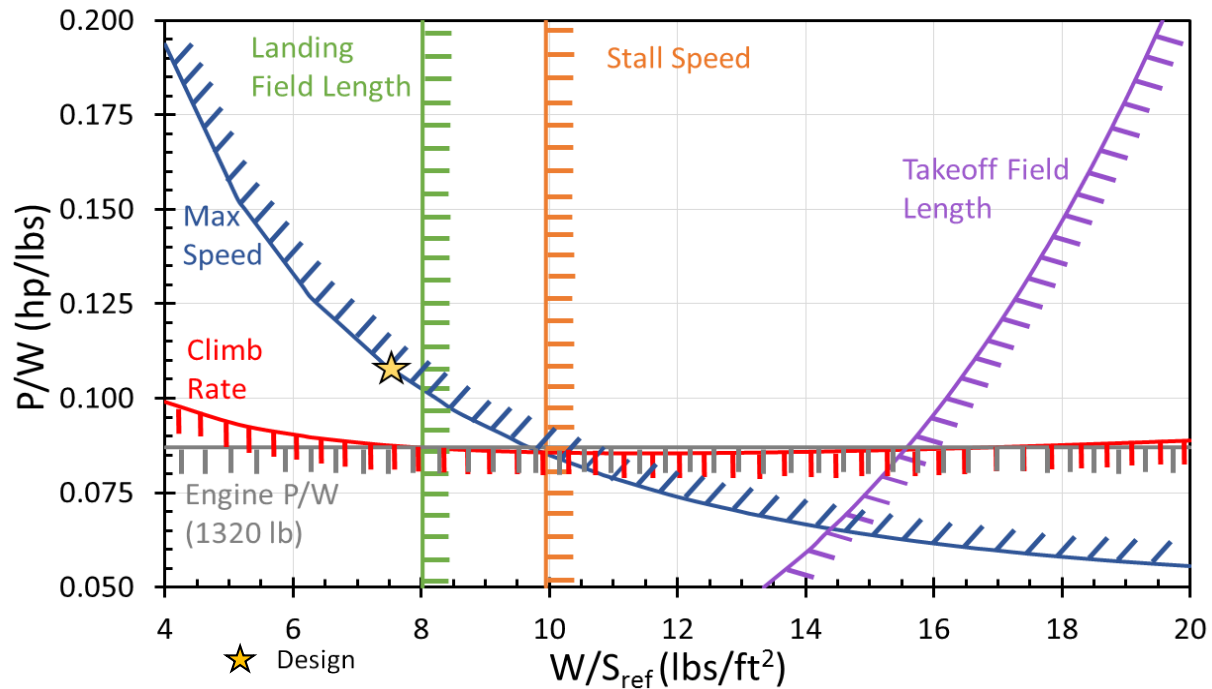


Figure 4: Constraint Diagram for Tempo

Takeoff and landing analysis was done using the method from Roskam and Lan's *Airplane Aerodynamics and Performance*,<sup>8</sup> which is further defined in Section 11.2. The takeoff and landing analysis methods were selected because they provide simplified integrals of takeoff and landing that are sufficiently accurate for conceptual design. The final constraint line is a derived requirement of minimum power-to-weight. As will be discussed in the propulsion section, a Lycoming AEIO-233 engine must be used because it is the least powerful aerobatic certified engine in the power range required for the aircraft. In addition to being restricted to one engine, the aircraft has a maximum weight of 1320lbs; combining these two requirements yields a minimum power-to-weight for both aircraft of 0.088 hp/lb. Performance above this line is only achieved with a higher weight or a less powerful engine. However, this is already the maximum weight allowed and less powerful engines cannot be used because they cannot work while inverted. Therefore, weight estimates for the aircraft set the power-to-weight.

The design for Tempo is governed mostly by the maximum speed, climb rate, and landing field length requirements. As seen in Figure 4, the design point is chosen to be at a wing loading of 7.6lbs/ft<sup>2</sup> and a power-to-weight of 0.107hp/lbf. Given Tempo's current weight of 1,087lbs, the wing area becomes 143ft<sup>2</sup> and the power required is 116hp (which is the rated horsepower for the Lycoming AEIO-233). Generally, when a design point is selected on a constraint diagram, the point is placed as close to the constraint boundaries as possible. However, the particular design point was selected for three reasons: because the propulsion system selected and the weight



estimate specify the power-to-weight required, to provide a margin for uncertainty, and to allow for the same wing area and engine in both aircraft. Based on the weight of Tempo and the engine selected, the power-to-weight of 0.107hp/lbs is required. In addition, the wing area selected places the design point slightly apart from the landing field length constraint. As a result, the current design point ensures that if Tempo's weight changes in future design iterations it does not violate the constraint.

As previously mentioned, the constraints for Encore are slightly different than those from Tempo. The maximum speed and stall speed requirements remain the same; however, the climb rate is more relaxed from 1,500fpm to 800fpm. Also, the takeoff and landing field length increases from 1,200ft to 1,500ft over a 50-foot obstacle. The design point is selected such that both aircraft have the same sized wings and use the same engine. Given the current weight of Encore, the design point is placed where the wing loading is 9.1lbs/ft<sup>2</sup> and a power-to-weight 0.09hp/lbs as shown in Figure 5. This design point leads to Encore having the same wing area and engine as Tempo. Additionally, as with Tempo, there is some margin for uncertainty associated with the selected design point for Encore, which ensures that Encore will not stall if the weight changes.

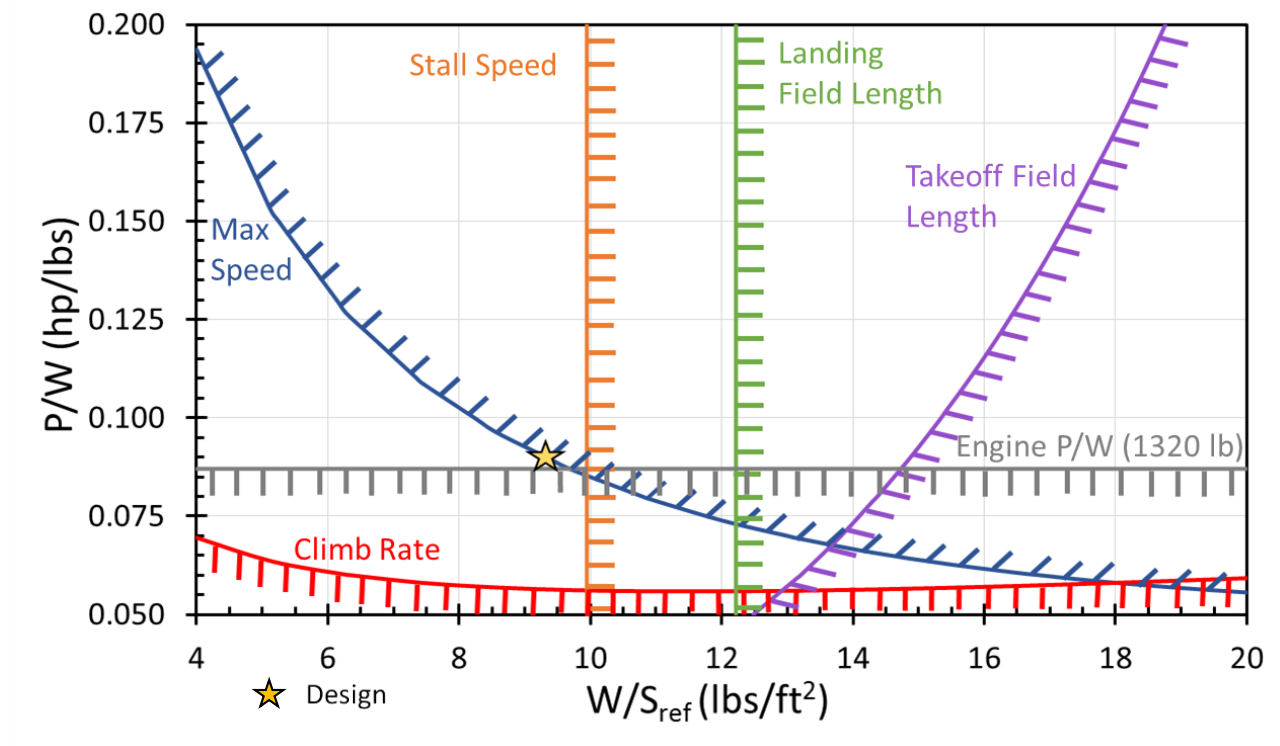


Figure 5: Constraint Diagram for Tempo

## 4.2 DERIVED MAXIMUM LIFT COEFFICIENT

As the constraint diagrams showed in the previous section, the landing field length requirement for Tempo and the stall speed requirement for Encore predominantly drive this LSA design. These two constraints are heavily influenced by the maximum lift coefficient,  $C_{L,max}$ , of the aircraft. Therefore,  $C_{L,max}$  essentially determines the wing area of the aircraft. Figure 6 depicts the constraint diagram for Tempo when  $C_{L,max}$  is varied from 1.2 to 1.45 and Figure 7 shows this relationship for Encore. These lines were generated with the same method as the constraint diagram.

The lines with hash marks represent the actual design space Avem Dynamics is working with while the dashed lines represent the change in the level of constraint of the requirements that depend on  $C_{L,max}$ . When examining these figures, it is apparent that a low  $C_{L,max}$  is not feasible for this design because the wings necessary for this would have an area that would be extremely large for an LSA. The landing field length constraints for Tempo and the stall speed constraints for Encore show that a maximum lift coefficient of at least 1.4 is needed for both aircraft. Section 6.2 will describe how the wing was designed to achieve a final  $C_{L,max}$  value of 1.45.

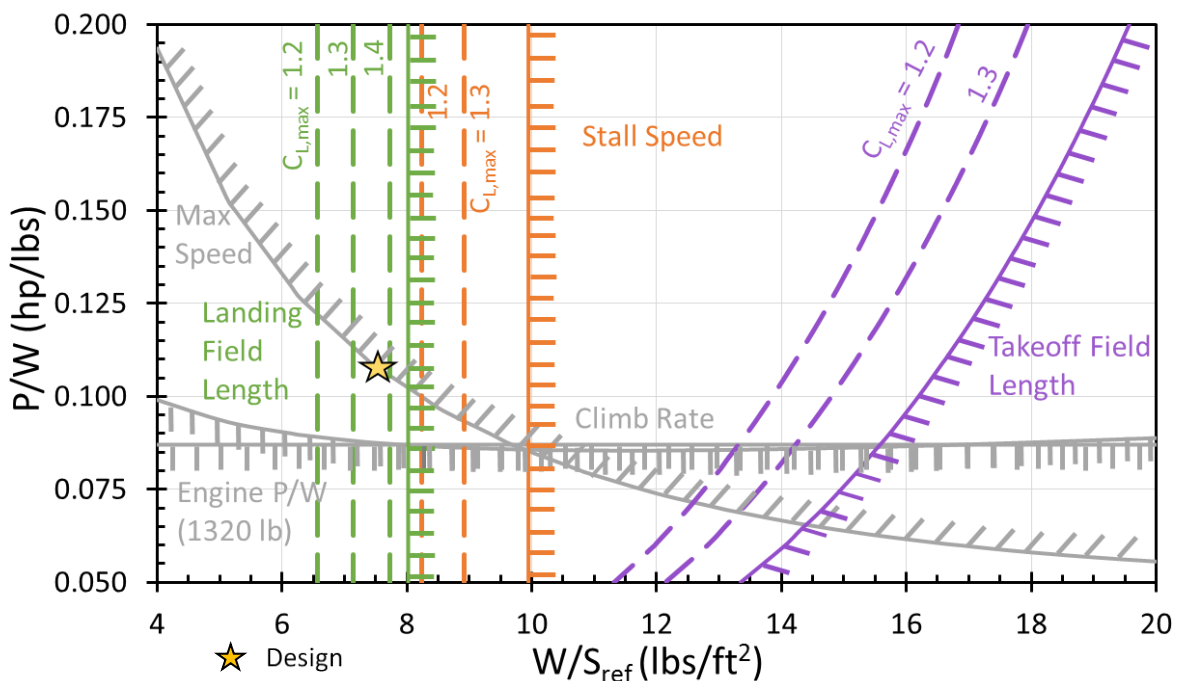


Figure 6:  $C_{L,max}$  Constraint Diagram for Tempo

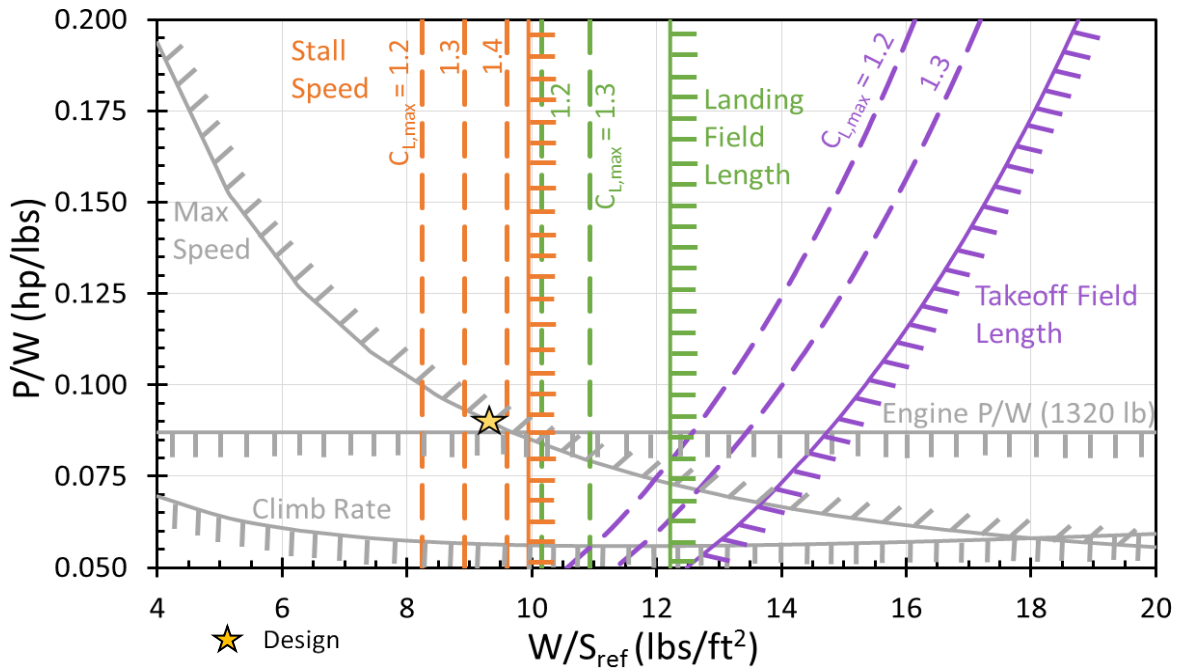


Figure 7:  $C_{L,max}$  Constraint Diagram for Encore

## 5 Configuration

The configuration of both aircraft is discussed below in regards to aesthetics, seating configuration, and landing gear discussions, followed by an inboard profile which shows the layout of the components for each aircraft.

### 5.1 AESTHETICS

When making configuration decisions it is important to recall the design objective of creating an aesthetically pleasing aircraft. It is often difficult to define what characteristics in an aircraft make it aesthetically pleasing. In order to gain a better understanding in airplane aesthetics, an interview<sup>5</sup> was conducted with an aerobatic aircraft designer, pilot, and competition judge, Dan Rihn, who designed the DR-107 and DR-109. Some of the most valuable information Rihn provided had to do with the effect of the shape of the fuselage and the placement of the wing on the appearance of the aircraft when performing aerobatics. Rihn recommended that the top view show the fuselage starting wide and converging to a point, and that the fuselage be symmetric about the longitudinal axis. Additionally, Rihn recommended that the wing be placed very near the vertical center of the fuselage, as opposed to having a high or low wing. These configuration decisions create a more aesthetically appealing aircraft because they make maneuvers such as a roll look very tight and clean. If the aircraft is not symmetric about the

longitudinal axis it would appear to wobble, or “banana”, when in roll. A tight roll is a sign of pilot skill, but even a “banana” will make a perfect roll look wobbly. For these reasons, both Tempo and Encore are mid-wing aircraft.

In order to validate if the current design of the aircraft was aesthetically pleasing, a survey was conducted. Two hundred Cal Poly students were presented with a picture of Tempo, and asked “Does this airplane look good?” The students were offered three options to respond with: “Yes”, “No”, or “Not Sure.” The results from the survey are shown in Figure 8, along with the picture that was provided for the survey. The results show that nearly twice as many students believed that the aircraft looked good than did not. This serves as a confirmation that the current design is aesthetically pleasing. While the students are not potential customers this survey provides initial data on the appeal of the aircraft.

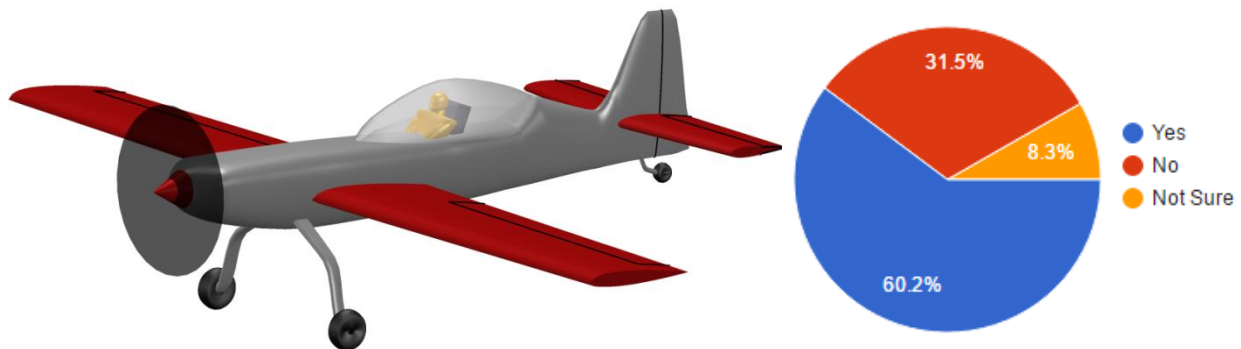


Figure 8: Aesthetics Survey Results

## 5.2 SEATING CONFIGURATION

Tandem and side-by-side seating, as shown in Figure 9, were the two configurations considered for the seating. The decision to utilize a tandem seating configuration was made by considering commonality, zero-lift drag coefficient, and the weight of the aircraft. While there are many qualitative factors to each configuration, such as comfort and flying experience, these factors are generally unquantifiable. Additionally, tandem seating is more

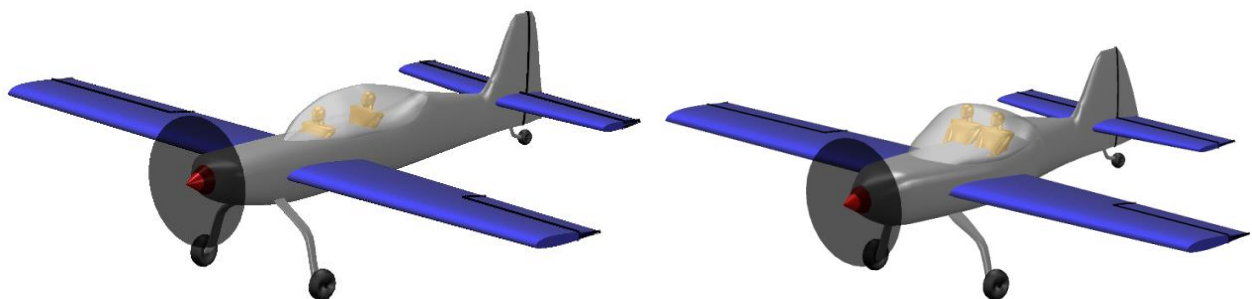


Figure 9: Side-by-Side versus Tandem Seating

streamline which makes this configuration more aesthetically appealing. In Table 5, these above mentioned characteristics are shown for each configuration. The commonality is calculated in Section 9.3, and is important to lower manufacturing costs and increase maintainability. The zero-lift drag coefficient for the entire aircraft is calculated in Section 6.3 and is found to be 0.0210 for tandem and 0.0220 for side-by-side. The difference in drag can be accounted for in the increase in diameter required for the side-by-side configuration. The final parameter, weight, is found from Section 9.2 and is 1297lbs for tandem and 1282lbs for side-by-side. The increase in weight between the two configurations is 0.3% which is so small it is almost insignificant. Tandem configuration was chosen since it has a higher commonality advantage and lower zero-lift drag coefficient.

	Gross Takeoff Weight (lbs)	$C_{D,0}$	% Commonality
<b>Tandem</b>	1297	0.0210	95
<b>Side by Side</b>	1282	0.0220	70

Table 5: Comparison of Seating Configuration

## 5.3 LANDING GEAR

When it comes to landing gear, a selection is required between tricycle landing gear or conventional landing gear. This section discusses the selection process of choosing the landing gear followed by how the gear was placed.

### 5.3.1 LANDING GEAR TYPE

Another configuration decision is what type of landing gear to use. Two options were identified: tricycle landing gear or conventional (taildragger) landing gear. There are advantages and disadvantages to both options. Taildragger landing gear causes the aircraft to be angled up while on the ground, leading to poor visibility while taxiing and can cause the pilot to ground loop, which is when the aircraft rotates in the yaw axis and the forward moving wing generates lift, possibly making the other wing tilt to hit the ground. These problems may be difficult to overcome for inexperienced pilots; however, Tempo and Encore are aerobatic aircraft so it is assumed that experienced pilots will be flying them or at least accompanied by one.

Taildragger landing gear is lighter than tricycle landing gear because the tail wheel is much smaller than the nose wheel. For example, the two seat Renegade Falcon LS 2 is made with both landing gear configurations and the taildragger aircraft is nineteen pounds lighter.<sup>9</sup> Similarly, the single-seat Sonex Onex LSA also comes with both configurations and the taildragger aircraft is 9lbs lighter.<sup>10</sup>

A drag buildup was also conducted to determine the zero-lift drag coefficient of the different landing gear configurations. An unfaired tricycle gear on Tempo was calculated to have a  $C_{D,0}$  of 0.0040 and an unfaired taildragger gear was found to have 7 less counts zero-lift coefficient of drag at 0.0033. The method of determining these values is discussed further in Section 6.3. Because the taildragger landing gear is lighter, has less drag, and pilots of aerobatic aircraft will be able to properly taxi, Tempo and Encore will have taildragger landing gear.

### 5.3.2 LANDING GEAR PLACEMENT

The location of the landing gear depends on the location of the aircraft's center of gravity. Methodology coming from Raymer<sup>11</sup> states that the most forward and aft CG should fall between  $15^\circ$  and  $25^\circ$  back from the location of the front wheels. Gear that is too far forward of the CG will cause the aircraft to be more prone to ground looping, and a gear that is too far aft will cause the aircraft to tip onto its nose. The location of the tail wheel must fall between an angle of  $10^\circ$  and  $15^\circ$  above the main wheels in the takeoff attitude. The change in angle and length that comes from the compression of the struts must also be taken into account when placing the gear. To prevent overturning, which can cause damage to the wingtips, the main wheels should be separated by a minimum of  $25^\circ$  off of the CG. This requirement could also be stated as the wheel track of the main wheels should be between 25% and 35% of the total wingspan. Figure 10 and Figure 11 shows that all of these requirements for landing gear placement have been met for both aircraft. The range of the most forward and aft CG locations for both aircraft span a distance that is 20% of the mean aerodynamic chord. Since the CG ranges of both Tempo and Encore are so similar, the landing gear between the two aircraft was kept common. In order to achieve the proper angles with the CG, the forward gear was placed 5.7ft aft of the spinner tip on Tempo and 5.2ft aft of the spinner tip on Encore as later described in Section 10.1. The gear is 5.1ft below the CG which is as short as possible while still satisfying the angle requirements of  $15^\circ$  to  $25^\circ$  from vertical.

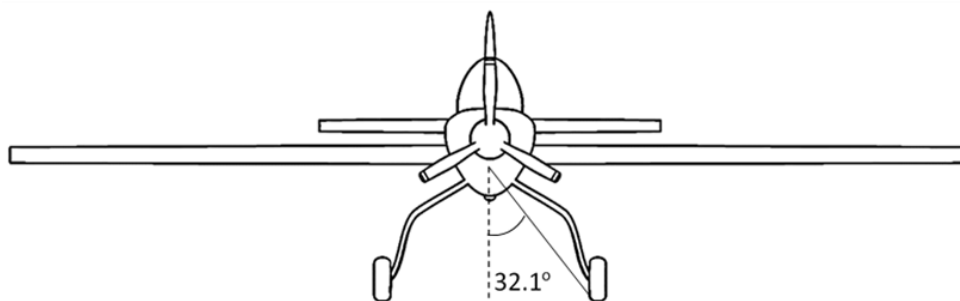


Figure 10: Landing Gear Placement with Main Track 25-35% of Wingspan

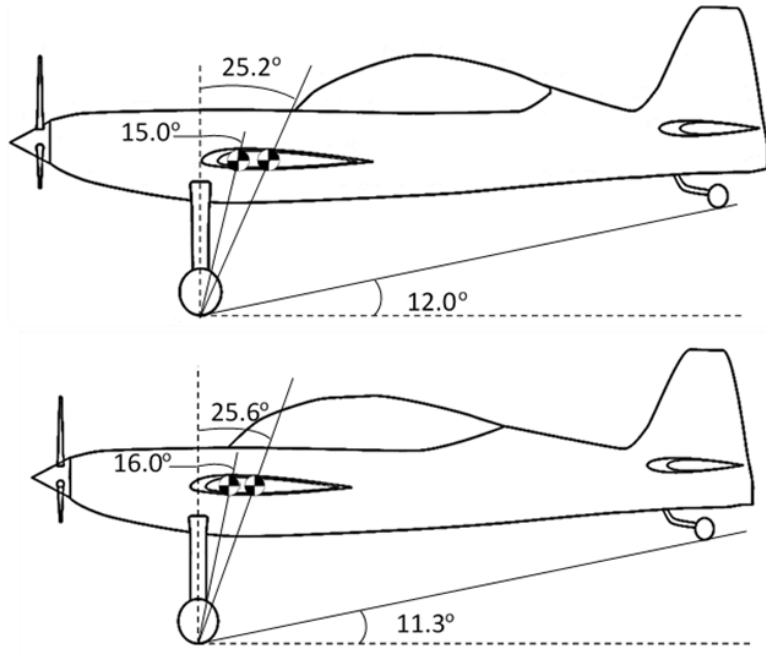


Figure 11: Tempo (top) and Encore (bottom) Landing Gear Placement

## 5.4 INBOARD PROFILE

The inboard profile for both aircraft are shown in Figure 12. The diagrams depict a side view of the aircraft indicating the location of various components and subsystems to ensure that the internal volume requirements are met. For both aircraft the propulsion system, which is the Lycoming AEIO-233 engine, fits in the nose of the fuselage. The shaft of the engine to the propeller is at a distance of 8in, which is the maximum distance before it is necessary to add an additional bearing.<sup>7</sup> Both figures display 6'2" pilots to demonstrate that the aircraft can be flown by a range of pilot sizes. Also, the pilot seats are each equipped with room for a seat pack parachute that is at most 3.5in thick. Parachutes such as Softie Seat or Softie Wedge Seat manufactured by Softie<sup>12</sup> are prime examples of parachutes that can easily be used. Additionally, each pilot has a control stick between their legs and foot pedals by their feet. The fuel for both aircraft is stored in the wing as shown in Figure 13. Both aircraft carry 12 gallons of fuel, as shown with the 2 six-gallon tanks within the wing or either side of the fuselage. Placing the fuel in the wing has two main benefits: it alleviates wing bending loads in positive g maneuvers, and it places a varying payload near the CG because the wing is near the CG, which shortens the distance between the forward and aft CG limits.

For the Tempo, a baggage area is situated directly behind the pilot and has a capacity of four cubic feet. To help balance the aircraft, the battery is placed near the empennage. A Concorde RG-12 battery is used as an example

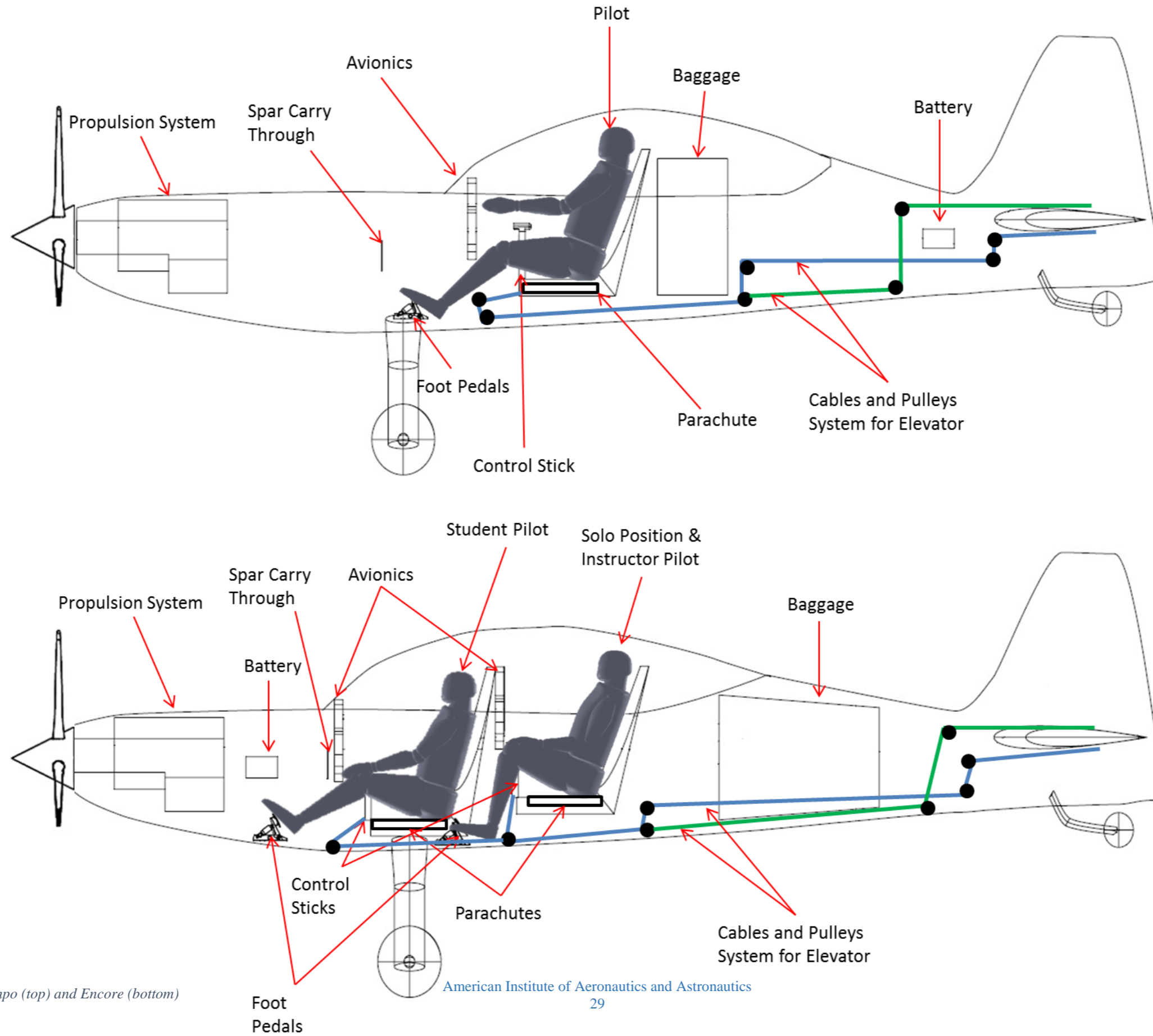
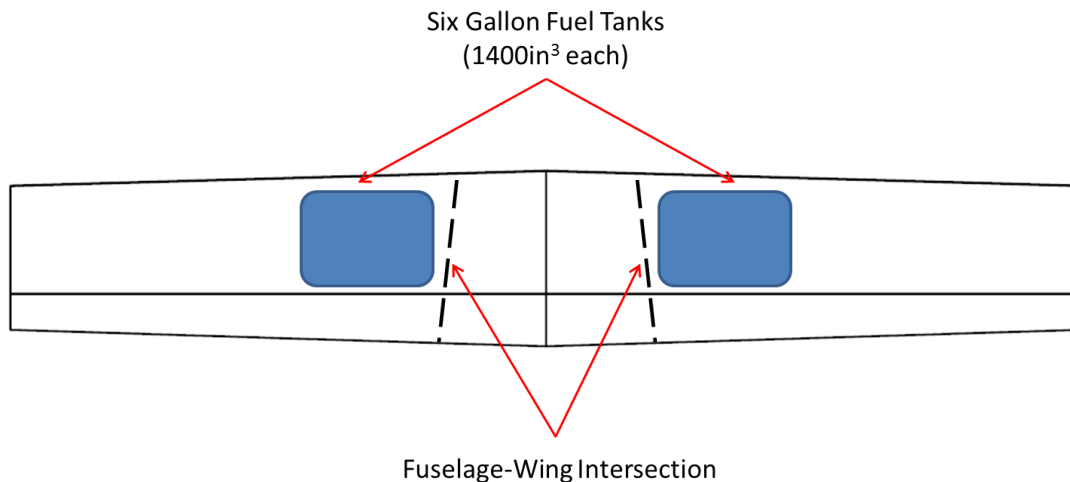


Figure 12: Inboard Profiles - Tempo (top) and Encore (bottom)



for both aircraft to model dimensions and weights.<sup>13</sup> The avionics panel is situated at a comfortable distance so that the pilot can reach all the instrumentation. The pilot is reclined to  $70^\circ$ , which assists in his ability to withstand g forces. The reclined position helps with resisting g forces because the vertical distance between the pilot's head and extremities is decreased, which lowers the effects of blood pooling in extremities due to aerobatic maneuvers.<sup>14</sup> The spar carry through location is also specified, with the dimensions calculated in Section 8.2.



*Figure 13: Location of Fuel in Wings*

In the Encore, the baggage is placed behind the rear pilot, and has a capacity for six cubic feet. The baggage is modeled as a tapered elliptical cylinder so that the volume fits in the rear section of the fuselage. The battery is placed towards the front of the aircraft for Encore as opposed to the rear for Tempo. For Encore, the pilots are seated in such a way to move the CG forward, while still fitting underneath the canopy. The front pilot is reclined to  $80^\circ$  to place the rear pilot as close to the front pilot as possible, while still reclined to assist in withstanding g forces, and the rear pilot is reclined to  $70^\circ$  as in Tempo. The front pilot is modeled with his hands on the avionics panel, and the rear pilot's hands are on the control stick, to demonstrate that the instruments are placed in reasonable locations. Finally, the spar carry through location is directly in front of the avionics panel of the front pilot. For both aircraft, the spar carry through location demonstrates that using a mid-wing is feasible.

## 6 Aerodynamics

The focus for aerodynamics is broken into three main components: the airfoil selection, design of the wing and the drag polar. The airfoil selected was made to help meet the requirements for the wing; however, this selected airfoil will not be the final one manufactured on the airplane since one will most likely be designed specifically for

Tempo and Encore. The goal will be to show that an airfoil, backed with experimental data, can effectively meet what is required.

The objective for the wing design is to ensure the requirements derived from the constraint diagram are met and will be able to meet the load requirements of aerobatic maneuvers. Currently, the outer geometry of the wing is being prioritized to meet the constraint diagram and the inner structures will be derived from the wing geometry.

## 6.1 AIRFOIL SELECTION

There is one key requirement that the airfoil will have to meet. This requirement is in conjunction with the planform of the wing, the airfoil must be able to meet the required  $C_{L,max}$  of 1.4 for landing and takeoff. Even though this  $C_{L,max}$  is a three dimensional requirement for the entire vehicle, it directly correlates back to the maximum two dimensional lift coefficient,  $c_{l,max}$ , of the airfoil. As soon as one span-wise location of the wing's  $c_l$  exceeds the  $c_{l,max}$  of the chosen airfoil, the wing has begun to stall at that angle of attack. It is also at this stall angle that the wing has reached its  $C_{L,max}$ . A larger  $c_{l,max}$  from the airfoil leads to a higher  $C_{L,max}$  from the wing planform which is favorable since the aircraft are not using high lift devices and the highest possible  $C_{L,max}$  is needed.

The RFP states that both aircraft have to be able to sustain at least five minutes of inverted flight, so the chosen airfoil must satisfy this requirement. Satisfying this requirement will have a similar method as finding  $C_{L,max}$  for normal flight. Along with having a  $c_{l,max}$ , an airfoil will also have a maximum negative  $c_l$ , or  $c_{l,min}$ . When the wing is upside down, if one of the sectional lift coefficients exceeds the  $c_{l,min}$  then the inverted wing has begun to stall. The minimum stall flight speed value can be obtained at this  $C_{L,min}$  value, and from this the inverted required flight speed of the aircraft can be found. An airfoil with a greater  $c_{l,min}$  value will perform better, pushing towards a more symmetrical airfoil.

These are the requirements that the airfoil will have to meet for both aircraft. However, there are a few things that directly correlate to the chosen airfoil. One of these fallouts is that the airfoil has to be thick enough to be able to fit the main spar and inner structure of the wing. Though the maximum thickness of the airfoil also affects both the amount of drag seen by the wing and where stall begins (leading or trailing edge), the necessary structures to meet the load limit requirements needs to be accommodated. Tempo will have to sustain +6/-5g's forces and Encore will have to sustain +6/-3g's. These kind of forces for aerobatic maneuvers will likely require a thicker main spar. If the airfoil is not thick enough to meet this requirement than it will not be viable.

Since most of the desired traits for the airfoil focus around the stalling characteristics, it was important to find experimental data. Many computer software programs that analyze airfoil aerodynamics assume inviscid solutions, which is not usable after stall since separated flow is inherently viscous, so data from both NASA Langley’s wind tunnels<sup>15</sup> and Sandia National Laboratories,<sup>16</sup> is used to find airfoils from existing LSA and aerobatic aircraft.

In order to equally compare values for each airfoil, the wing planform was chosen to have the reference area derived from the constraint diagram of 143ft<sup>2</sup>, with a wingspan of 30ft, chord of 6ft, and no twist, taper, or sweep. The rectangular wing was chosen so that the performance of the airfoils could be properly be compared with minimal influence from the geometry of the wing. The results from this study are shown in Table 6.

*Table 6: Airfoil Trade Study*

Airfoil	Aircraft	Max Camber	$C_{L, \max}$	Angle of Stall
NACA 1412	Super Decathlon	1.0%	1.28	17.5
NACA 2412	Cessna 150	2.0%	1.35	18.3
NACA 23012	Taylorcraft L2-A	1.8%	1.36	19.0
NACA 0015	Pitts Special (lower wing)	0.0%	1.00	15.2
NACA 64 <sub>2</sub> - 415	Sonex Onex	2.2%	1.25	17.0

The method used for calculating  $C_{L, \max}$  values is described in Section 6.2.2. From Table 6, unfortunately there are no airfoils that exceed the required  $C_{L, \max}$  required of 1.4. However, the airfoil with the largest  $C_{L, \max}$  and  $C_{L, \min}$  value is the NACA 23012, and this airfoil extremely close to meeting these requirements. The next step will be to take this airfoil and use it for designing the wing so that the wing will be able to meet and exceed the requirements set out for  $C_{L, \max}$  and inverted flight, described in the next section.

## 6.2 WING DESIGN

The wing should not only meet the constraints but it should also allow Tempo and Encore to excel in the IAC competition. The wing design must be executed in steps, starting with the constraint diagram which is discussed in Section 4.1. From the constraint diagram a wing reference area was chosen to be 143ft<sup>2</sup> and the maximum lift coefficient of the aircraft is 1.45. This section will further develop the design of the wing, specifically the wing span and wing taper.

### 6.2.1 WING SPAN

Instead of choosing an aspect ratio for the wings, the wingspan was sized for an aerobatic aircraft. It is expected that both aircraft will be stored in a T-Hanger, the largest of which have a 48ft width.<sup>17</sup> The next constraint is the root bending moment of the wing. As span increases, the root bending moment will also increase, driving up the necessary structure required to hold the moment and increasing the weight. The final constraint considered is the root bending moment during roll of the aircraft, since during roll the wing will experience higher root bending moments than in level flight. These higher root bending moments will add to the required structure and increase weight accordingly. With these constraints, the sizing of the wing span was accomplished.

The root bending moment for steady level flight is found for wingspans between 15ft and 48ft by finding the lift distribution on the wing for the given wingspan<sup>18</sup> and then integrating the lift distribution to find the moment. The wing is assumed to be rectangular, with no sweep or taper, of a constant wing area of 143ft<sup>2</sup>. A moment was found for each positive g-loading case (1 to 6 g's) according to the Requirement 10.1 and for the given range of wingspans. The plot of root bending moment verses g-loading is shown in Figure 14 for a 15-foot wingspan, 31-foot wingspan, and a 48-foot wingspan. According to spar sizing discussed in Section 8.2, the maximum root bending moment allowed is 68,000ft-lbs. The maximum root bending moment will change with thickness of the wing and therefore chord; however, there needs to be a structural constraint on the wing to limit wingspan. This estimation of the

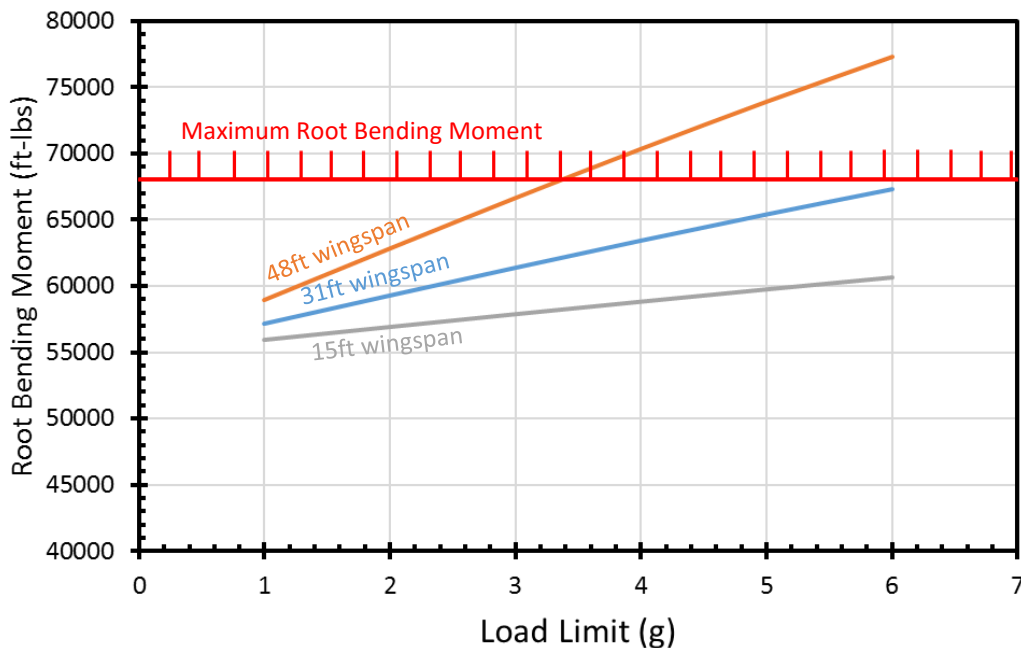


Figure 14: Root bending moment for a given load limits and wingspans

maximum root bending moment is a conservative one and can be refined in preliminary design. Given this top moment constraint, the maximum wingspan allowed is 31ft.

A plot of wingspan versus wing weight is shown in Figure 15. The wing weight model is discussed in further depth in Section 9, but the GASP weight model<sup>17</sup> recommends that the wing weight be maximum of 20% of the weight of the entire aircraft. With the predicted weight of Tempo being 1087lbs, the maximum weight of the wing can be 217lbs. Shown in Figure 15, this maximum wing weight limits the maximum span to be 42ft. Since the

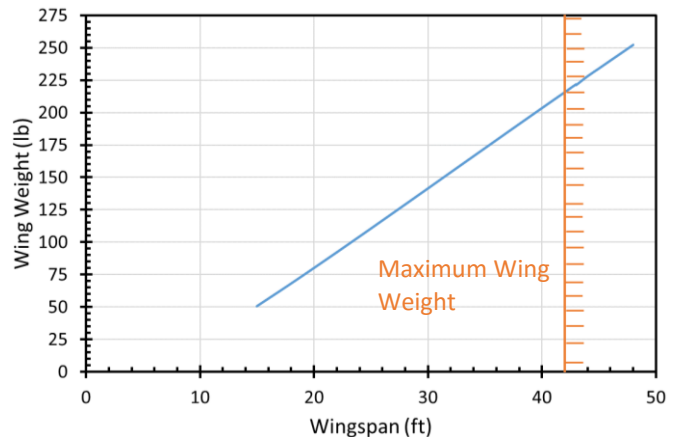


Figure 15: Wing weight versus wingspan, with the maximum wing weight allowed shown

required  $C_{L,max}$  of the aircraft must be met without the use of flaps, and the wing area is set from the constraints on the constraint diagram, the parameters that can be changed to meet the required  $C_{L,max}$  are the wingspan, taper, and twist. Taper will be discussed in Section 6.2.2 and twist will not be included in the design to lower manufacturing costs. The requirements for  $C_{l,max}$  for airfoil selection is discussed in Section 6.1, and the minimum wingspan to meet the lowest required  $C_{l,max}$  of 1.4 is 28ft. With this lower constraint on the wingspan, the range in which the wingspan can fall is between 28ft and 31ft.

The final constraint on the design was determined to be the roll rate requirement of 180°/sec. The total roll rate will increase the root bending moment from the steady level flight root bending moment. The root bending moment for the roll condition is calculated using the steady state roll rate equation given by:

$$\dot{\phi} = \frac{L_{\delta_a} \delta_a}{-L_p}$$

where  $L_{\delta_a}$  is the non-dimensional variation of the airplane rolling moment coefficient with aileron deflection,  $L_p$  is the non-dimensional variation of airplane rolling moment with pitch, and  $\delta_a$  is the aileron deflection. The maximum aileron deflection is assumed to be 20° for initial sizing, and the derivatives are calculated using Datcom.<sup>19</sup> The root bending moment is:

$$L = L_{\delta_a} \delta_a I_{xx}$$

where  $I_{xx}$  is the roll moment of inertia of the entire airplane. This value for root bending moment can be found for multiple roll rates; however, the minimum requirement for roll rate was investigated to ensure compliance with the RFP. Figure 16 shows the variation of root bending moment with wingspan for a roll rate of  $180^\circ/\text{sec}$ . When rolling root bending moment is added to the steady level flight root bending moment for 1g case, it is possible that this moment could exceed the 6g maximum moment. However, it can be seen from Figure 16 that at the maximum wingspan, the rolling moment does not even come close to the 6g case of the root bending moment. For completeness, a roll rate of  $360^\circ/\text{sec}$  is also plotted on the same figure, and was also shown to not affect the maximum root bending moment at 6g's.

With the maximum root bending moment of 68,000ft-lbs, the required  $C_{L,max}$ , from Section 4.2 of 1.4, and the weight constraints of the wing, the wingspan of the aircraft comes out to 31ft and an aspect ratio of 6.72.

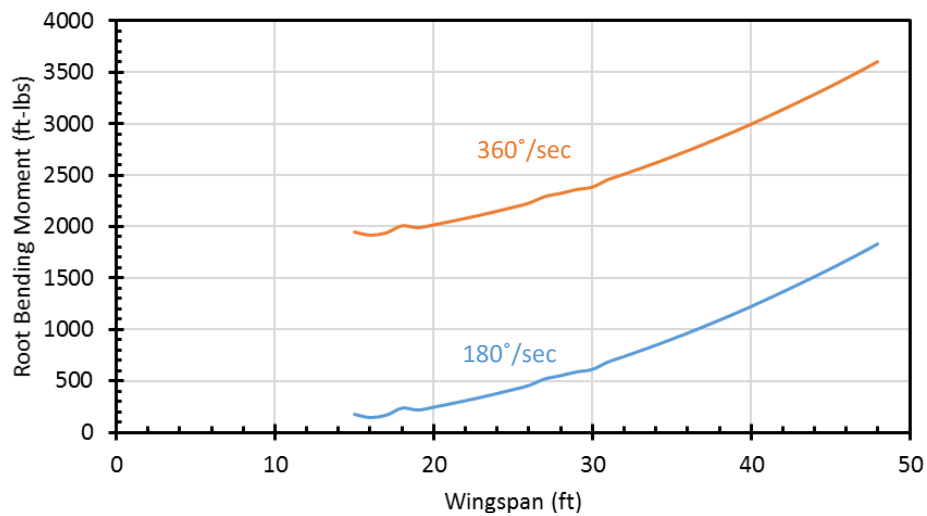


Figure 16: Variation of root bending moment in roll with wingspan

### 6.2.2 WING TAPER

A standard rectangular wing with  $143\text{ft}^2$  reference area was unable to meet the required  $C_{L,max}$ , so it was decided that adding taper to the wing could help meet this requirement. Avem Dynamics would also like to design Tempo and Encore to be a modern and attractive aircraft, and adding a slight amount of taper to the wings adds to the overall appeal. While adding taper can increase manufacturing costs from added complexity, the price will be worthwhile because both aircraft will become more aesthetically pleasing and perform better. The focus of this study is to show that the resultant lift distribution will still be favorable for stall location span-wise along the wing and be able to meet requirements for  $C_{L,max}$  for normal and inverted flight.

The first step was to calculate the lift distributions for both a non-tapered and tapered wing and compare. The method for calculating the various lift distribution was as follows: using the NACA 23012, the basic lift distribution was found using VSPAERO,<sup>20</sup> a vortex lattice code, at an angle of attack of 0°. The lift distribution was then found at angle of attack of 1°. The additional lift distribution was found by subtracting the baseline lift distribution and the lift distribution at 1°. The change in lift distribution is linear, meaning it can be propagated forward with respect to increasing angle of attack. This propagation can continue until a point along the wing span where the sectional lift coefficient exceeds the  $c_{l,max}$  of the airfoil, and it is at this point the wing has begun to stall. The area under the lift distribution curve is the total  $C_L$  for the wing, and as soon as the wing has begun to stall, the area under the curve is the  $C_{L,max}$ . Figure 17 shows an example of this process where the  $c_{l,max}$  is of the NACA 23012 airfoil and the shaded area is the additional lift distribution and is the total change that is propagated forward. This increase can be seen to propagate to the stall angle of 19°. It is at this angle that the wing has begun to exceed the  $c_{l,max}$  of the airfoil.

This process was done for the wing in inverted and normal flight for non-tapered and tapered wing planforms as part of a trade study to find the optimum taper ratio. The optimum taper ratio for the wing maximizes  $C_{L,max}$  whilst still trying to keep the stall location as inboard as possible to try to avoid stalling where the ailerons are located. This ensures that the pilot will be able to retain control of the aircraft even when wing has begun to stall.

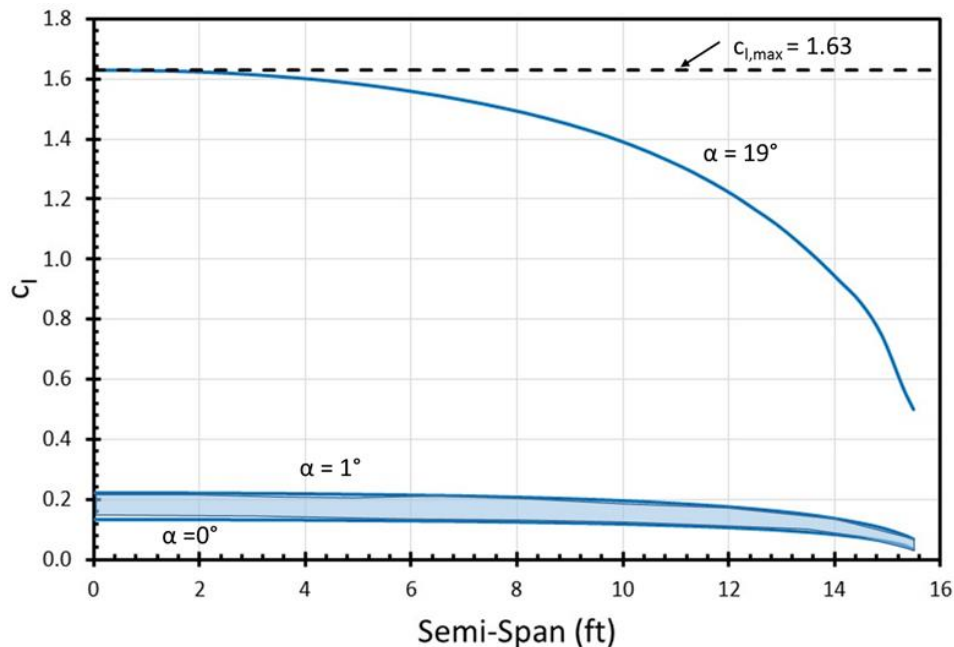


Figure 17: Lift Distributions for NACA 23012 Airfoil. Shaded region is the additional lift distribution

The resulting lift distributions and values are seen in and Figure 18 and Table 7. As the wing becomes more tapered, the lift distribution of the wing begins to shift from purely elliptical to more evenly distributed. The stall point of the wing starts to move outboard and the wing starts to stall closer to the tip.

In Figure 18, the dashed line across the top represents the  $c_{l,max}$  of the NACA 23012, and the filled circles

Table 7: Varying Taper Ratios

Taper Ratio	Stall Location (% span)	$C_{l,max}$
1.00	0.0%	1.38
0.82	24.4%	1.45
0.75	32.0%	1.46
0.50	52.3%	1.48

along this line represent the location that that specific taper ratio began to stall. As expected, the lift distribution plot shows that as the wing begins to taper, the stall location moves away from the root. The taper ratio of 0.82 was found to have the highest  $C_{L,max}$  value whilst still avoiding stalling near the ailerons. This line, shown in red, more evenly distributes the lift across the span when compared to the standard elliptical lift distribution. This yields a

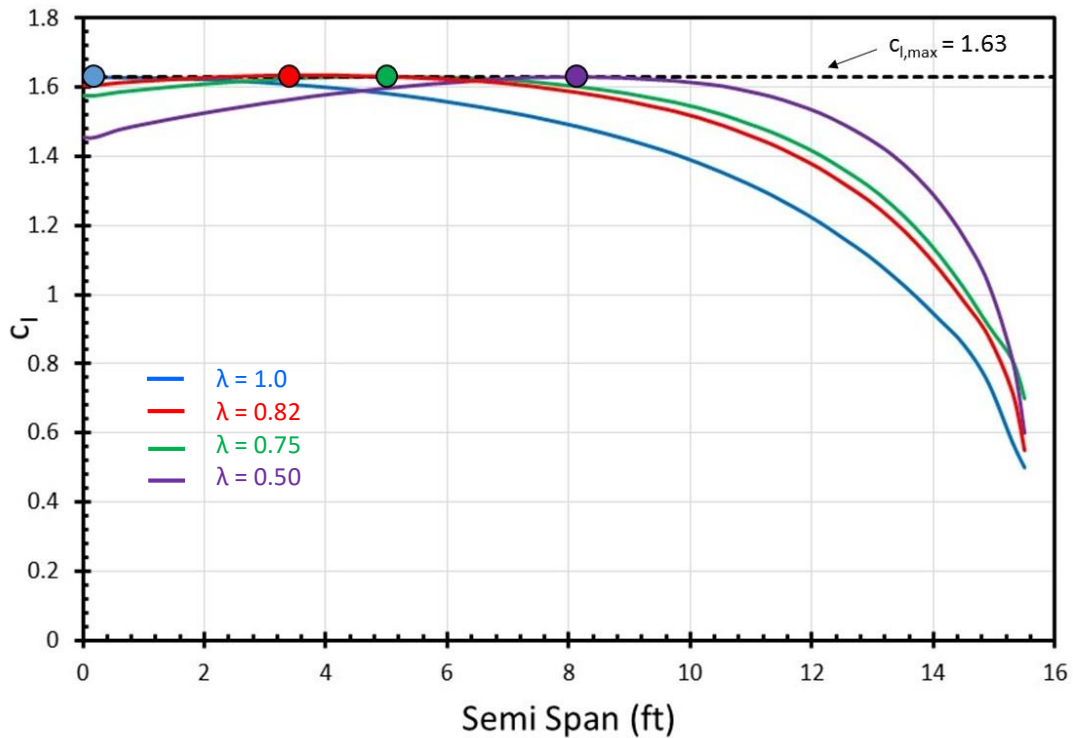


Figure 18: Comparison of Various Taper Ratios



$C_{L,max}$  value of 1.45 . This taper ratio begun to stall at 24.4% of the span, and the root of the aileron begins at 38.7% of the span, resulting in 2ft of clearance between stall location and control surface.

The inverted lift distribution shows the tapered wing for inverted flight in Figure 19. The tapered wing had a  $C_{L,min} = -1.09$ . From this  $C_{L,min}$  value and the wing loading of both aircraft, an inverted stall speed of 45.3 KCAS can be backed out. This speed is much lower than standard aerobatic maneuvers, so this wing should be more than sufficient at sustaining inverted flight for at least five minutes as stated by the RFP.

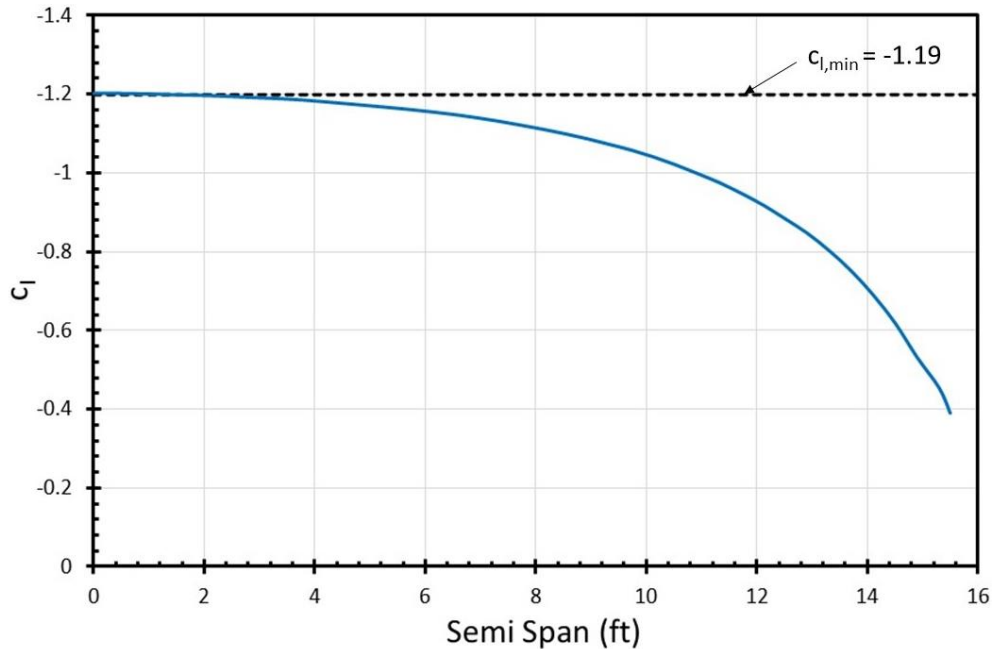


Figure 19: Inverted Lift Distribution

### 6.3 DRAG ESTIMATION

A form factor method is used to complete a drag buildup for both aircraft.<sup>21</sup> This method involves a series of analytical equations which account for each component’s contribution to the total drag of the aircraft and is a common, widely accepted method of calculating the zero-lift drag coefficient. The drag build-up is done at an altitude of 3000 feet MSL for a speed of 168ft/s (115 KCAS). The skin friction coefficient ( $C_f$ ) is found using Reynolds number at that speed and then calculated for an assumed turbulent boundary layer from Schlichting’s equation for skin friction coefficient. Form factors for the fuselage are found using the largest diameter and the length of the aircraft, and form factor for the wing is found assuming a thickness to chord ( $t/c$ ) ratio of 0.12 which corresponds to the NACA 23012 thickness to chord. The reference area ( $S_{ref}$ ) for Tempo and Encore is 143ft<sup>2</sup>, since commonality is maintained by keeping the wing area constant. The  $C_{D,0}$  for Tempo is 0.0201 or 201 counts and is

shown in Table 8. While the drag build-up for Encore is not shown in tabular form, it was found in a similar method to Tempo, and is 210 counts.

Table 8 shows the component breakdown of the contributing elements to the zero-lift coefficient of drag. The wing is the largest contributor to the  $C_{D,0}$  at 72 counts. The value for the  $C_{D,0}$  of the landing gear was estimated from Hoerner,<sup>22</sup> and sized for common LSA wheels, the dimensions of which were found from Grove Aircraft Landing Gear Systems Inc.<sup>23</sup> The wetted areas for each of the components is found by modeling both aircraft on VSP,<sup>20</sup> and obtaining the wetted areas from those models. Roughness of the surface is accounted for in this method where aluminum is the material. Interference factors are found for the wing/fuselage and horizontal tail/fuselage from Roskam's book, where he has suggested values for the interference based on Reynold's number. The miscellaneous drag is a conservative estimate on the  $C_{D,0}$  that is unaccounted for, including excrescence drag, cooling drag, and trim drag, and is roughly 25% of the base zero-lift coefficient of drag.<sup>24</sup>

Table 8: Drag Component Build-up for Tempo

Component	$S_{wet}$ - (ft <sup>2</sup> )	Characteristic Length (ft)	$\frac{t}{c}$ or $\frac{Len}{Dia}$	Reynolds Number (x10 <sup>6</sup> )	$C_f$	Form Factor	$C_{D,0}$
Fuselage	115	21	5.07	2.52	0.0023	1.47	0.0033
Wing ( $S_{ref} = 143 \text{ ft}^2$ )	275	31	0.12	4.96	0.0029	1.23	0.0072
Horizontal Tail	24	2.7	0.15	2.67	0.0031	1.23	0.0018
Vertical Tail	36	2.5	0.15	2.79	0.0032	1.23	0.0010
Landing Gear	0.36	5.25	~	~	~	~	0.0028
Miscellaneous	~	~	~	~	~	~	0.0040
$C_{D,0 \text{ tot}}$							0.0201

### 6.3.1 DRAG BUILDUP COMPARISON

The drag build-up method described above is checked by performing a drag build up on the Cessna 162 and 150. Since both of these aircraft are high-wing aircraft, the method was modified to account for the strut braces and the larger size of the aircraft. Dimensions for both aircraft were found on Cessna's website, and inputted into the drag build-up. Wetted areas were found using VSP and all these drag build-ups were done at 3000ft MSL and a speed of 115 KCAS.

$C_{D,0}$  for the Cessna 162 and 150 were found to be 245 counts and 242 counts respectively. For comparison, values for  $C_{D,0}$  were taken from a tabulation of zero-lift drag coefficients for general aviation aircraft.<sup>25</sup> The “actual” value for  $C_{D,0}$  for the 162 is reported to be 250 counts, making the error between the calculated and actual values 2%. The “actual” value for  $C_{D,0}$  of the Cessna 150 is reported to be 260 counts, making the error between the calculated and actual value 7%. A 7% error is acceptable for conceptual design, and the accuracy of the model is acceptable for the level of design work being executed.

### 6.3.2 DRAG POLAR

Once the drag build-up is completed at a certain altitude, it is possible to obtain a drag polar for the aircraft as seen in Figure 20. The induced drag for the aircraft is calculated with VSPAERO<sup>20</sup> which is a vortex lattice method. The drag polar for Tempo and Encore are both included in the figure; however, due to the high amount of commonality between the two aircraft, they essentially have the same drag polar. Negative values for coefficient of lift have been included to account for the inverted flight requirement.

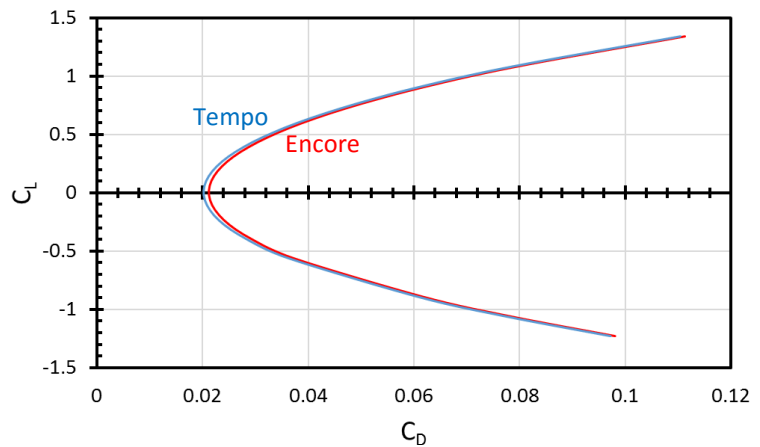


Figure 20: Drag Polar for Tempo and Encore

## 7 Propulsion

The design of the propulsion system is crucial to defining the performance capabilities of the aircraft. The main components in the propulsion system are the engine, which provides power, and the propeller, which converts engine power into thrust. The LSA ASTM International Standards<sup>2</sup> state that the aircraft may have no more than one reciprocating piston engine. This rule was created to prohibit the use of turbine engines from appearing on LSA, but also had the effect of limiting the potential use of electric or other experimental engine types. Additionally, the propeller must be either fixed pitch or ground-adjustable.

### 7.1 METHODOLOGY

There are several performance constraints defined in the RFP and the ASTM International Standards for LSA that influence the design of the propulsion system. The most notable of these constraints are the 1500fpm climb

rate requirement and the maximum cruise speed of 120 KCAS. These requirements pose a challenge, as the climb rate requirement demands a powerful engine while the maximum speed requirement limits engine power.

During the design of the propulsion system, the engine, propeller, or both can be specifically designed to try to meet the requirements. The engine must be certified with the ASTM Standards International or 14 CFR Part 33.<sup>26</sup> Any design work or changes made to the engine by Avem Dynamics would cause the engine to need to be recertified. Because of the extra cost and time necessary to undergo these certifications, Avem is electing to not make any changes to the chosen engine, but rather to use it as it would be provided by the manufacturer. Therefore, the propeller will be the major focus of design work in the propulsion system.

In order to not exceed the 120 KCAS limit, the system will be designed so that at 120 KCAS, the maximum thrust provided by the propeller is equal to the drag on the aircraft. This design should prevent the pilot from exceeding the limit, since at higher speeds the drag would be greater than thrust.

### **7.1.1 FIXED PITCH PROPELLERS**

Fixed pitch and ground adjustable propellers cannot be changed during flight, and therefore can only be optimized to absorb full engine power at a single point of the flight envelope. If the flight condition changes from that optimal point (i.e. different atmospheric conditions or airspeed), the propeller will be unable to absorb the maximum available power from the engine. With this system, the rotation speed of the engine is more directly related to thrust, as in general, increasing engine speed increases thrust.

## **7.2 ENGINE TRADE METHODOLOGY**

Because the LSA industry is still fairly new, very few LSA engines are certified, and only one commercially available engine below 150hp is capable of aerobatics. There do exist modifications and aftermarket parts for many LSA engines at lower power ratings that provide them with aerobatic capabilities. However, these changes and parts would require recertification of the engine. As mentioned in Section 7.1, Avem Dynamics is currently avoiding the need for engine certification due to the added time and cost. If an engine is not already certified, it is expected that the engine manufacturer would be willing to certify the engine given the number of engines to be purchased by Avem and would certify the engine by the entry into service (EIS) date of 2020.

## **7.3 ENGINE SELECTION**

Several LSA engines were viewed and compared by weight, maximum power, and power to weight ratio, as seen in Table 9 below. Cost was not taken into account due to the fact that engine prices often fluctuate after certification, and as some engines are not yet certified, a comparison could not be made.

In order to hopefully lower the engine acquisition cost, the same engine will be used in both aircraft. According to the constraint diagram, for the chosen wing area the design calls for an engine that can provide between 100 and 130 horsepower. Avem has chosen to use the Lycoming AEIO-233 engine. Although the Lycoming engine has a lower power to weight ratio, the decision ultimately came down to the fact that it is the only fully aerobatic engine in this power range. In addition to being capable of continuous inverted flight, it also has the highest time between overhaul (TBO), which is highly desirable for pilots.

Table 9: Engine Comparison

Engine	Weight (lbs)	Maximum Power (Hp)	Power to Weight	TBO (hours)	Aerobatic
ULPower UL350iS <sup>19</sup>	173	130	0.75	1500	No
Rotax 912 S <sup>20</sup>	141	100	0.71	2000	No
Rotax 914 F <sup>21</sup>	166	115	0.69	2000	No
Lycoming AEIO-233 <sup>22</sup>	200	116	0.55	2200	Yes
Rotec R2800 <sup>23</sup>	224	110	0.49	1000	No

## 7.4 PROPELLER MATCHING

The propeller design uses code from NASA CR 114289.<sup>27</sup> This code was originally written for NASA by Hamilton Standard, a propeller manufacturing company. The report specifies that there are five characteristics of a propeller that will define its performance. Given this set of characteristics, Hamilton Standard guaranteed to manufacture a propeller that met the promised performance.

### 7.4.1 PROPELLER CHARACTERISTICS

The five characteristics are: the number of blades ( $N_{blade}$ ), the tip diameter, the angle of each blade at  $\frac{3}{4}$  the length ( $\beta_{3/4}$ ), the activity factor (AF), and the integrated design lift coefficient per blade ( $C_{L,i}$ ). The code in the NASA report is able to take these five variables, as well as other parameters, such as flight conditions, and output the expected power and thrust that the propeller would provide. From the expected power and thrust, the propeller efficiency can be found.

### 7.4.2 PROPELLER DESIGN PROCESS

Figure 21 shows the general design process for the propeller. The code allows for each variable to vary within some range. Initially, the propeller characteristics are chosen by making an informed guess within these ranges and are run through the code to find the expected performance. That performance is combined with the

engine data and drag polar information in order to find the overall propulsion system performance. Next the system is checked to see if the climb rate and top speed requirements are met. If the requirements are not met with the current propeller, some adjustments are made to the initial guess and the loop is run through again. This process occurs until a working set of characteristics are found. As there are five separate input variables to this loop, the number of possibilities are extremely high. To find a working solution, an optimization function was utilized from the MATLAB optimization toolbox. This nonlinear optimization tool chose how to change the variables and was able to converge quickly to an acceptable set of propeller characteristics.

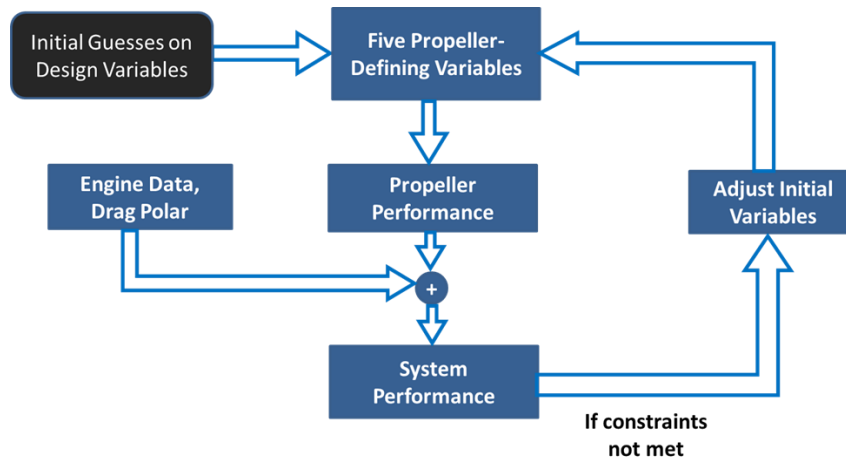


Figure 21: Propeller design process

### 7.4.3 PROPELLER PERFORMANCE

The set of characteristics found for the design are shown in Table 10. For a LSA, these characteristics are seemingly normal. LSA typically have between 2 and 4 blades on their propellers and a diameter between 4 and 6 feet. This propeller is similar to a climb propeller, which tend to have a high activity factor and low blade angle. These characteristics allow the propeller to absorb more power at lower speeds, but lowers efficiency at high speeds.

Table 10: Propeller Characteristics

Propeller Characteristics
$N_{blade} = 3$
Diameter = 5.1 ft
$\beta_{34} = 20.4^\circ$
AF = 126
$C_{L,i} = 0.3$

As mentioned in Section 7.1.2, fixed pitch propellers have a single flight condition in which they can absorb the maximum horsepower provided by the engine. This flight condition was designed to occur at the climb speed in order to maximize climb rate. For this propeller, that flight condition is at sea level, standard day conditions and with an airspeed of 67 KCAS. The curve of absorbable horsepower at this flight condition can be seen in Figure 22.

The blue curve is the propeller load line which represents the maximum power the propeller can absorb over a range of rpms, while the red curve represents the area in which the engine can perform. For the Lycoming AEIO-233 engine, the maximum power available is 116hp and the maximum rpm is 2800. As the speed is changed, the blue line would shift around, but this is the only point at which the propeller can absorb the full available engine power.

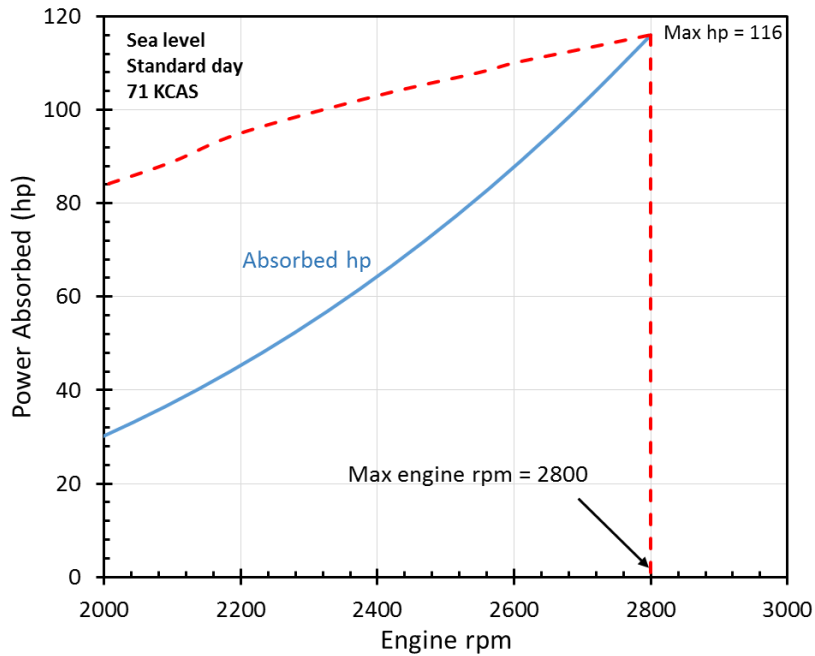


Figure 22: Optimal Propeller Load Curve

Given the specific constraints placed upon the design, the flight condition at which the propeller performance should be optimized is the maximum climb speed at sea level, standard day. This is because the climb condition requires the most power to be more competitive. Sea level standard day was chosen because it represents the optimal flight condition, ensuring that the maximum speed requirement could not be exceeded at any condition.

Figure 23 shows the propeller’s expected coefficients of thrust and power at varying advance

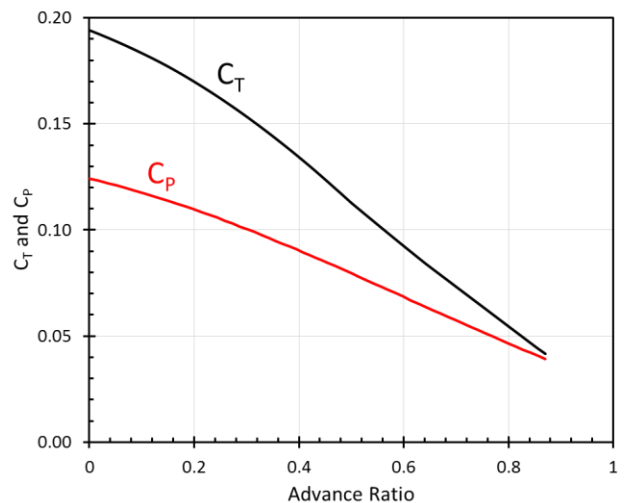


Figure 23: Thrust and Power at Varying Advance Ratios

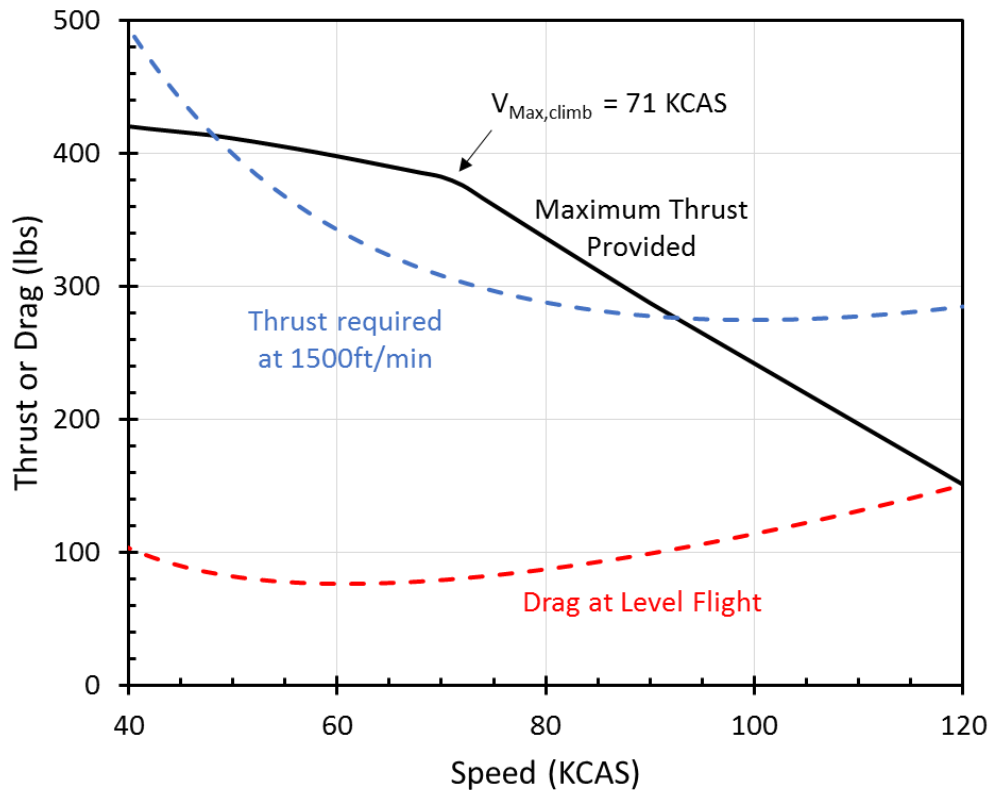


Figure 24: Maximum Thrust Performance

ratios. The advance ratio is the ratio between the freestream velocity and the propeller tip speed.

Using these chosen propeller characteristics, both the 1500fpm climb rate and the 120 KCAS maximum speed requirements were met, as seen in Figure 24. The red curve represents the drag acting on the aircraft at steady, level flight over a range of speeds from stall speed to the maximum allowed speed (39 KCAS to 120 KCAS). The blue curve shows the thrust that is required at any speed in order to climb at 1500fpm. The black curve shows the maximum thrust provided by the propulsion system. It can be seen that the aircraft is able to climb at higher than 1500fpm since the black curve passes above the blue curve. Additionally, the provided thrust drops down and is equal to the red curve at 120 KCAS. This decline means that at level flight, if the aircraft tries to go faster than 120 KCAS it will not be able to provide the required thrust to maintain that faster speed.

Figure 25 shows the how the system would perform when providing the maximum thrust over a range of speeds. The red curve shows how much horsepower the propeller can absorb, while the black curve represents the engine speed. It can be seen that at speeds slower than the maximum climb speed of 71 KCAS, the engine rpm and absorbed power rise together. At 71 KCAS the engine is providing the maximum power of 116hp at its maximum



rpm of 2800. At higher speeds, because the engine speed can no longer increase, the pilot would need to reduce the throttle in order to not over-rev the engine. This shows how the system is more powerful at lower speeds, allowing the climb rate to be met, but is also limited at higher speeds so as to not exceed the speed limit.

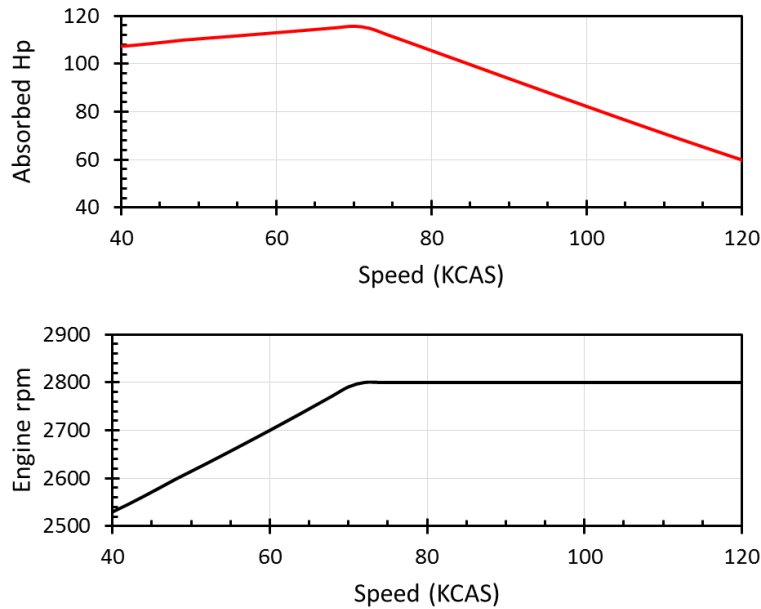


Figure 25: Engine Performance

Figure 26 shows how the overall propulsion system efficiency is found. The leftmost graph depicts the amount of usable power as a ratio of absorbed power over maximum power. The middle graph shows the propeller

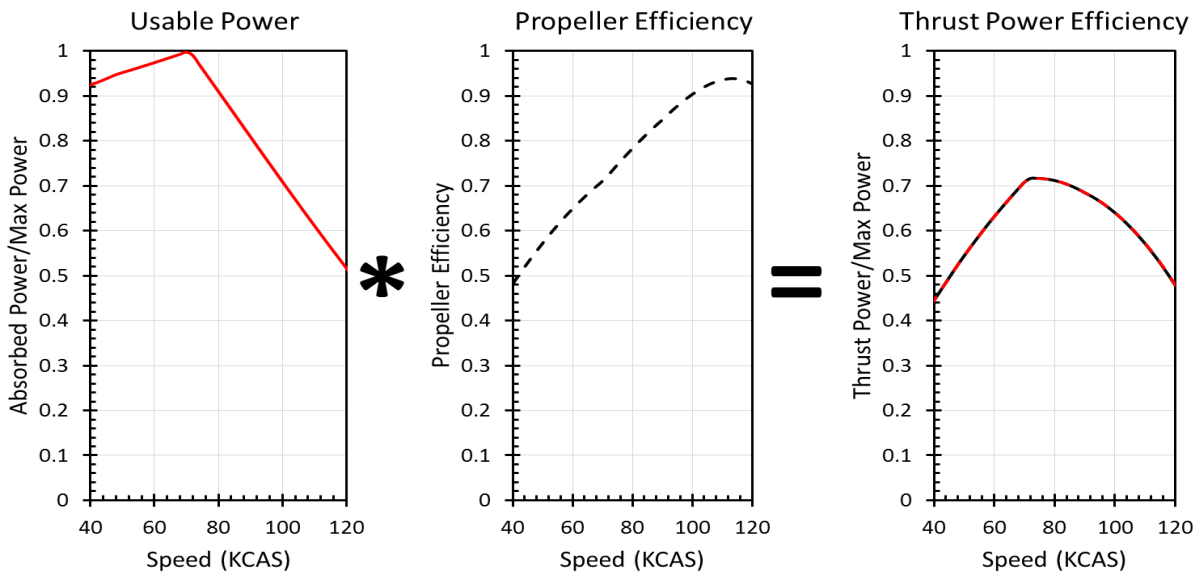


Figure 26: Overall Propulsion System Efficiency

efficiency. When these two graphs are multiplied together at each speed, the resulting graph, shown to the right, represents the amount of the maximum power can be converted into thrust by the propeller. This final efficiency becomes an input to the constraint diagram.

## 8 Structures

The structures of the aircraft are crucial to meet the desired maneuvering capabilities set forth by the requirements. Most of the structural analysis in conceptual design involves demonstrating strength capability of the aircraft at load limits and determining structural plausibility, such as demonstrating load paths. The loadings on the aircraft are accounted for in a V-n diagram and a feasibility analysis will be performed on the wing spar.

### 8.1 V-N DIAGRAM

The V-n diagram is generated to establish load requirements of the aircraft. From the RFP, Tempo must be designed to withstand flight loads of +6/-5g's, while Encore must withstand flight loads of +6/-3g's. The stall lines for Tempo are generated using a  $C_{L,max}$  of 1.45 and a wing loading of 7.52lbs/ft<sup>2</sup>, while the gust lines are generated using a  $C_{L\alpha}$  of 2.24 rad<sup>-1</sup>. The  $C_{L\alpha}$  of 2.24 rad<sup>-1</sup> was found by plotting the  $C_L$  for various angles of attack, which were calculated using VSPAERO, and finding the slope of the linear portion of the plot. The resulting maneuvering speed for Tempo is found to be 96 KCAS. Based on the upper and lower limits set on the design cruise speed in 14 CFR Part 23,<sup>26</sup> the design cruise speed for both aircraft is calculated to be 108 KCAS. Finally, Tempo has a dive speed of 154 KCAS, also calculated from 14 CFR Part 23. The V-n Diagram for Tempo can be seen in Figure 27.

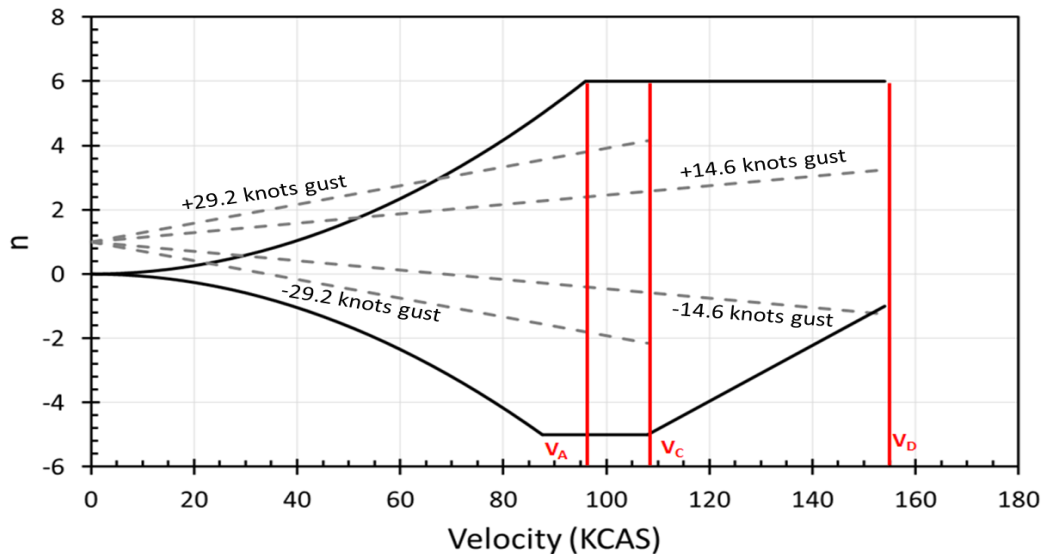


Figure 27: V-n Diagram for Tempo

The V-n Diagram for Encore can be seen in Figure 28, and closely resembles the V-n diagram for Tempo because both aircraft use the same wing, and therefore have the same  $C_{L,max}$  and  $C_{L\alpha}$ . There are two main differences between the V-n diagram for Tempo and for Encore. The first is that Encore only needs to withstand negative flight loads down to -3g's. The second difference is that Encore has a larger wing loading than Tempo because Encore weighs more than Tempo, but still using the same wing area. Encore has the same design cruise speed as Tempo, but the maneuvering speed is 105 KCAS and the dive speed is 168 KCAS.

Taking a closer look at the two V-n diagrams reveals a challenging point when it comes to maintaining commonality. Although both aircraft have similar limits on this diagram, since Encore is heavier, its structure must be stronger to withstand the forces and stresses. Therefore, to maintain commonality between aircraft, the structure of both aircraft must be based on the flight loads of Encore. The strength capabilities, and thus structural compliance, will be discussed in Section 9.

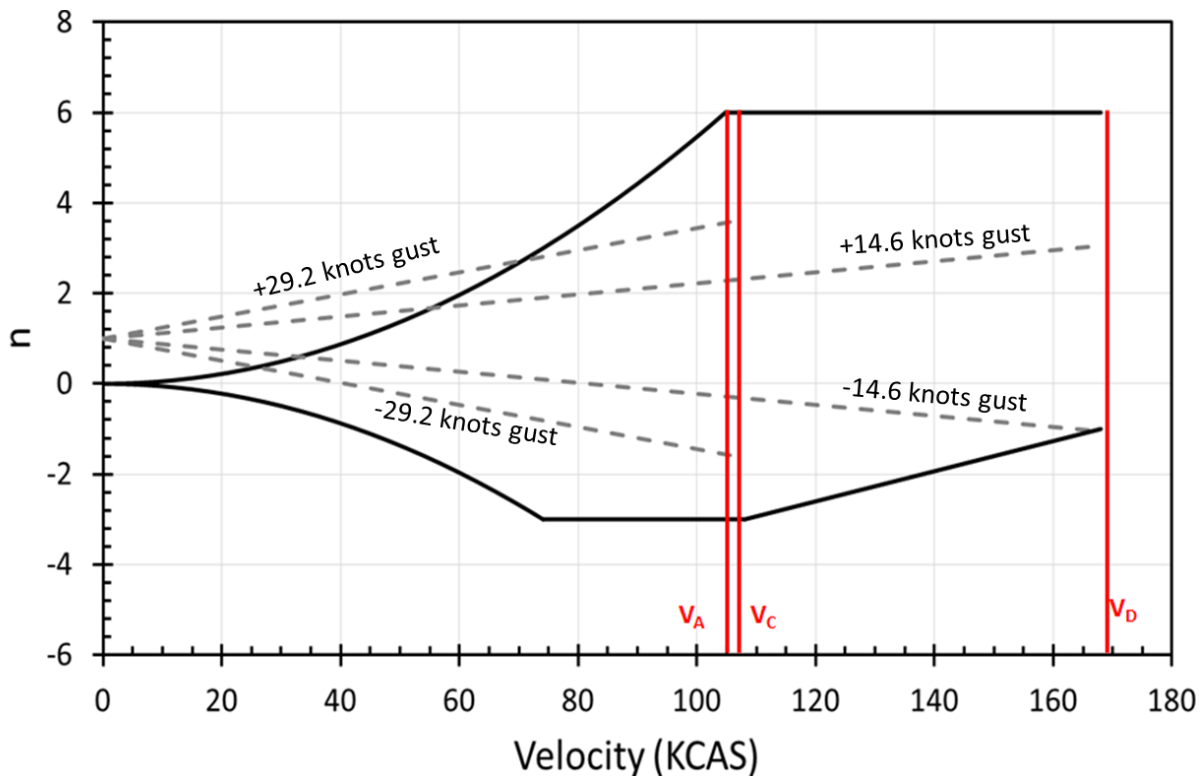


Figure 28: V-n Diagram for Encore

## 8.2 SPAR SIZING

A structural component that can be analyzed during conceptual design is the spar size and location. In order to demonstrate a plausible load path, the spar must be sized and the location of the spar carry through must be specified. It is assumed that the critical load which sizes the spar is the bending caused by a 6g maneuver in Encore (to maintain commonality). Additionally, the spar was sized by assuming it to be a rectangular beam. The lift distribution of the wing for a 6g maneuver was found using VSPAERO. The lift distribution was then integrated to find that the root bending of the wing equals 68,000ft-lb. The spar is placed at the maximum thickness location of 29.8% of the root chord for the chosen airfoil (NACA 23012). Because the airfoil has a maximum thickness of 12% of the chord, it is desired to demonstrate that this airfoil is thick enough to maintain structural compliance without a wide spar. The root chord of the wing is 5.075ft, which yields a root wing thickness of 7.3in at the maximum thickness of the airfoil. A yield strength of 60,000psi was used along with a factor of safety of 1.5. Using these numbers and the classic formula for determining bending stress in a beam:

$$\sigma = \frac{Mc}{I}$$

the root spar width was found to be approximately 0.130in, which is reasonable given the size and class of aircraft. The spar placement in the wing can be seen in Figure 29. With the spar sized, the carry through location was determined, and is specified in the inboard profile in Section 4.5.

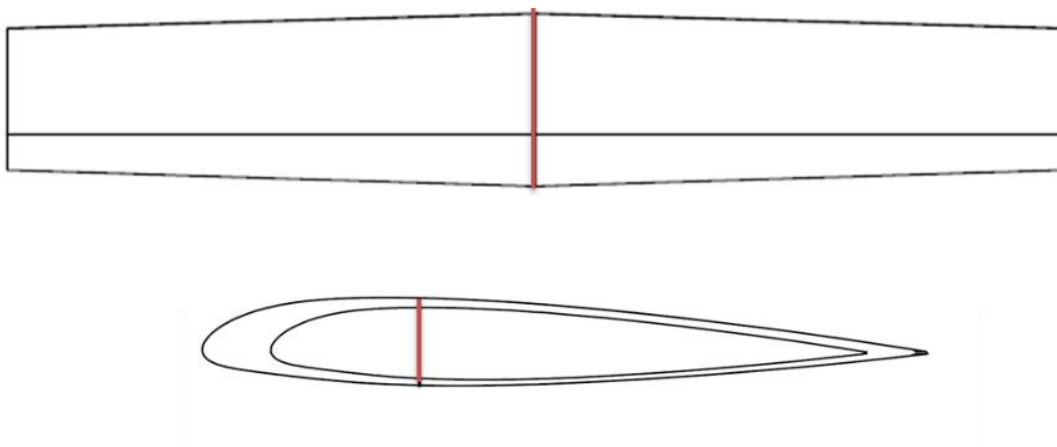


Figure 29: Spar Location in Wing

## 8.3 MATERIALS AND MANUFACTURING

### 8.3.1 MATERIAL SELECTION

Material selection is an important consideration when designing an aircraft due to the impact that the material has on both the geometry that can be implemented and the manufacturing process. Aluminum and composites are the two most common materials used in LSA and their advantages and disadvantages are taken into account in this section. Avem Dynamics did not consider the used of wood and fabric as a potential material due to the fact that the design team is looking to build a sleek, modern family of aircraft.

Aluminum has certain advantages over composite materials and Avem Dynamics has decided that those advantages justify its use over more modern composite materials. Aluminum, such as 2024-aluminum, is widely used in the light aircraft industry due to its high strength to weight ratio, its fatigue resistance properties, and its ability to resist corrosion. The most persuasive argument for manufacturing with aluminum is that it has high familiarity since it has long been used in the aircraft industry. The Avem Dynamics could take advantage of the knowledge about aluminum that is so widely available and apply that to the LSA family. Another inherent advantage of aluminum is that it is more conductive than composites so any static buildup that occurs on the airplane can be easily discharged with no modification of the material. Generally, the raw material and manufacturing cost of aluminum will be less than carbon composite.

Manufacturing must be taken into consideration before selecting a material since material selection has a major impact on the type of labor and facilities required for production. Aluminum manufacturing could be advantageous since it does not require the purchase of an autoclave which could be an expense of millions of dollars. Since the aesthetics of the airplane are an important consideration, aluminum could potentially have a disadvantage because of the difficulty in shaping aluminum into compound curvature. However, it has been shown in the past with airplanes such as the P-51 that it is possible to make an aesthetically pleasing aircraft with aluminum. As shown in Figure 30 the geometry of the Tempo and Encore share some similarities to the P-51, particularly in the wing, tail, bubble-style canopy and narrow fuselage. Components of Tempo and Encore such as the wing and empennage will be easily made with aluminum due to their minimum compound curvature. It is expected that the parts of the aircraft with compound curves, such as the fuselage and canopy, could be manufactured with aluminum but with less ease.

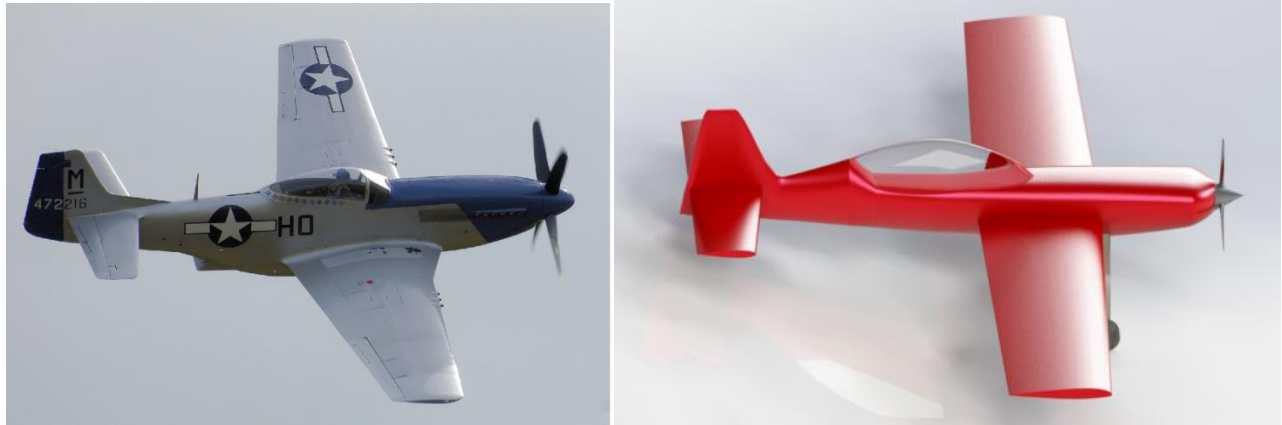


Figure 30: Tempo Shares Geometric Similarities with P-51 (also made of aluminum)

In larger airplanes, skin thickness would be driven by aerodynamic and structural loads. It is likely that the aerodynamic and structural forces that Tempo and Encore experience will be less of a driving factor in sizing the skin thickness than minimum gauge requirements. Therefore, the difference in weight between composite and aluminum will likely be insignificant in an aircraft of size. Additionally, based on the preliminary cost models, an aluminum aircraft is less costly to build, discussed further in Section 12. It is estimated that if Encore is constructed with aluminum it will cost \$82,650 to build; whereas, it would cost \$102,000 if Encore was constructed with composite materials. The cost of the raw materials for aluminum is significantly lower than composites, so in order to make a 10% profit, as the RFP states, Tempo's selling price would be approximately \$120,000 for an aluminum aircraft or \$170,000 for a composite aircraft. Assuming that the performance of the aircraft does not change based on material, customers will be more inclined to purchase a cheaper aircraft.

### 8.3.2 MANUFACTURING

The current LSA market indicates that it is reasonable to expect Avem Dynamics to sell approximately 4 aircraft per month. This number of projected sales combined with the inherent simplicity of the aircraft means that it will be the most cost effective to manufacture the aircraft primarily by hand and to minimize the amount of costly, automated machinery.

It is vital to consider the producibility of an aircraft in conceptual design. This was done by maximizing simple geometric shapes with straight edges and square corners when reasonable. To reduce cost, it is also helpful to minimize the number of major structures. The Tempo and Encore were designed with commonality as a main objective and therefore have several identical components such as the wing, vertical tail, landing gear, and most of the fuselage. As stated in Section 8.3.1, the structure of the Tempo and Encore will be built predominantly with

aluminum. The geometry of the fuselage supports the use of a semi-monocoque structure which is the preferred structure for an all-aluminum fuselage. A series of frames in the shape of the fuselage cross sections, or jig, will be made from 2024-aluminum tubing and joined with stringers to provide longitudinal rigidity. Skin made from 2024-aluminum sheet metal satisfying minimum gage can be shaped to wrap around the structural support tubes and riveted to the frame by a machinist. Many small aircraft companies utilize water jet cutters to cut precisely fitting pieces such as the wing ribs and an instrument panel frame. Automated water jet cutting can be programmed to cut many different parts with high precision and repeatability. This will be more cost effective than making tooling specific to each part. Investing in a water jet cutter will lower the long term manufacturing cost.

Since Avem will be selling fully assembled aircraft and not kit-built planes, facilities required for manufacturing will need to be large enough to support a small assembly line of aircraft. ALCOA is the world's third largest producer of aluminum and its operational base is in Pittsburg, Pennsylvania. They are a highly reputable company whose products are used by many aerospace companies worldwide, including Airbus and Pratt & Whitney. Shipping costs can be reduced by setting up a manufacturing facility in a location near ALCOA's main facility.

## 9 Mass Properties

According to FAA and ASTM International standards, LSA cannot exceed a maximum gross takeoff weight of 1,320lbs. The airframe weight of the Tempo and Encore includes the wing, empennage, and fuselage of the aircraft and is determined based on a model developed by Avem Dynamics. The remaining weights are based on a detailed weight breakdown from K.D. Wood's aircraft design book<sup>28</sup> and supplier information for various components. This approach to weights was chosen since there is little to no common weight model specifically for LSA and to gain an accurate understanding of the total weight of the aircraft, a new method must be created.

### 9.1 METHODOLOGY

The most relevant publicly available weight models for LSA are made for the general aviation category of aircraft. Since this category includes a large range of aircraft from gliders to business jets, a more relevant model was developed based on light sport aircraft.

Unfortunately, complete weight breakdowns for aircraft as small as LSA are limited. The five aircraft, the Cessna 150, 172, 175, 180, and 182, from K.D. Wood's design book,<sup>28</sup> make up the dataset used to develop the airframe weight models and will be referred to as the Cessna dataset. All of these aircraft are single engine, propeller driven, strut-braced, high wing aircraft with gross takeoff weights ranging from 1,500 to 2,650lbs. This dataset is

then compared to another dataset of aircraft, created from the Aerocrafter Kit Airplane Catalog,<sup>29</sup> which includes the P96 Golf, EV-97 Eurostar, KP-2U Sova, Midget Mustang, Mustang II, Storm 300 Special, and Sonex Onex. This dataset will be referred to as the comparison dataset. The range of gross takeoff weights for this dataset is from 950 to 1,600lbs and are comprised of single engine, propeller driven, low or mid wing monoplanes that have aluminum airframes. The gross takeoff weight, empty weight, and the engine names are listed in the Aerocrafter Catalog,<sup>29</sup> but it does not include a component weight breakdown for the seven aircraft. The comparison of the two datasets is done based on the empty weight of the aircraft without the engine.

The comparison dataset is used to adjust the results of the Cessna dataset to better estimate the weight of light sport aerobatic aircraft. The aircraft from the Cessna dataset are much larger, have strut-braced high wings, and different fuselage designs when compared with Tempo and Encore; however, the Cessna dataset is used because of the detail in its weight breakdown. The comparison dataset is necessary to account for the mentioned differences. The aircraft that comprise the comparison dataset were chosen based on their similarity, design, and material to Tempo and Encore. These changes to the Cessna dataset improve the accuracy of the weight models.

The remaining component weights are based on actual weights. These weights are taken directly from the Cessna 150 in K.D. Wood's design book or from supplier information. The landing gear, avionics systems, and the battery are the only weights based on supplier information with the supplier for landing gear being Grove Aircraft Landing Gear Systems Inc,<sup>23</sup> the supplier for the avionics system being Garmin,<sup>30</sup> and the battery supplier being Concorde Batteries<sup>13</sup>.

### 9.1.1 WING

The wing weight of the aircraft is based on a linear equation with two inputs, the skin and the spar weights. The wing weight equation is of the form:

$$W_{\text{wing}} = k_1 W_{\text{skin}} + k_2 W_{\text{spar}} + k_3$$

The skin thickness is approximated as 0.025in as discussed in Section 8, small aircraft skin thicknesses is often limited by minimum gage rather than structural constraints. The minimum gage skin thickness for light aircraft is between 0.015 and 0.025in,<sup>28</sup> with the higher end of this range chosen to provide a more conservative estimate. The total skin area is approximated as 2.02 times the wing area. Because the ailerons are included in the wing area, the aileron weight is counted as part of the skin weight. This skin volume is then multiplied by the skin density to yield the skin weight input into the wing weight equation with a skin density of 0.095lbs/in<sup>3</sup> (density of aluminum).



The semi-span spar weight was approximated as a rectangular cantilever beam and then doubled for the total spar weight. The spar length is half the wingspan and the spar height is calculated with thickness-to-chord of the wing at the root. The thickness of the cross-section is calculated based on the wing loading and the material yield strength with a triangular load placed on the wing. The total wing loading is equal to the product of the design gross takeoff weight of the aircraft (1,320lbs), the g-loading (6g's), and the factor of safety (1.5). The 6g loading is based on the V-n diagram as described in (Section 8.1). The yield strength is set equal to 60ksi with a factor of safety of 1.5. With the spar thickness approximated, the volume of the spar could be calculated and spar weight is found by multiplying spar volume by the density of aluminum.

The three k values used in the wing weight equation are constants that are varied to fit the datasets and will be referred to as  $k_{w1}$ ,  $k_{w2}$ , and  $k_{w3}$ . The three  $k_w$ s values are determined based on a least squares fit of the wing weight of the Cessna dataset. The comparison of the calculated wing weights and the actual wing weights can be seen in Figure 31. After the k-constant are determined,  $k_{w3}$  is adjusted to better match the comparison dataset. Note that the skin, internal structure, ailerons, and hardware are all accounted for in this model.

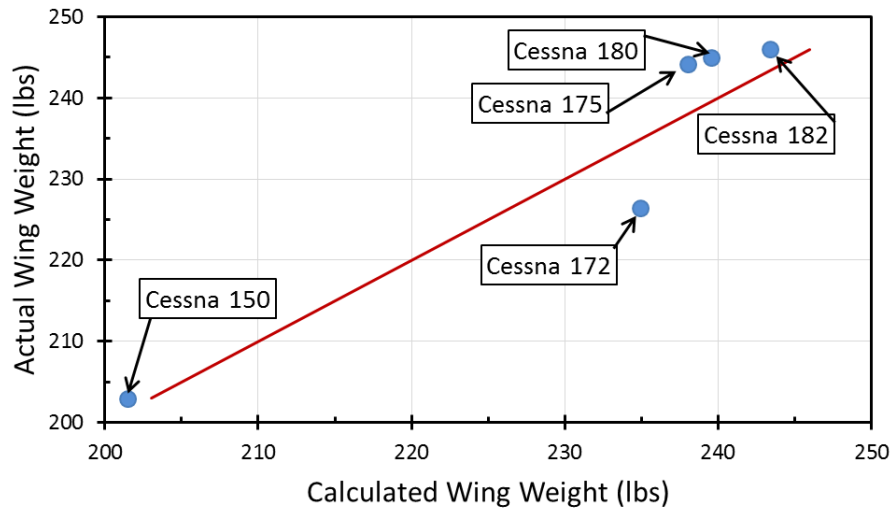


Figure 31: Wing Weight Linear Fit to Cessna Dataset

### 9.1.2 EMPENNAGE

Both the horizontal and vertical tail weights are modeled in the same manner as the wing weight and accordingly the empennage weight equation follows the same form as the wing weight equation. The elevator and rudder weights are included in the horizontal and vertical tail weights with a density of  $0.0951\text{lb/in}^3$  and a yield strength of 60ksi used since aluminum is the selected material. Like with the wing weight, the horizontal and

vertical tail constant ( $k$ ) values are determined from a linear fit of the Cessna dataset and will be referred to as  $k_{h1}$ ,  $k_{h2}$ , and  $k_{h3}$  for the horizontal tail and  $k_{v1}$ ,  $k_{v2}$ , and  $k_{v3}$  for the vertical tail. Figures 32 and Figure 33 compare the calculated horizontal and vertical tail weights to the actual horizontal and vertical tail weights from the Cessna dataset. To fit the comparison dataset  $k_{h3}$  and  $k_{v3}$  are varied. Note that the model accounts for the skin, internal structure, control surfaces, and hardware.

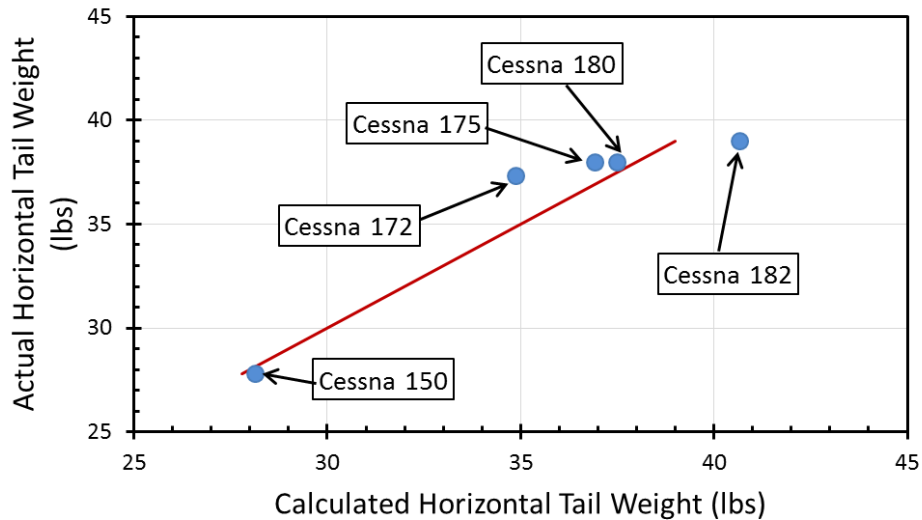


Figure 32: Horizontal Tail Linear Fit to Cessna Dataset

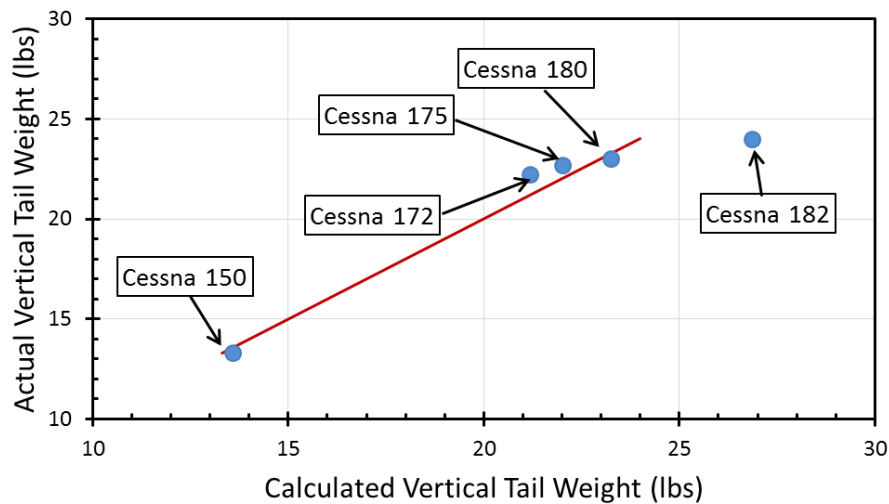


Figure 33: Vertical Tail Linear Fit to Cessna Dataset

### 9.1.3 FUSELAGE

Like the wing and the empennage, the fuselage weight is calculated with a similar equation that is a linear fit with two inputs, the skin weight of the front fuselage and the skin weight of the rear fuselage. The shape of the

front fuselage is assumed to be a half cylinder and the rear fuselage is assumed to be a cone without the tip. The maximum width of the fuselage is used as the base circles of the cylinder and the cone

A skin thickness of 0.025in is used with the internal structure of the fuselage being made up of stringers and ribs. The stringers are assumed to have a one-inch by one-inch square cross section, are placed one foot away from each other, run the length of the fuselage, and are made of aluminum. The placement of the stringers ensures that one stringer will run across each square foot of skin, and so the stringer volume is spread evenly over the entire skin area. The stringer thickness is 0.083in, with the fuselage skin weight being the sum of the fuselage skin thickness and fuselage stringer thickness multiplied by density, as described earlier.

A fourth set of constant (k) values, referred to as  $k_{f1}$ ,  $k_{f2}$ , and  $k_{f3}$ , are determined for the fuselage weight mode and are based on a least squares fit of the fuselage weight from the Cessna dataset. The calculated fuselage weight is compared to the actual fuselage weight in Figure 34. The constant (k) value,  $k_{f3}$ , is varied to better fit the comparison dataset.

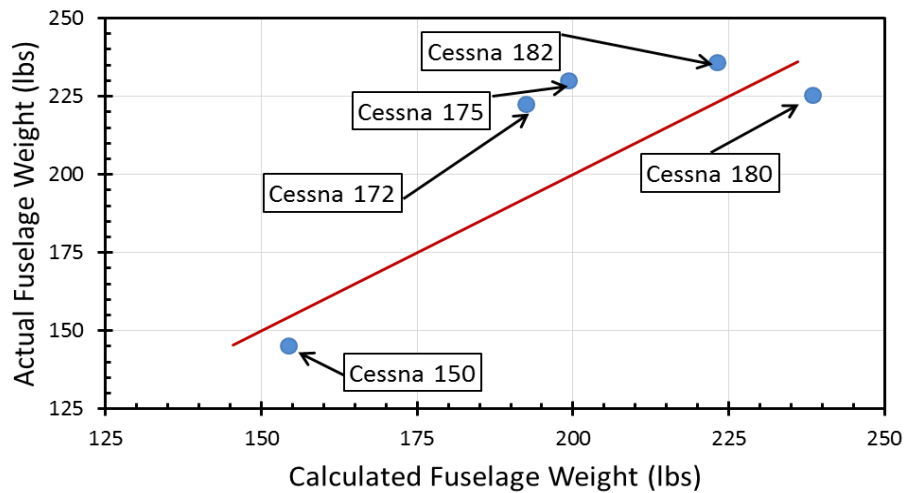


Figure 34: Fuselage Linear Fit to Cessna Dataset

The inputs to the fuselage weight model are the fuselage length and the maximum fuselage width, and note that the skin, internal structure, and hardware are accounted for by this model. The canopy, floorboard, instrument panel, and baggage door weights are added to the weight determined by the developed model. These three weights are taken directly from the Cessna dataset.

#### 9.1.4 SYSTEMS

The systems weight includes the electronics, avionics, and controls systems. The controls system weight which includes the cockpit controls, cables, and pulleys is nearly the same for all of the aircraft in the Cessna dataset, therefore these weights are used exactly. The control surface weight is approximately 20lbs and the cockpit control is 5lbs per pilot. The electronics weight includes the battery, battery box, generator, and wiring, and with the exception of the battery, these weights are taken directly from the Cessna dataset. The same battery is used in both aircraft and weighs 13lbs which is taken from the Concorde Battery database.<sup>13</sup> The avionics system used is the Garmin G300<sup>30</sup> avionics system which consists of two screens weighing 2.5lbs each for a total weight of 5lbs per pilot.

#### 9.1.5 FURNISHING

The furnishings weight is taken directly from the Cessna dataset, which includes the seats, seatbelts, seat mounts, and carpet. The seat, seatbelts, and seat mounts weigh 12.5lbs per seat for a total furnishings weight for Tempo of 15lbs and for Encore of 27.5lbs.

#### 9.1.6 LANDING GEAR

The landing gear system weight includes the gear springs, wheels, tires, axles, hydraulic brakes, brake pads, steering, and additional hardware. The hydraulic brakes weight, brake pads, and steering weights are taken directly from the Cessna dataset. The remaining weights come from Grove Aircraft Landing Gear Systems Inc<sup>23</sup> who design, manufacture, and sell landing gear by component. Using Grove's part catalog, a complete landing gear is put together for Tempo and Encore and is 62lbs.

### 9.2 WEIGHT SUMMARY

With weight model complete, it was used to determine the weights of the Tempo and Encore. The component weights of the two airplanes can be seen below in Table 10. Neither of the airplanes exceed the maximum gross takeoff weight of 1320lbs.

### 9.3 COMMONALITY

As previously mentioned, one of the objectives for the aircraft family is to be 75% common by weight without the propulsion system. In order to meet this objective, a number of components must remain the same for both aircraft. The empty weight of the two aircraft without the propulsion systems are 430lbs and 460lbs for Tempo and Encore, respectively. The components that are exactly the same on both aircraft are the wing, vertical tail, landing gear, and the electronics system. The combined weight is 237lbs for both aircraft. The components that are

Table 11: Component Weight Breakdown

Component	Tempo Weight (lbs)	Encore Weight (lbs)	Tempo Longitudinal CG Location (ft)	Encore Longitudinal CG Location (ft)	
<b>Wing</b> (Internal Structure, Skin, Ailerons,)	155		5.75	5	
<b>Empennage</b>	40	42	-		
Horizontal Tail (Internal Structure, Skin, Elevator)	26	28	19.7		
Vertical Tail (Internal Structure, Skin, Rudder)	14	14	20.7		
<b>Fuselage</b>	128	128	11	8	
Internal Structure and Skin	108.5	102	“	“	
Canopy	13	18			
Floor Boards	3				
Instrumental Panel	1.5	3			
Baggage Door	2				
<b>Propulsion</b>	267		-		
Engine	213		2.6		
Air Intake System	3				
Exhaust System	9				
Cooling System	3				
Fuel System (Fuel Tanks, Plumbing)	12		7.75	7	
Engine Controls	2		2.6		
Starting System	5		0.6		
Propeller System (Propeller, Propeller Mounts)	20		0.6		
<b>Nacelle</b>	23		2.61		
Cowling	9		“		
Firewall	5				
Engine Mounts	7.5				
Miscellaneous	1.5				
<b>Landing Gear</b>	62		-		
Front Gear Springs	32.2		5.7	5.24	
Front Wheels and Tires	14				
Rear Gear Spring	5		21.7		
Rear Wheels and Tires	4				
Axles	0.8		-		
Hydraulic Brakes	2.5		-		
Brake Pads	0.5		-		
Steering	2		0.6		
Miscellaneous	1		-		
<b>Avionics</b> (Avionic Panels, Navigation, Instruments)	5	10	10	6.0 (front seat)	8.9 ( rear seat)
<b>Pilot Control Instruments</b>	25	30	-		
Cockpit Controls	5	10	10.8	6.8 (front seat)	9.7 ( rear seat)
Cables and Pulleys	20	20	14	11.1	
<b>Electrical Group</b>	22		-		
Battery	13		17.2	4.2	
Generator	7				
Wiring	0.5		-		
Power Control	0.5		-		
Lights	1		5.75	5	
<b>Furnishings</b>	13	26	11.7	8.85 (front seat)	11.4 ( rear seat)
Seating Assembly (Seats, Seating Mounts)	12	24	“	“	
Generator	0.5	1			
Wiring	0.5	1			
<b>Empty Weight</b>	740	765	6.77	6.29	
Fuel	72		7.75	7	
Crew	230	400	11.7	8.1 (front seat)	10.6 (rear seat)
Parachute	15	30			
Baggage	30		13.5	13.5	
<b>Gross Takeoff Weight</b>	<b>1087</b>	<b>1297</b>	<b>7.51</b>	<b>7.04</b>	

added due to the second pilot in Encore but are still “common” between both aircraft are the avionics, controls, and furnishings and weighs 161lbs for Tempo. The uncommon components are the canopy and horizontal tail which make up 32lbs of the empty weight for Tempo. Commonality is calculated by dividing the weight of completely common components by the weight of the uncommon components. Tempo and Encore are 92% common by weight without the propulsion system.

## 10 Stability and Controls

This section discusses the stability and control analysis for both Tempo and Encore. The method used for calculating the center of gravity placement includes considering all the different combinations of varying payloads and determining how these combinations affect the stability of the aircraft. Longitudinal stability is determined based on static margin for both aircraft to size the horizontal tail and a trim analysis is completed to size the elevator. Directional stability is determined by appropriately sizing the vertical tail. The rudder is sized by taking into consideration various constraints such as spin recovery, crosswind landing, and coordinated turn. Spin recovery is investigated in more depth to ensure that the aircraft comply with the FAA Fars Part 23.221.<sup>31</sup> The aileron is sized to ensure compliance with the roll rate requirement in the RFP as well as providing the necessary maneuverability for a competitive aerobatic aircraft.

### 10.1 CENTER OF GRAVITY

Once the weights of the aircraft are established the center of gravity, CG, is estimated using the longitudinal CG location of each component. First, the fixed components CG are located and then the removable, varying payloads are placed in order to find the smallest possible shift in CG. A loading diagram is generated for the multiple cases determined by considering all the conservative combinations of the varying payloads, including maximum and minimum weight of the people, fuel, and baggage, which is shown in Table 12. For Tempo the

Table 12: Varying Payload Weights for Tempo and Encore

	Maximum Weight (lbs)		Minimum Weight (lbs)	
<b>Pilot (Tempo)</b>	230		120	
<b>Pilot (Encore)</b>	Front 200	Rear 200	Front 0	Rear 120
<b>Fuel</b>	72		0	
<b>Baggage</b>	30		0	

maximum weight of the pilot is 230lbs and a minimum weight is 120lbs. The maximum pilot weight for Encore is 400lbs (two pilots weighing 200lbs each) and the minimum weight is set by considering the case where one pilot, weighing 120lbs, is flying in the rear seat. The minimum pilot weight is chosen to be nonzero because the aircraft requires a pilot to fly. The maximum weight of the fuel for both Tempo and Encore is 72lbs which accounts for 12 gallons of fuel, while the baggage has a maximum weight of 30lbs.

Due to the placements of the payloads as shown previously in Section 9.2, the most forward CG limit for Tempo is with the minimum pilot and no fuel or baggage, and is located 7.05ft back from the tip of the spinner. The most aft CG limit for Tempo is with

maximum pilot, maximum baggage and no fuel, and is located 7.96ft from the tip of the spinner. These cases are shown in the loading diagram for Tempo in Figure 35.

The same type of analysis is done for Encore. The forward CG limit is set by the same scenario as Tempo, minimum pilot, no fuel and no

baggage, and is located 6.59ft from the spinner. However, due to the different wing locations the fuel location changes, causing the aft CG limit for Encore to be defined by a different scenario. The aft CG limit is defined by maximum pilots, fuel, and baggage, and is at a distance of 7.48ft back from the tip of the spinner.

Figure 36 shows the loading diagram for Encore. The loading diagrams are

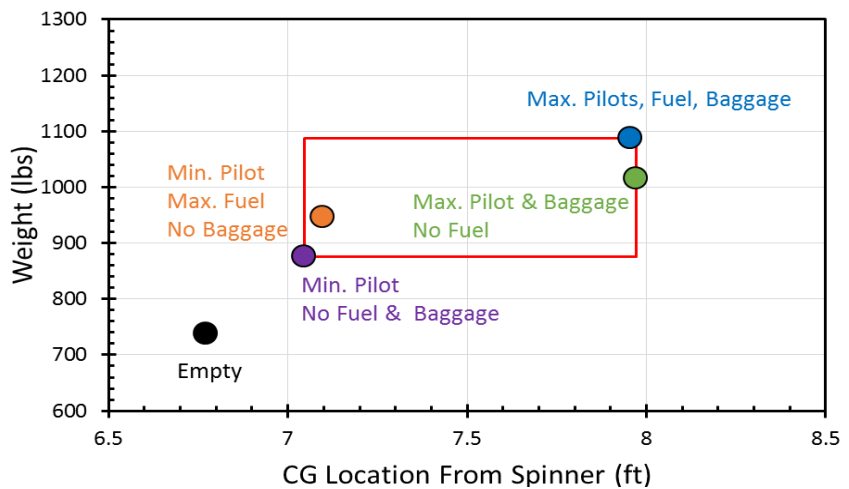


Figure 35: Loading Diagram for Tempo

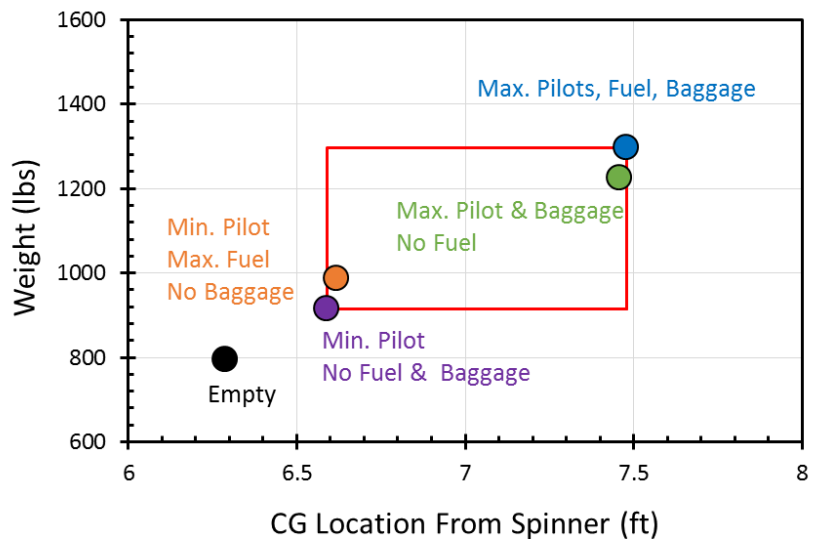


Figure 36: Loading Diagram for Encore

used to size the empennage and control surfaces, described later throughout this section.

The travel of the CG for both aircraft is 1 foot, which is 22% of the mean aerodynamic chord. The varying payloads are placed in such a way to minimize CG travel. The largest factor in CG travel is the variance in pilot weight, which accounts for a quarter and a third of the total weight for Tempo and Encore, respectively. After CG travel is minimized, the wing is placed so that the location of the aerodynamic center (AC) produces a static margin described in Section 10.2

## 10.2 LONGITUDINAL STABILITY

The horizontal tail is sized by using Roskam's X-plot method<sup>32</sup> and Athena Vortex Lattice (AVL).<sup>33</sup> The horizontal tail geometry is sized to meet an acceptable static stability. AVL is used to determine the horizontal tail area by varying the area until the desired static margin is achieved. Then the results are depicted using Roskam's X-plot method. The X-plot method requires finding the AC and CG as a function of horizontal tail area with the difference between the two lines corresponding to the static margin at different horizontal tail areas.

For light sport aircraft, it is typical to have a shift in most forward and aft CG location static margin of 20-25%.<sup>32</sup> This allows the aircraft to refrain from becoming too stable or unstable within the range of CG limits. For aerobatic aircraft static margin is important when performing maneuvers; the aircraft cannot be too stable or else the aerobatic maneuvers cannot be performed adequately, and for safety reasons the aircraft cannot be too maneuverable. Therefore, for conceptual design the static margin for the most aft CG limit was chosen to be 12% and 14% of the mean aerodynamic chord (MAC) for Tempo and Encore, respectively. After more in-depth wind tunnel testing, these numbers will be refined. Since Tempo is meant to be competitive in intermediate aerobatic competition, the smallest static margin is used when sizing the horizontal tail to obtain the most maneuverable aircraft. Due to the desired aerobatic training objective for Encore, the static margin is slightly higher to allow for more control during the maneuvers.

Figure 37 depicts the X-plot for Tempo with a static margin of 12%, resulting in a horizontal tail area of 30ft<sup>2</sup>. Figure 38 depicts the X-plot for Encore with a static margin of 14%, resulting in a horizontal tail area of 32ft<sup>2</sup>. To ensure that the shift in static margin is within the reasonable range, the static margin was calculated for the forward CG limit using the calculated horizontal tail areas. This results in a static margin of 34% and 36% of MAC for Tempo and Encore, respectively. Thus, the shift in static margin for the two aircraft are 22% which lies within the range of 20 to 25%.



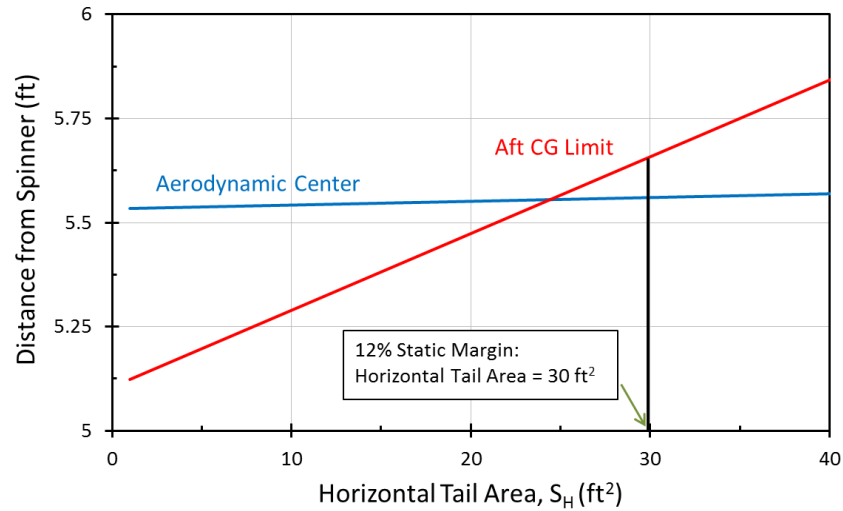


Figure 38: X-Plot for Tempo

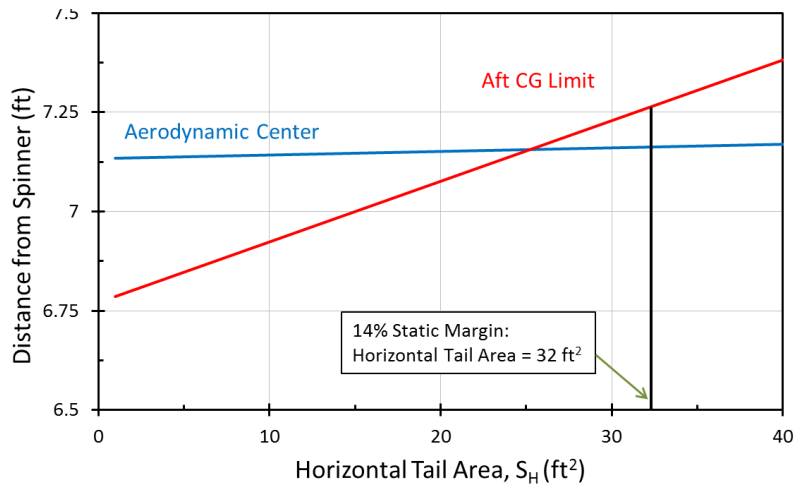


Figure 37: X-Plot for Encore

### 10.3 TRIM ANALYSIS

Once the longitudinal static stability analysis is completed, a trim analysis is conducted to ensure that the aircraft can be trimmed with reasonable elevator deflection angles. This analysis is done at both the forward and aft CG locations for Tempo and Encore. Figure 39 and Figure 40 depict Tempo’s  $C_M$  vs.  $C_L$  plot with various elevator deflections at the forward and aft CG limits of 7.05ft and 7.96ft, respectively. From Figure 39 it can be seen that Tempo can be trimmed at the  $C_{L,max}$  value of 1.45 at a deflection of  $-22^\circ$ . Since there is an inverted cruise flight requirement, it is important to note that Tempo can also be trimmed at the  $C_{L,min}$  value of  $-1.09$  at a deflection of  $16^\circ$ . By looking at Figure 40 for the aft CG limit, it can be seen that the maximum and minimum elevator deflections to

ensure trim at  $C_{L,max}$  and  $C_{L,min}$  are  $-8^\circ$  and  $6^\circ$ , respectively. Thus, the elevator is sized to handle deflections ranging from  $-22^\circ$  to  $16^\circ$  (total of  $38^\circ$ ), which is a typical range for light aircraft.

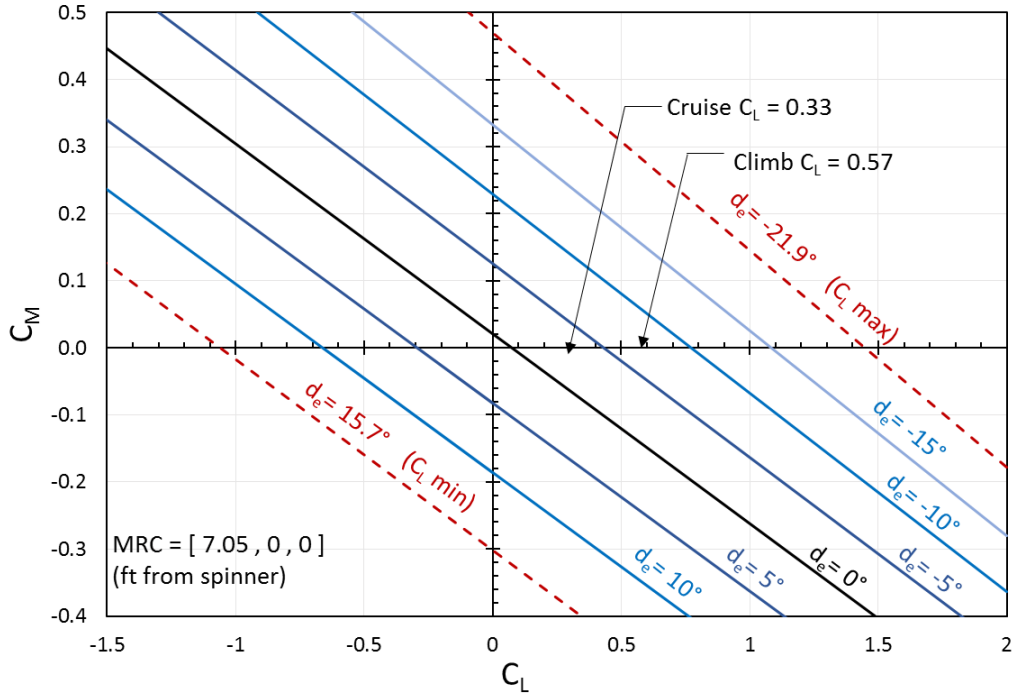


Figure 39: Trim Diagram for Tempo at Forward CG Limit

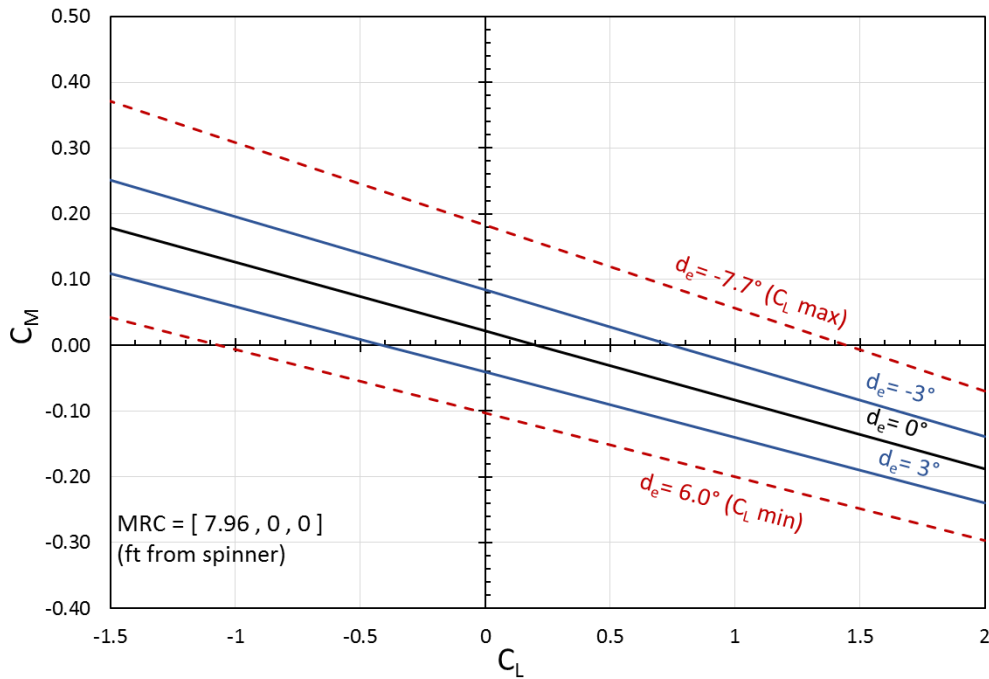


Figure 40: Trim Diagram for Tempo Aft CG Limit

Similarly Figure 41 and Figure 42 depict Encore's  $C_M$  vs.  $C_L$  plot with various elevator deflections at the forward and aft CG limits of 6.59ft and 7.48ft, respectively. By comparing the maximum and minimum elevator deflections for the forward and aft CG limits, it can be seen that the forward CG limit produces a larger deflection range requirement of  $-16^\circ$  to  $12^\circ$ . In order for Encore to trim at the  $C_{L,max}$  and  $C_{L,min}$ , the elevator must deflect a total of  $28^\circ$  and is sized accordingly, as discussed in Section 10.3.1.  $C_{L,cruise}$  and  $C_{L,climb}$  are depicted to show that the aircraft can be trimmed at these conditions.

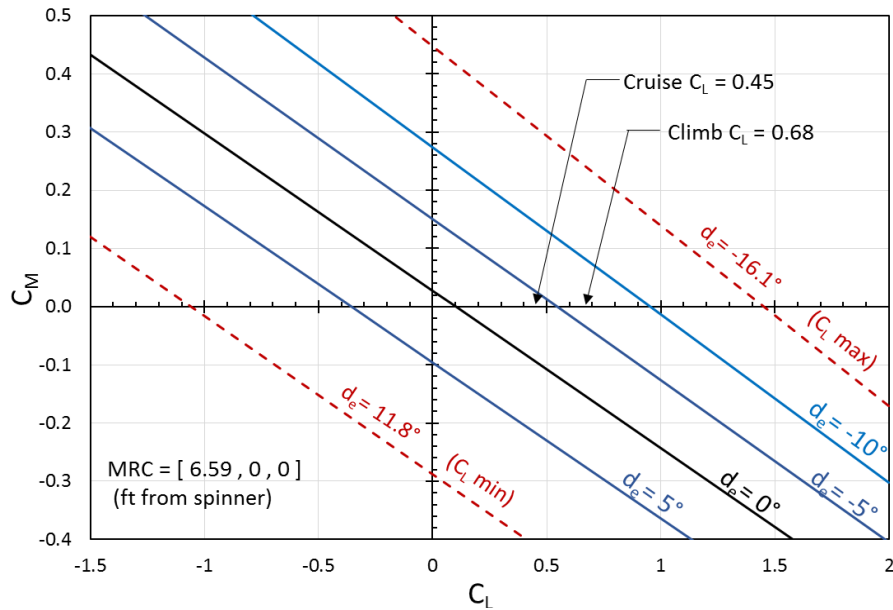


Figure 42: Trim Diagram for Encore at Forward CG Limit

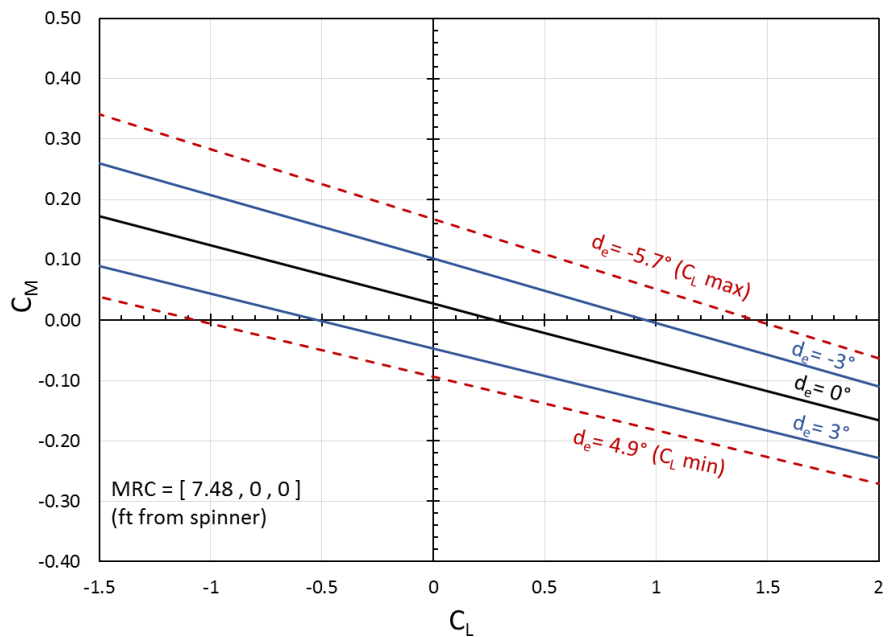


Figure 41: Trim Diagram for Encore at Aft CG Limit

### 10.3.1 ELEVATOR SIZING

As commonly seen, the elevator spans across the entire span of the horizontal tail. The elevator is sized based off the trim analysis. As previously discussed in Section 10.3 for Tempo, the maximum elevator deflection in order to trim at  $C_{L,max}$  is  $22^\circ$ . By limiting the deflection in AVL to this maximum deflection resulted in an elevator sized to 25% of the chord from the trailing edge for Tempo. Similarly, for Encore, it was previously determined that the maximum elevator deflection is  $16^\circ$  which resulted in an elevator encompassing 25% of the chord.

## 10.4 DIRECTIONAL STABILITY

Once the horizontal tail is sized correctly for longitudinal stability, directional stability is analyzed by sizing the vertical tail. Then the rudder is sized by considering spin recovery, crosswind landing, and coordinated turn. Then spin recovery is analyzed in depth by considering shielding of the rudder, tail effectiveness in recovery from spin, and aircraft moment of inertia.

### 10.4.1 VERTICAL TAIL SIZING

Directional stability ( $C_{n_\beta}$ ) for the aircraft family is achieved by sizing the vertical tail with Roskam's X-plot method,<sup>32</sup> which determines the minimum size for the vertical tail to satisfy the required directional stability level. A minimum  $C_{n_\beta}$  of  $0.001 \text{ deg}^{-1}$  is recommended for preliminary design.  $C_{n_\beta}$  encompasses the aircraft wings and body  $C_{n_\beta}$  contributions, the vertical tail  $C_{n_\beta}$  contributions, and the total value is found using an equation that is depended on the dimensions of the aircraft and vertical tail. When  $C_{n_\beta}$  is plotted against varying vertical tail area, as shown in Figure 43, it is determined that a vertical tail area ( $S_v$ ) of  $16.2 \text{ ft}^2$  is needed to satisfy the minimum directional stability requirement for Tempo.

Directional stability for Encore is determined the same way, by using its dimensions and the equations given by Roskam. Variation in  $C_{n_\beta}$  for Encore is also shown in Figure 43. The difference between directional stability for Tempo and Encore is negligible due to almost identical fuselages. For this reason, as well as the

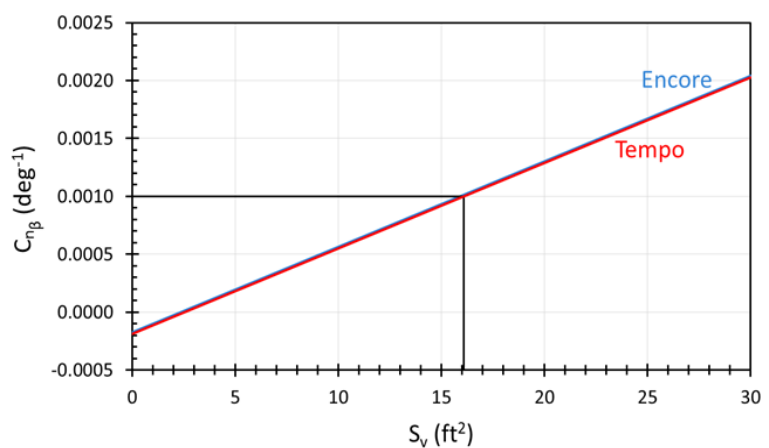


Figure 43: Directional Stability X-plot

design objective for commonality between the aircraft, the same vertical tail will be used for both family members.

#### 10.4.1 RUDDER SIZING

The rudder size is based off two requirements for directional stability stated in FAR part 23,<sup>31</sup> the aircraft must be able to recover from a spin and the aircraft must be able to land in crosswind conditions. There is also a third requirement of being able to perform a coordinated (banked) turn, which is a basic maneuvering capability that all aircraft shall be able to perform. These requirements will drive the minimum size for the rudder.

The first requirement is the ability to recover from spin. LSA are required to successfully enter and recover from a one full turn spin in less than three seconds as designated in FAR part 23.221.<sup>31</sup> This requirement is modified so that Tempo and Encore will be able to recover from a high spin rate maneuver in less than three seconds. A NASA study done on spin recovery is used to quantify high spin rates.<sup>35</sup> In this study, the largest spin rate used is 2.4rad/sec. This value equates to being able to recover from a 420°/sec spin maneuver in three seconds. This worst case scenario is used for as a constraint for Tempo and Encore.

The severity of the spin can be classed into the angle of attack that the aircraft is at, ranging from steep spin at the smallest angle of attack to flat spin at the largest angle of attack. Tempo and Encore should be able handle the worst case scenario of spin, and therefore the rudder sizing is done for flat spin, which starts at 65° angle of attack and ends at 90°. The moment of inertia is then calculated in the directional ( $I_x$ ), lateral ( $I_z$ ) and coupled lateral-directional ( $I_{xz}$ ) coordinates. Using these parameters, the rudder power derivatives are calculated for both Tempo and Encore.<sup>34</sup> The final design consideration is rudder shielding by the horizontal tail, which is when the wake of the horizontal tail decreases rudder effectiveness and the effective tail volume coefficient of the vertical tail. With these control derivatives and the previous variables calculated, the rudder size is varied in terms of chord length and span of the vertical tail to meet the minimum rudder deflection needed to satisfy these requirements, as shown in Figure 44.

The next requirement, as stated in FAR part 23.233, is that the aircraft must be able to land in a steady side slip with level wings in a crosswind up to 25 KCAS. The aircraft landing speed is approximated at 1.1 times greater than stall speed and the total wind force is calculated using a projected side area of the aircraft of 102ft<sup>2</sup>. Using control derivatives from AVL, force and moment equations are solved simultaneously that varied with crab angle (difference between heading and course angle) and again the maximum rudder deflection.

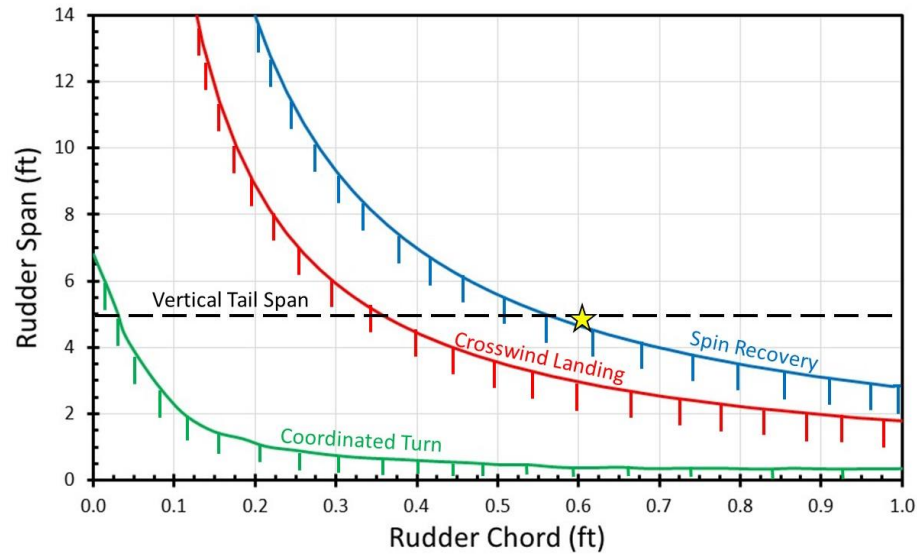


Figure 44: Constraint Diagram for Rudder Sizing

The last requirement for the rudder to meet is to be able to perform a coordinated turn. In a coordinated turn, the ailerons bank the aircraft and the rudder is used to correct for adverse yaw. Avem Dynamics would like for the rudder to be able to perform this maneuver in an aerobatic situation. The maneuvering speed for the aircraft is 98 KCAS and the bank angle is chosen to be 90°, which is the maximum angle any pilot would perform a maneuver, such as a lazy eight. The control derivatives are again used in conjunction with the steady-state yaw and pitch rates in the lateral-directional axes to find the aileron deflection, side-slip angle, and the rudder deflection.

The goal for these requirements are not to exceed the maximum rudder deflection that most aerobatic aircraft experience. With data from the Federal Aviation Administration website,<sup>37</sup> values for maximum rudder deflection are sampled from aerobatic aircraft with the largest deflection being 30° and the smallest being 25°. The above requirements are plotted as constraints against varying span of rudder and rudder chord length, with a maximum rudder deflection of 25°. This result can be seen in Figure 44.

The black dotted line is the span of the vertical tail and is the maximum span of the rudder. The rudder span is 5ft (spanning the entire vertical tail) and the chord length is 0.6ft.

### 10.4.2 SPIN RECOVERY

The FAA Federal Aviation Regulations (FAR) Part 23, Section 221 says that the aircraft must recover from a one-turn spin, or a three-second spin, in no more than one additional turn after initiation of the first control action for recovery. In Section 10.4.1, this requirement is shown to be met with rudder size, but there are other characteristics that influence recovery from spin.

Shielding of the rudder by the horizontal tail, tail effectiveness in recovering spin, and airplane moment of inertia can cause unsatisfactory spin recovery. The first determination is the amount of usable rudder when in spin. It is recommended that 30% of the rudder be out of the wake of the horizontal tail<sup>37</sup> to achieve the necessary rudder reversal for satisfactory spin recovery, shown in Figure 45. A line must be drawn 60° from the leading edge of the horizontal tail and the part of the rudder covered by that angle is considered in the wake of the horizontal tail. The next factors considered are the aircraft relative density, tail-damping power factor, and inertia yawing-moment parameter. Relative density ( $\mu$ ) is related to the interaction of inertia, aerodynamic forces, and moments acting on the aircraft during spin and can be empirically determined from wingspan and wing loading. The tail-damping power factor (TDPF) is an indication of the vertical tail effectiveness in recovering spin. Figure 46 shows the necessary values for determining TDPF, and is highly dependent on how much of the rudder is unshielded by the horizontal tail.

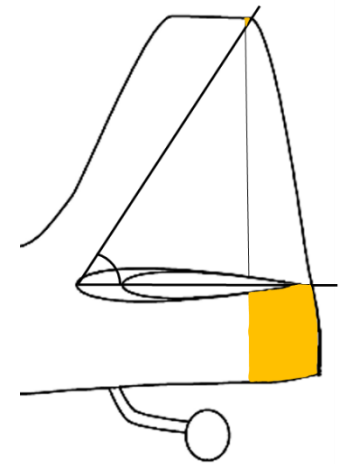


Figure 45: Part of the rudder unshielded by horizontal tail is shown in yellow.

The final parameter considered is the inertia yawing moment parameter which indicates how the mass is distributed along the wings or fuselage and can be a predictor of how effective control surfaces are in spin recovery. Figure 47 is from a NACA report from 1947.<sup>38</sup> Most of the spin recovery data from these reports<sup>38,39,40</sup> is empirically determined from the spin tunnels at NASA Langley for light aircraft, so the figure shows the results of experimental data. Since both aircraft have the same wing and very similar fuselage, the values for  $\mu$ , TDPF, and inertia yawing moment will be the same for Tempo and Encore. The value  $\mu$  is four, once again, determined empirically from wing-

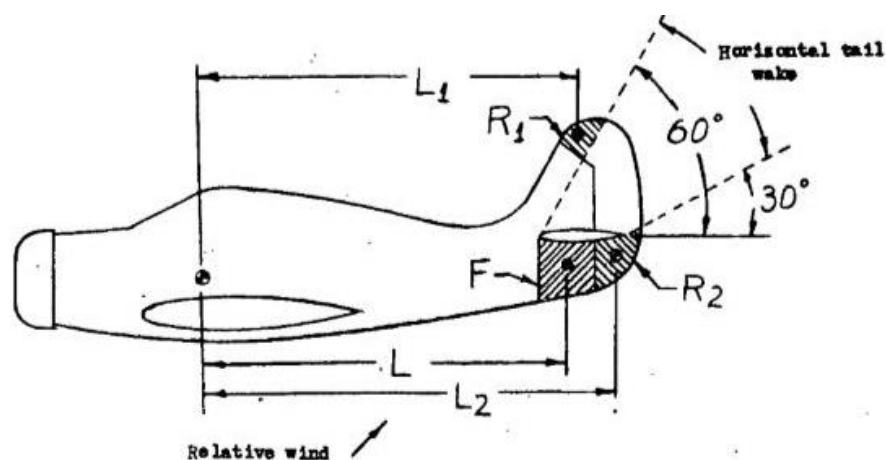


Figure 46: Necessary Components to find TDPF

loading and wingspan.<sup>41</sup> The TDPF is determined to be  $570 \times 10^{-6}$ . To determine the inertia yawing moment, experimental values of radius of gyration were found for early fighter type aircraft.<sup>41</sup> The radii of gyration ( $R_x$ ,  $R_y$ ,  $R_z$ ) for 15 aircraft were plotted against the wingspan and a line of best fit was determined. From this, the radii of gyration for Tempo and Encore were determined and multiplied by the weight to find the moments of inertias and resulted in an inertia yawing moment of  $-21 \times 10^{-4} \text{ft}^2/\text{lb}$ .

Figure 47 shows the required parameters plotted against each other. An interesting phenomenon occurs when considering the effect of the elevator on the rudder effectiveness. If the rudder movement proceeds the elevator movement, the rudder effectiveness is increased and the aircraft can recover from spin faster. However, if the elevator movement proceeds the rudder movement, the rate of spin of the aircraft is increased. These facts imply that the pilot knows the proper technique for adequate spin recovery. Since the pilots of Tempo and Encore will be experienced enough to fly in the intermediate category, it is assumed that they will properly know how to recover from spin or are accompanied by an experienced enough pilot. However, it is desired to have a recovery from spin through rudder reversal alone since it is the simpler technique and will add to the safety of the aircraft. From Figure 47, it can be seen that the aircraft satisfactorily recover from spin through rudder reversal alone.

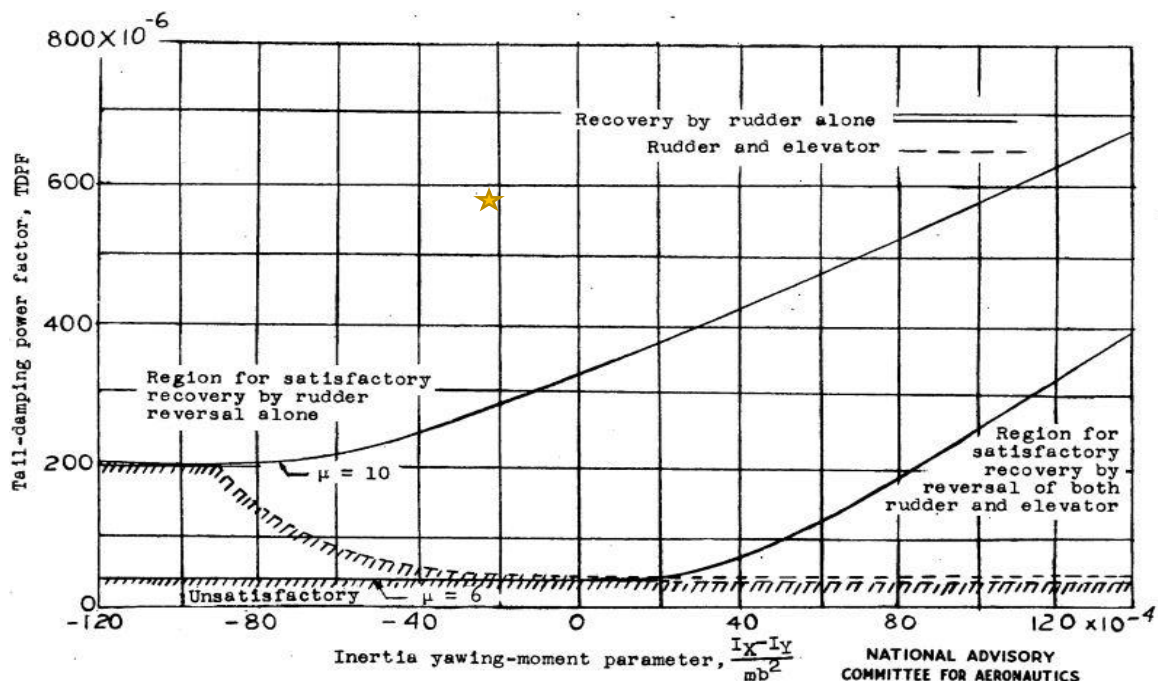


Figure 47: Determination of Satisfactory Spin Recovery



## 10.5 AILERON SIZING

The ailerons for Tempo and Encore were sized in regards to roll rate. A roll rate of  $180^\circ/\text{sec}$  is the minimum roll rate required by the RFP; however, in order to be more competitive in the intermediate category aerobatics competition, a larger roll rate is necessary. Using the roll rate index from Cassidy's book,<sup>42</sup> and by comparing a variety of aerobatic aircraft, a roll rate of  $360^\circ/\text{sec}$  is determined to be the target roll rate. This roll rate will allow for the aircraft to remain competitive while having controls that are not being too sensitive. Using both Roskam's equation for steady state roll rate<sup>43</sup> and Datcom's equations for roll damping and roll authority,<sup>19</sup> the ailerons are sized to fit the desired roll rate. Six ailerons deflection angles are analyzed along with five aileron widths at various velocities.

Of the six aileron deflection angles,  $15^\circ$  is chosen. This angle was chosen because it will not experience flow separation over the aileron and reduces the risk of losing roll control at high angles of attack. Of the five aileron widths, 30% of the chord is chosen to allow for two aileron spars while still being able to produce high roll rates. By using an aileron width of 30% of the chord, Tempo and Encore can reach roll rates far beyond the minimum required roll rate.

A set of velocities ranging from 80 KCAS to the maximum speed of 120 KCAS are tested for the chosen aileron deflection angle and width. The outer most edge of the aileron is set to 6in in from the tip of the wing. As seen in Figure 48, the semi-span location of the inner edge of the aileron is plotted against the steady state roll rate

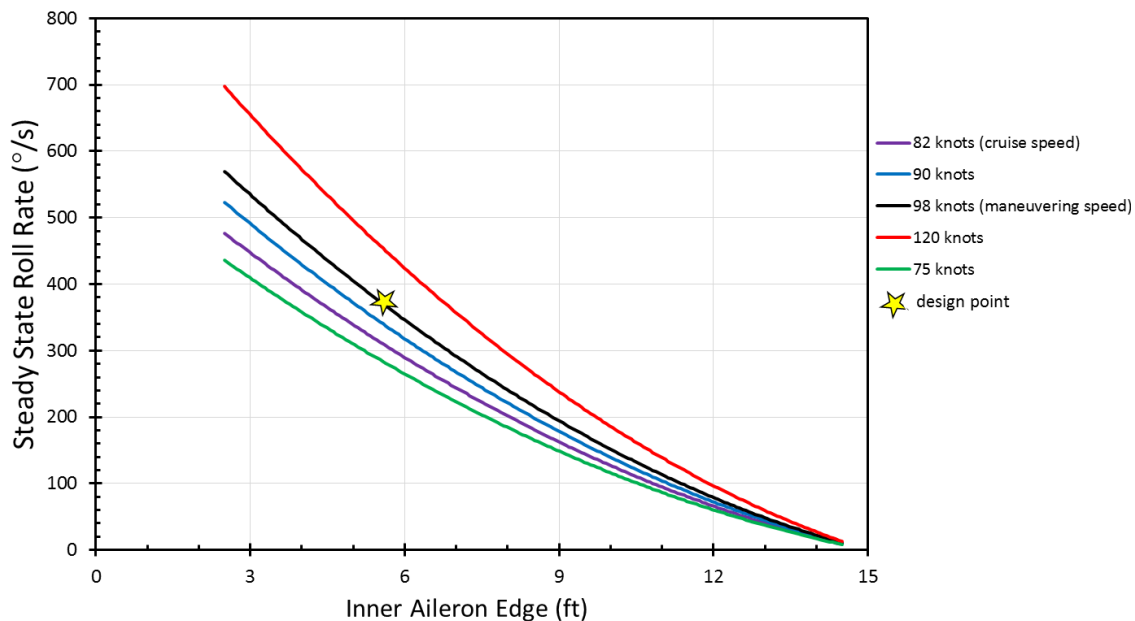


Figure 48: Ranging Velocities for Aileron Sizing

for the range of velocities. The cruise and maneuvering velocities determined in Section 11.4 are of particular interest. In order to be competitive in the intermediate category aerobatic competition, the maneuvering velocity is determined to be the most important. The inner edge of the aileron was determined from this plot (Figure 48) based on a steady state roll rate of  $360^\circ/\text{sec}$ , aileron deflection angle of  $15^\circ$ , aileron width of 30% of the chord, and the outer edge of the aileron set 6in away from the wingtip. The resulting inner edge aileron location is 5.75ft from the aircraft's centerline. Figure 49 depicts the details of the sized aileron.

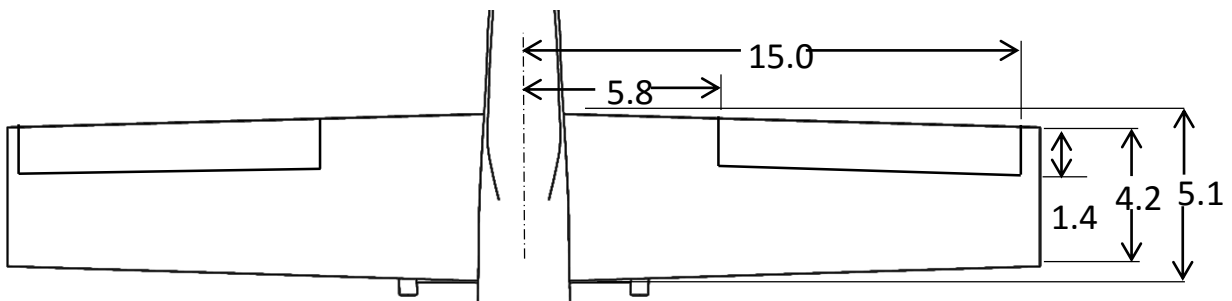


Figure 49: Sized Ailerons on Wing

### 10.6 EMPENNAGE SUMMARY

A summary of the empennage configuration is given below in Figure 50. Tempo and Encore share a common vertical tail with a  $16.2\text{ft}^2$  area ( $V_V = 0.0522$ ). Tempo's horizontal tail area is  $30\text{ft}^2$  ( $V_H = 0.698$ ) and

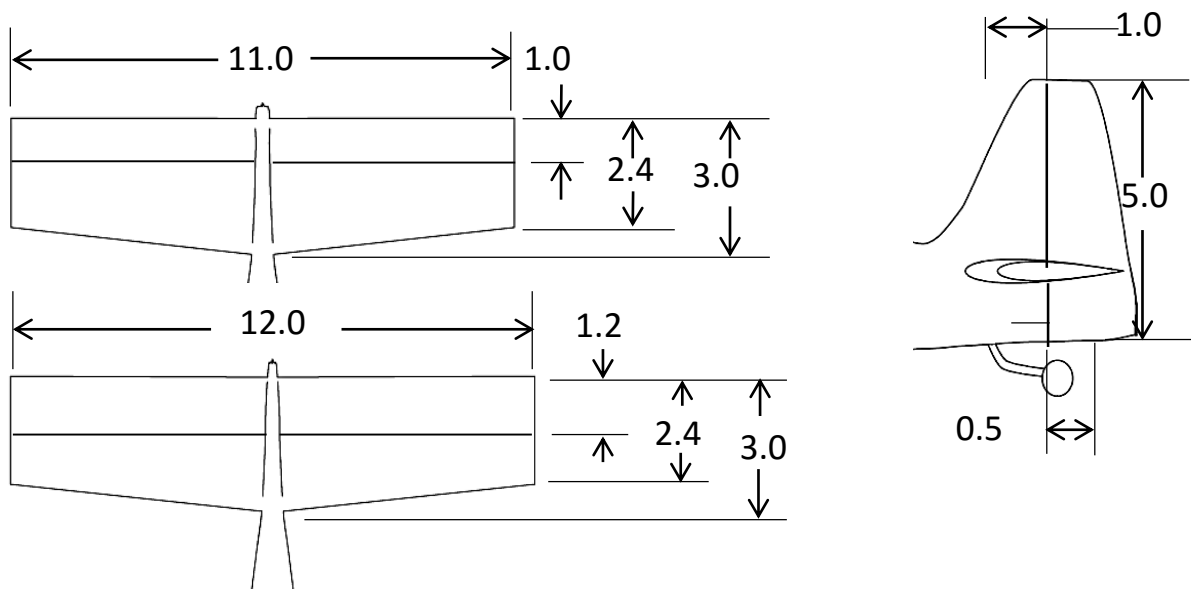


Figure 50: The horizontal and vertical tail and their dimensions for Tempo (top left) and Encore (bottom left). The vertical tail (top right) is common between the two aircraft

Encore’s horizontal tail is 32ft<sup>2</sup> ( $V_H = 0.763$ ). The tail areas are determined from equations that depend on the dimensions of the aircraft. The design objective to make the aircraft visually appealing encouraged the use of taper and sweep in both the horizontal and vertical tails. Completely rectangular shapes may be simpler to manufacture, but Avem Dynamics decided this detracted from the appeal of the aircraft family. The sweep angles and taper ratios are determined by eye for achieving aesthetically pleasing, proportional tails.

In Table 13, the empennage of the Tempo and Encore can be compared to tails of other small single piston engine aircraft using tail volume coefficients.<sup>46</sup> The Mudry aircraft are aerobatic airplanes, the Cessna is a high wing general aviation aircraft, while the last three aircraft listed are low-wing monoplanes. It is seen that the tail areas obtained for Avem Dynamics’ aircraft seem reasonable as the tail volume coefficients are similar to those of existing aircraft.

Table 13: Comparison of Volume Coefficients

	Tempo	Encore	Mudry Cap10	Mudry Cap232	Cessna 152	Beagle Pup	Diamond DA20	Lancair Legacy
Takeoff Weight (lbs)	1087	1297	1676	1609	1670	1600	1764	2200
$V_H$	0.698	0.763	0.743	0.499	0.557	0.723	0.820	0.568
$V_V$	0.0522	0.0522	0.0710	0.0580	0.0337	0.0523	0.0351	0.0563

## 11 Performance

Performance of the aircraft is analyzed starting with the flight envelope to determine the overall performance of the aircraft throughout all possible speeds and altitude. Taking and landing performance are demonstrated to meet the RFP requirements for both Tempo and Encore, using simplified equations for single engine, piston driven aircraft. The maximum rate of climb is shown for various atmospheric conditions and is closely tied to the performance of the propulsion system described in Section 7. Cruise performance is analyzed by considering the fuel consumption for the Lycoming AEIO-233. A payload range diagram is shown to demonstrate the maximum ranges for various payload configurations for both aircraft. Finally, turn performance is analyzed using specific excess power curves for given weights and altitudes.

## 11.1 FLIGHT ENVELOPE

The boundaries for the flight envelope of Tempo and Encore are defined by the stall speed, the visual flight rules (VFR) ceiling, the never exceed speed, and the 120 KCAS speed limit for level flight. The service ceiling of an aircraft is generally defined as the altitudes at which the aircraft has a maximum rate of climb of 100fpm to 300fpm. This range of climb rates for Tempo and Encore, shown by the specific excess power curves, is well above the VFR ceiling as seen in Figures 51 and Figure 52. However, because LSA are only allowed to fly under VFR, the FAA's limit for VFR of 18,000ft<sup>45</sup> is the maximum ceiling of both aircraft. The FAA also dictates in 14 CFR Part 91<sup>26</sup> that when flying at 12,500ft MSL or higher, pilots must be on supplemental oxygen if they are at those altitudes for more than 30 minutes. At altitudes of 14,000ft MSL or higher, pilots must be on supplemental oxygen at all times. These boundaries are very important for pilots to understand when they are flying Avem Dynamics' LSA family members.

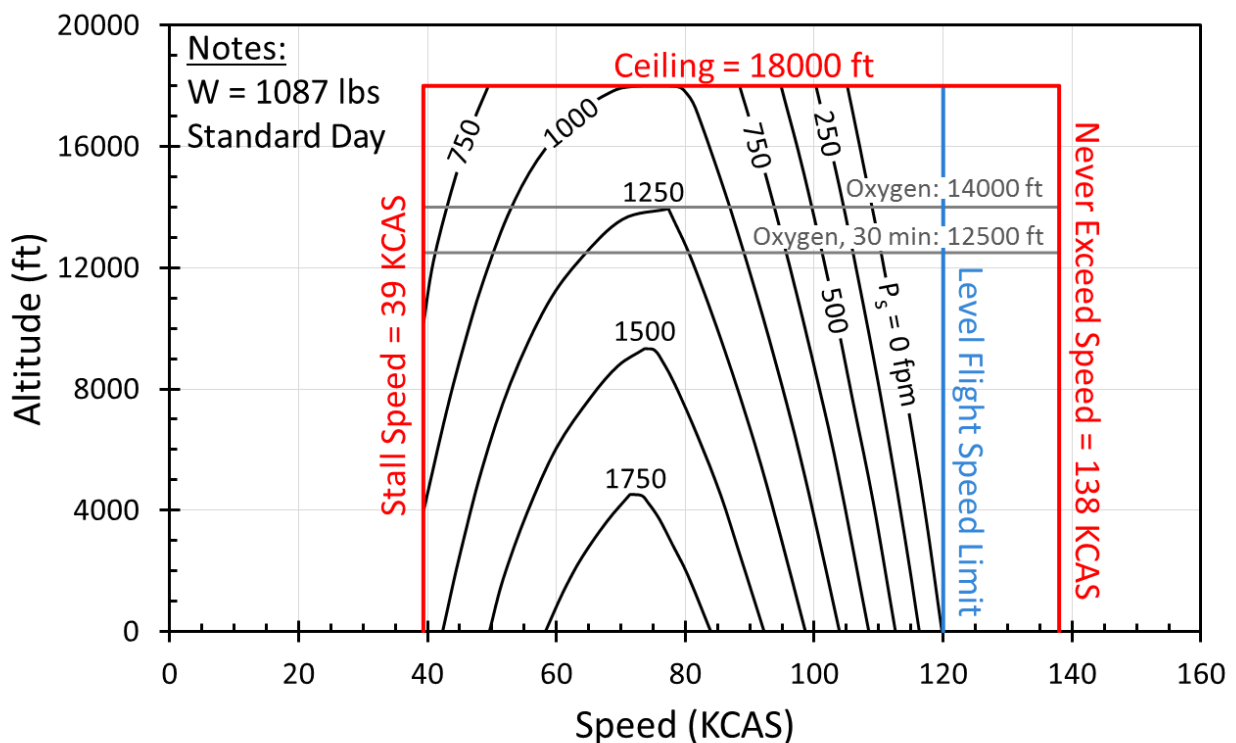


Figure 51: Flight Envelope for Tempo

As seen in Tempo's flight envelope, shown in Figure 51, the aircraft has a stall speed of 39 KCAS and a never exceed speed of 138 KCAS which is calculated from the definitions in 14 CFR Part 23<sup>26</sup> and the ASTM International standard for LSA.<sup>2</sup> The units for aircraft speed are given in calibrated knots to easily depict the distinct

speed boundaries and because Mach number is not relevant for these small aircraft. Tempo achieves a maximum rate of climb of 1980 fpm at sea level at a speed ( $V_y$ ) of 71 KCAS. The speed for maximum climb angle ( $V_x$ ) is 51 KCAS.

The flight envelope for Encore is shown in Figure 52 and it is seen that the stall speed for this larger aircraft is 43 KCAS and the never exceed speed is also higher at 150 KCAS. The specific excess power curves also show that Encore achieves lower maximum rates of climb than Tempo. At sea level, Encore has a maximum rate of climb of 1590fpm at 71 KCAS and  $V_x$  is 54 KCAS. It is important to note that both aircraft have a specific excess power of 0 fpm at 120 KCAS at sea level as was designed by the propeller which was discussed in Section 7.4.

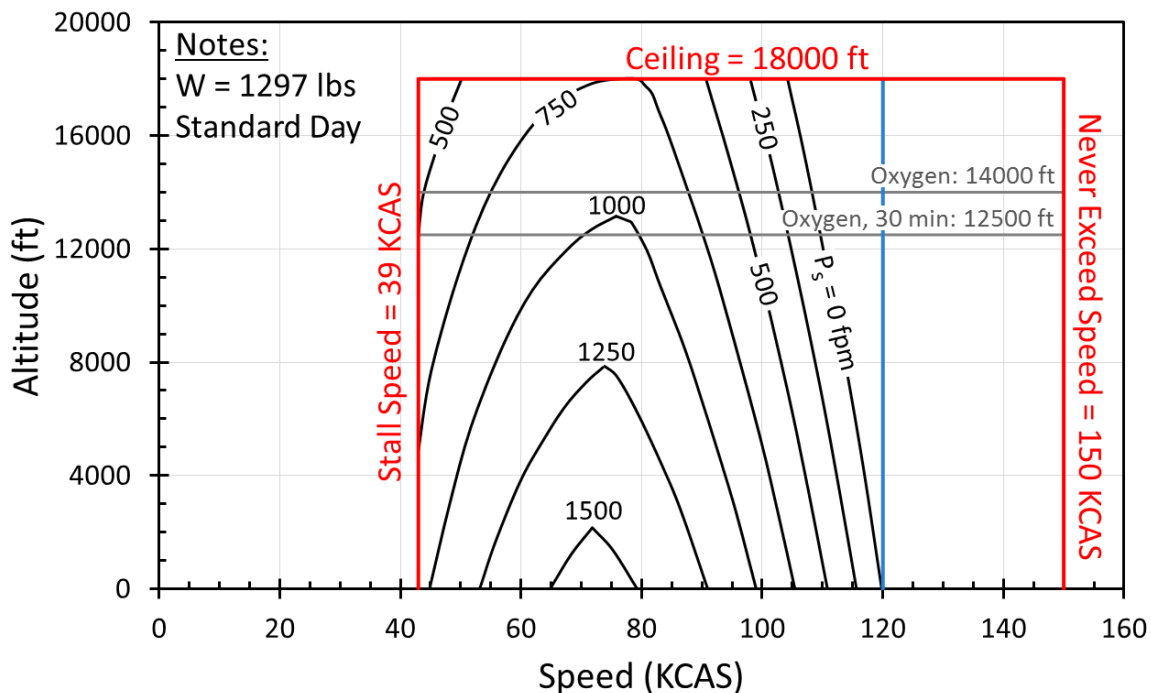


Figure 52: Flight Envelope for Encore

## 11.2 TAKEOFF AND LANDING

### 11.2.1 TAKEOFF

Takeoff and landing performance are calculated using equations developed in Roskam and Lan's *Airplane Aerodynamics and Performance*<sup>8</sup> for single propeller, piston engine driven aircraft. The total takeoff field length equation is broken down into three major components: ground roll, rotation, and climb over an obstacle. The ground roll segment is when all wheels are still on the ground, rotation is when the plane transitions into lifting its front

wheels off the ground, and climb is when the aircraft has all wheels off the ground and has begun to ascend. A rolling ground coefficient of 0.025 is used for taking off from dry pavement and 0.075 is used for grass. The RFP requires the single seat aircraft to takeoff in 1200ft over a 50-foot obstacle and the two-seat to have a maximum takeoff field length of 1500ft, both from dry pavement and at sea level and International Standard Atmosphere (ISA) + 10°C. Tempo takeoff performance from elevations of 0ft to 10,000ft is plotted in Figure 53. Calculations are done at the gross takeoff weight for dry pavement at ISA + 10°C (red), grass at ISA (green), dry pavement at ISA (orange), and grass at ISA + 10°C (blue). Tempo can takeoff at sea level and ISA + 10°C from dry pavement in 715ft, from grass at sea level and ISA + 10°C in 710ft, and from dry pavement at ISA + 10°C from an elevation of 5000ft MSL in 813ft.

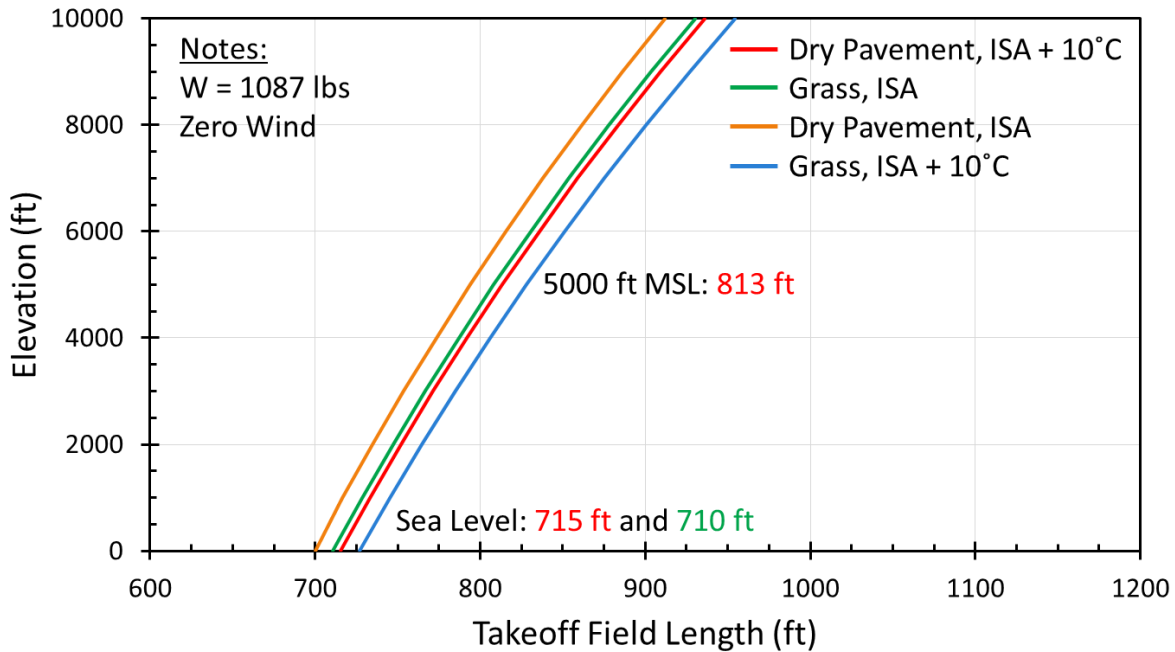


Figure 53: Takeoff Field Length for Tempo at Various Conditions

Encore takeoff performance is shown in Figure 54. Encore can takeoff at sea level and ISA + 10°C from dry pavement in 858ft, from grass at sea level and ISA + 10°C in 858ft, and from dry pavement at ISA + 10°C from an elevation of 5000ft MSL in 987ft. Both aircraft in the Avem Dynamics LSA family meet the takeoff requirements.

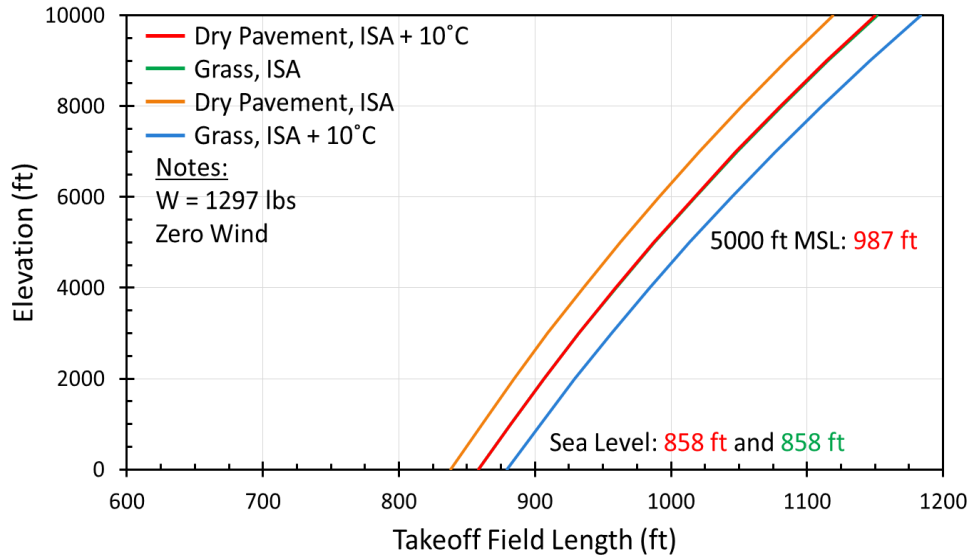


Figure 54: Takeoff Field Length for Encore at Various Conditions

### 11.2.2 LANDING

Total landing field length is also broken up into three components: descent from an obstacle, rotation, and ground roll. The calculation is simplified from performance over time to an instantaneous maneuver by stating that the average speed is 70% of the speed at touchdown which is estimated as 130% of the stall speed of 39 KCAS and 43 KCAS for Tempo and Encore, respectively. The braking coefficient of friction used for calculations is 0.7 for landing on dry pavement and 0.6 for landing on grass. The drag and lift forces are calculated based on the flight conditions and speed. Because aircraft do not apply thrust when landing, the landing field length is not a function of power-to-weight which is reflected in the constraint diagrams in Section 4.1. Like takeoff, the single seat is required to land within 1200ft over a 50-foot obstacle from dry pavement and at sea level and International Standard Atmosphere (ISA) + 10°C and the two-seat must land within 1500ft under the same conditions.

Landing performance data for Tempo is plotted in Figure 55. Tempo can land at sea level and ISA + 10°C on dry pavement in 1157ft, on grass at sea level and ISA in 1161ft, and on dry pavement at ISA + 10°C at an elevation of 5000 feet MSL in 1237ft. These values can be seen for Encore in Figure 56. Encore can land at sea level and ISA + 10°C on dry pavement in 1262ft, on grass at sea level and ISA in 1272ft, and on dry pavement at ISA + 10°C at an elevation of 5000ft MSL in 1363ft. Both aircraft in the Avem Dynamics LSA family meet the landing requirements.

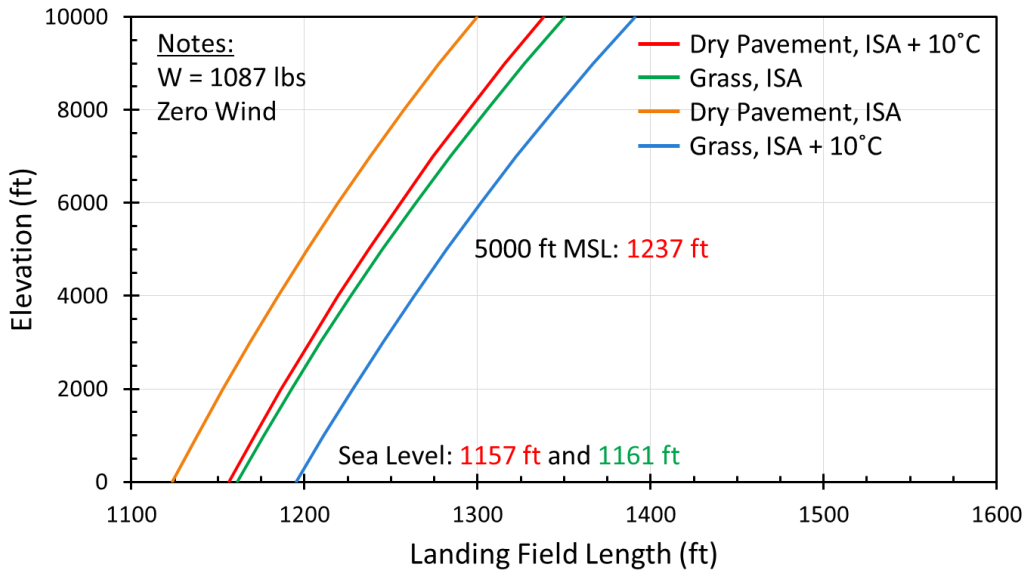


Figure 56: Landing Field Length for Tempo at Various Conditions

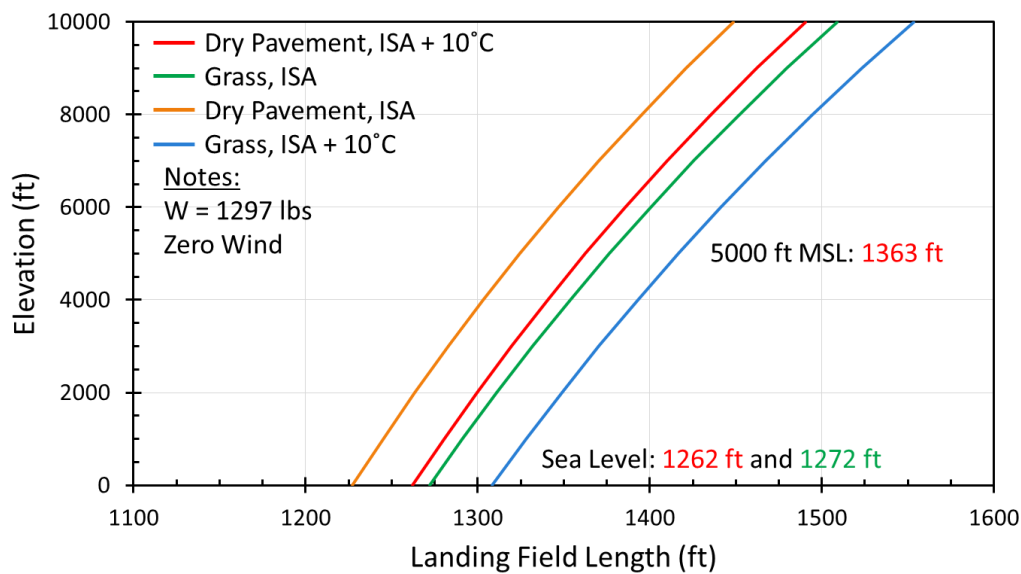


Figure 55: Landing Field Length for Encore at Various Conditions

### 11.3 MAXIMUM RATE OF CLIMB

At the beginning of the design process, the requirement to meet a 1500fpm climb rate for the single seat aircraft seemed very challenging because of the 120 KCAS speed limit requirement. As discussed in Section 7.4, the propeller is optimized with the engine so that aircraft would have enough thrust at lower speeds to climb faster than the requirement but would have thrust equal to drag at 120 KCAS to not surpass the speed limit. With a custom propeller and the Lycoming AEIO-233 engine, Avem Dynamics is able to design both aircraft so that they far exceed the requirements. Fortunately, the requirements are exceeded by a large amount due only to the propeller



characteristics and not from any performance sacrifices in other areas. The maximum rate of climb for all altitudes within the flight envelope are shown for both Tempo and Encore in Figure 57. The single seat is required to climb at 1500fpm at sea level and ISA + 10°C and the two seat must climb at 800fpm at sea level and ISA + 10°C, shown by the triangles. Tempo achieves a maximum rate of climb of 1980fpm at a forward speed ( $V_y$ ) of 71 KCAS and Encore can climb up to 1590fpm at the same speed.

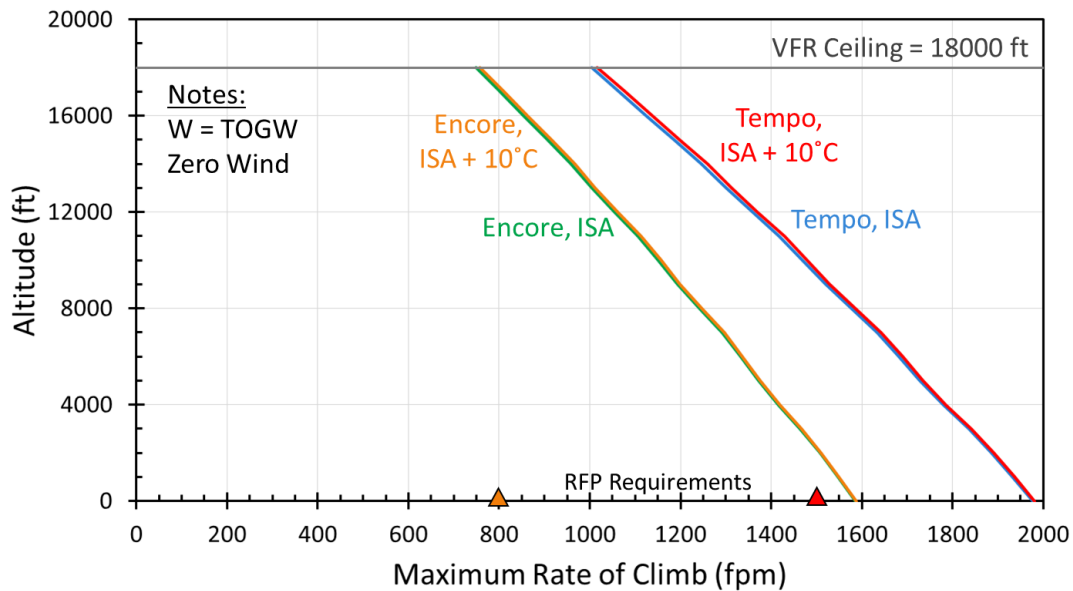


Figure 57: Maximum Rate of Climb for Tempo and Encore

### 11.4 CRUISE PERFORMANCE

While flying Tempo or Encore, the pilot could choose to cruise at any speed from the stall speed to the 120 KCAS speed limit. However, it would not be practical to fly cross-country at slow speeds near stall and it would not be fuel efficient to cruise at the highest speed. Fuel consumption during cruise for the Lycoming AEIO-233 engine is calculated from the percentage of horsepower used and the efficiency, and the data is shown in Figures 58

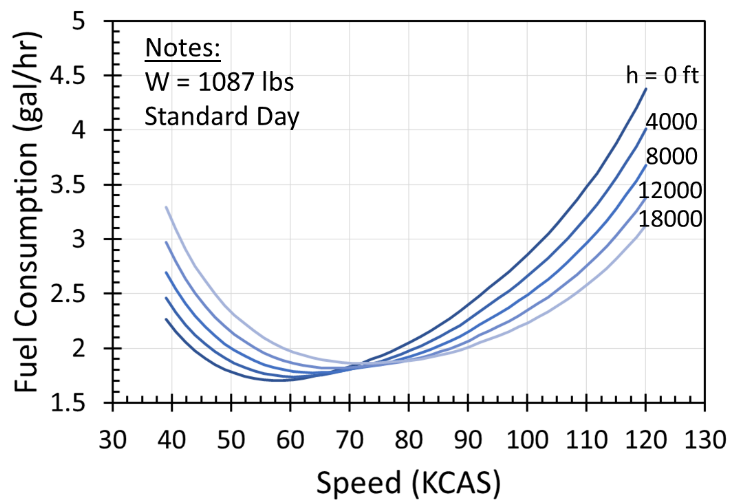


Figure 58: Tempo Fuel Consumption

and 59 for Tempo and Encore, respectively. It turns out that cruising at sea level at 58 KCAS for Tempo and 62 KCAS for Encore uses the least amount of fuel per hour but cruising at sea level is not possible and these are very slow cruise speeds.

If the pilot wishes to cruise at the level flight speed limit, it can be seen that higher altitudes provide lower fuel consumption but that the engine speed is at the maximum limit at 2800 RPM, as shown in Figures 60 and 61. Although the maximum engine speed is reached, the engine is not at full power because of the “inefficiency” of the propeller at that speed. This is why fuel consumption at 120 KCAS is less than the maximum continuous fuel consumption of 9.8gal/hr.

A typical cross-country cruising altitude for general aviation aircraft under VFR is 8000ft MSL. This altitude also provides the farthest range compared to higher altitudes when taking into account the amount of fuel used to climb. The cruise speed for maximum range is then 82 KCAS for Tempo and 85 KCAS for Encore.

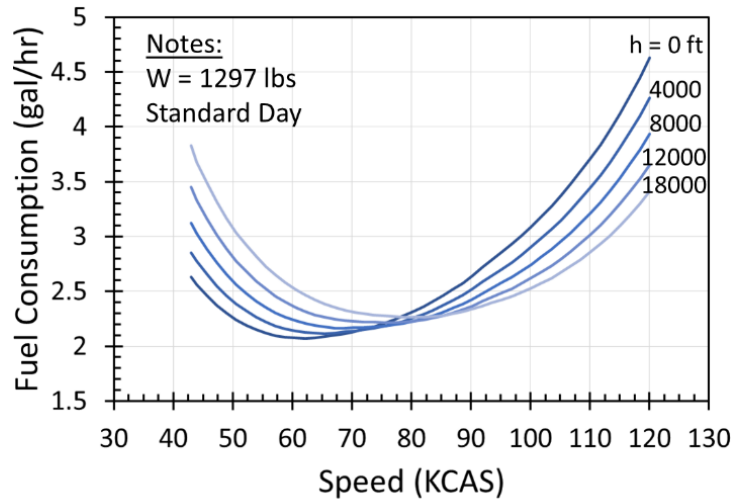


Figure 59: Fuel Consumption for Encore

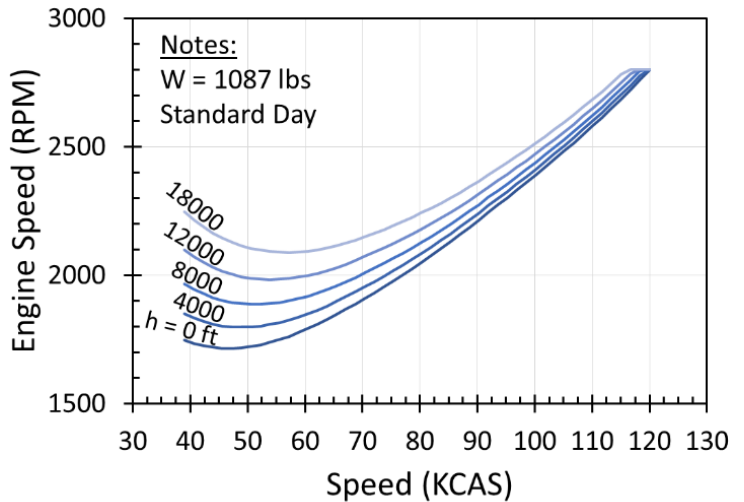


Figure 60: Tempo Engine RPM and Speed

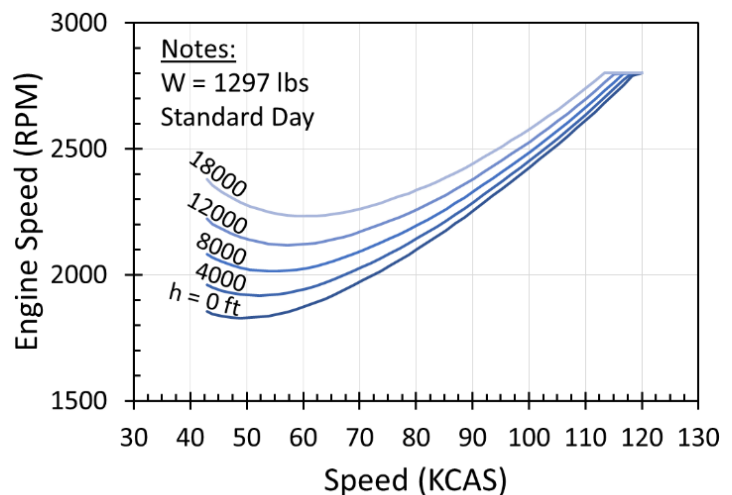


Figure 61: Encore Engine RPM and Speed

## 11.5 PAYLOAD RANGE

The Encore may be used more as a general aviation aircraft than the Tempo which will primarily be used for aerobatics. This means the pilot should understand the ferry range of the aircraft, as well as the available payload. This is illustrated by the payload-range diagram for the Tempo and Encore shown in Figure 62. Maximum payload is calculated from the empty weight subtracted from the gross takeoff weight, so the weight of the pilot and fuel are included. Fuel consumption information for the engine is taken to calculate the range of the aircraft. Calculations were done at an altitude of 8000ft MSL as this is a typical cross-country cruising altitude for general aviation. Maximum range is achieved at an 82 KCAS cruise speed for Tempo and a cruise speed of 85 KCAS for Encore. As shown in the figure, Tempo, shown in red, has a higher specific range than Encore at 5.5nm/lbs compared to 4.6nm/lbs. This means that Tempo is able to travel 0.9nm farther than Encore for each pound of fuel consumed.

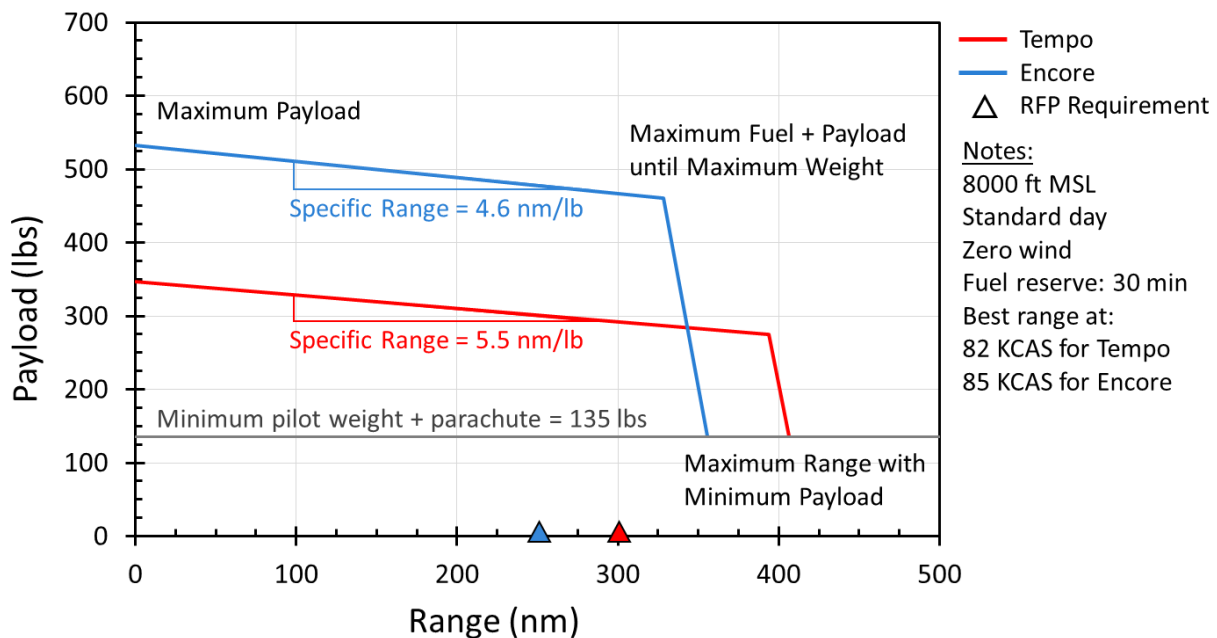


Figure 62: Payload Range Diagram for Tempo and Encore

Maximum payload for the aircraft are 347lbs and 532lbs for Tempo and Encore, respectively. The minimum payload weight is the minimum weight of a single pilot plus the required parachute which is 135lbs total. This makes the Tempo achieve a maximum range, not including the 30 minute fuel reserve, of 405nm while the Encore can travel 355nm. Avem Dynamics' aircraft family surpasses the RFP's minimum ferry range requirement of 300nm for the single-seat and 250nm for the two seat aircraft.

## 11.6 TURN PERFORMANCE

Maneuverability is an important feature of aerobatic aircraft. Turn performance is one way to quantify maneuverability. Tempo's turn rate, shown in Figure 63 is calculated at the competition weight of 1005lbs and the average altitude of an intermediate aerobatic routine if the ground is at sea level, 2350ft. The black specific excess power curves are calculated at this weight and altitude as opposed to the gross takeoff weight and at sea level for which the propeller is optimized (as explained in Section 7.4). The green line is the aircraft's stall boundary based on a  $C_{L,max}$  of 1.45, the blue line is the plus 6g limit load, and the red line is the aircraft's never exceed speed which is 138 KCAS. The Tempo's maneuvering speed is shown by the top corner of the plot at the intersection of the stall boundary and the limit load lines and it is 96 KCAS which gives Tempo a maximum instantaneous turn rate of  $67^\circ/\text{sec}$ . Maximum sustained turn rate is represented by the peak of the 0fpm specific excess power curve and it is  $31^\circ/\text{sec}$  when Tempo is travelling at 76 KCAS.

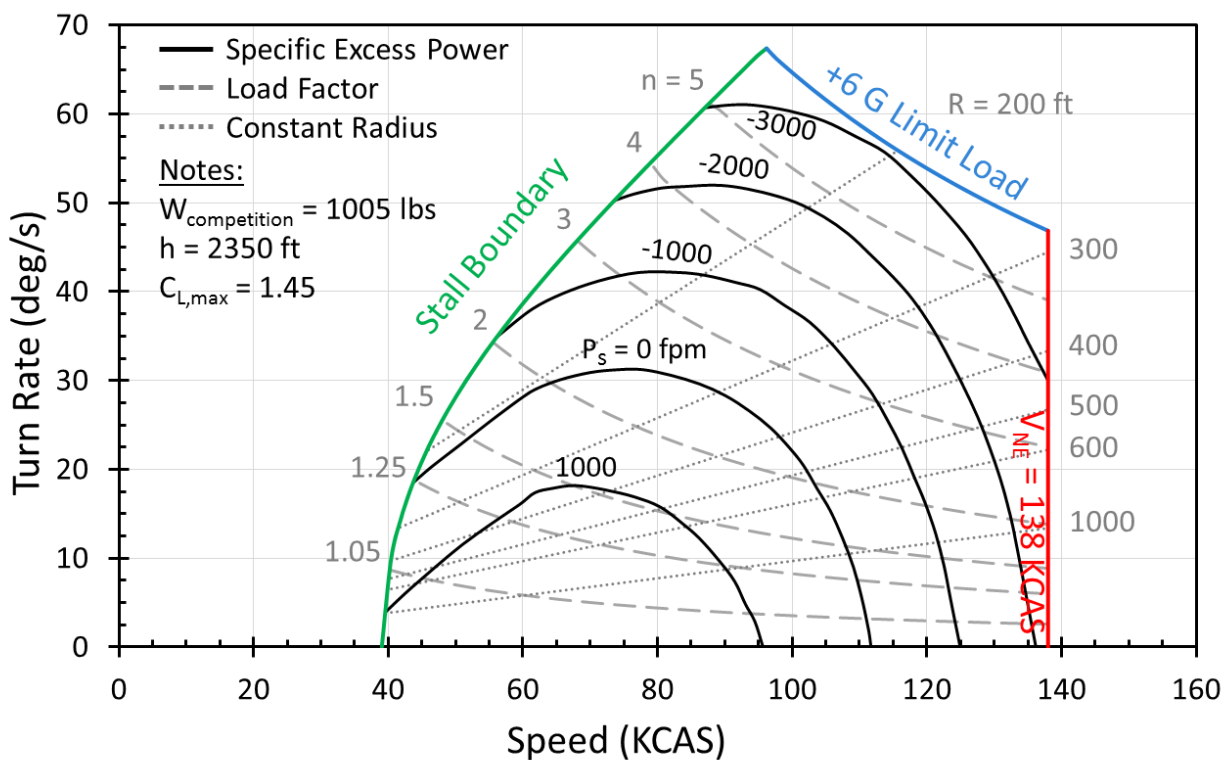


Figure 63: Turn Performance for Tempo

To assess the maneuverability of the trainer variant, Encore, turn performance is calculated at the same altitude and a comparable training weight of 1220lbs. This training weight is based on needing fuel for about 100 minutes of flight time (including the 30 minute fuel reserve) as well as having two pilots that are the maximum

weight the RFP requires which equals 400lbs. As seen in Figure 64, Encore has a never exceed speed of 150 KCAS and a higher speed stall boundary. Maneuvering speed is also higher at 106 KCAS and this gives a lower maximum instantaneous turn rate of 61°/sec. The maximum sustained turn rate for Encore is 26°/sec when the aircraft is travelling at 80 KCAS.

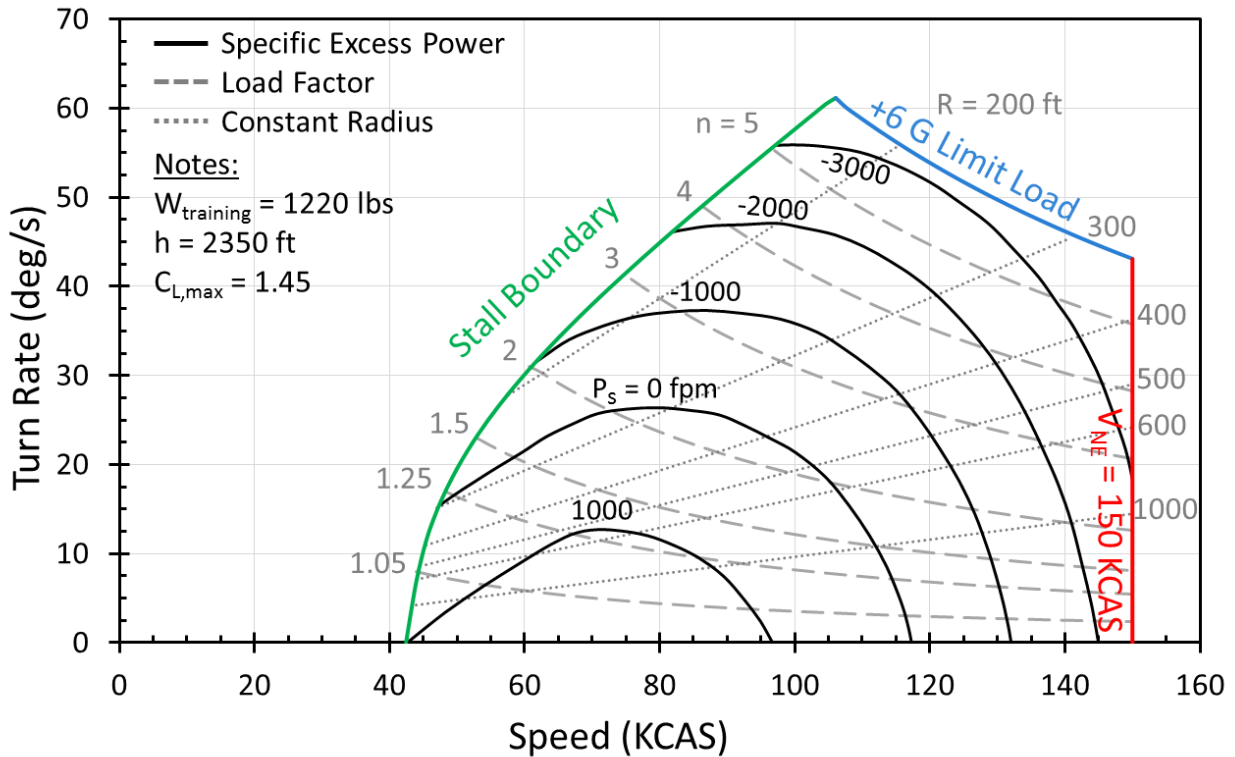


Figure 64: Turn Performance for Encore

## 12 Cost Estimate

As a new company entering the LSA market, Avem Dynamics has calculated cost estimates to determine a profit timeline. Based on the conducted market analysis that is described in Section 2, it is assumed that four aircraft will be sold per month. This leads to Avem Dynamics making a 10% profit after selling 240 aircraft total over five years.

### 12.1 DEVELOPMENT COST

The cost to develop an aircraft includes the non-recurring costs of engineering, tooling, testing, and additional overhead costs. These costs are calculated using cost models from Gudmundsson<sup>44</sup> which use equivalent 2012 dollars, but are adjusted to account for inflation. With these adjustments, they yield costs in equivalent 2016 dollars. The total development cost of Tempo and Encore is \$6.5 million.

The engineering cost model takes into account the maximum level airspeed of the aircraft, the amount of composites used in the airframe, the weight of the airframe, the use of flaps, the number sold after five years, the cost of engineering labor, cabin pressurization, and if the aircraft is a LSA. The weight is based on Encore since it is the heavier airframe and will result in a larger cost of engineering. Due to the high degree of commonality, only one aircraft in the family needs to be analyzed, so Encore is used to yield a more conservative cost estimate. The rate of engineering labor is the fully burdened labor rate which is approximately 2.2 times the engineering salary.<sup>46</sup> The salary is determined to be \$50/hr based on the national average for aerospace engineers.<sup>47</sup> The total cost of engineering came out to be \$2.34 million and makes up about one-third of the total development cost.

Tooling cost is about two-thirds of the total development cost and includes the cost to build and acquire tools for manufacturing the aircraft. The same inputs are used for the cost model with the addition of the taper on the wing and results in a tooling cost of \$4 million.

Testing and additional costs make up the small remaining portion of the total development cost and is the cost of certification through the component and flight testing phases. This model accounts for the maximum level airspeed, airframe weight, and if the aircraft is a LSA. The resulting cost of testing is \$53,000. The additional costs include facilities, overhead costs, and the cost of supporting staff. The supporting staff include administration and human resources staff. Using the same inputs as the engineering model with the exception of the fully burdened labor rate, the additional costs come to \$41,000.

## 12.2 FLYAWAY COST

The flyaway cost is how much money is needed to produce a single unit, which includes the manufacturing cost, materials, quality control, and the engine and propeller costs. Using Gudmundsson's models,<sup>44</sup> it is determined that the total cost to build each aircraft is \$90,000.

The manufacturing cost is the amount of money required to manufacture the parts and assemble them into the completed aircraft with inputs of maximum level airspeed, the amount of composites in the aircraft, airframe weight, the number of aircraft sold in 5 years, fully burdened labor rate, and if the aircraft is a LSA. The fully burdened labor rate is 2.2 times the hourly wage of a manufacturer which is \$25/hr, based on the national average wage for an aircraft assembly worker.<sup>47</sup> The total manufacturing cost is calculated to be \$15 million to manufacture all 240 aircraft which comes out to \$62,500 each. This accounts for over two-thirds of the cost of building each aircraft.

The materials cost is simply the price of the raw materials that will make up the aircraft. Note that this model assumes that the airframe is made from aluminum, composites, or a combination of both. For the case of Tempo and Encore, only aluminum is used so this and other previously mentioned inputs are used. The total materials cost for each aircraft is \$6,200.

Quality control cost is the cost of the technicians and equipment necessary to demonstrate that the product is made to the proper standards and is based on the amount of composites in the airframe and the cost of manufacturing. The quality control cost is \$4,000 per aircraft.

The other major costs of building the aircraft are the cost of the engine and propeller. The Lycoming AEIO-233 costs<sup>49</sup> approximately \$23,000 while a cost model determined the propeller to be \$3,145. The engine and propeller costs are then reduced based on a quantity discount factor for purchasing a large number of engines and propellers at once. The exponential function takes into account how many engines are purchased and the speed at which personnel can learn based on a learning curve. For Tempo and Encore, a learning speed of 0.95 is used because it is the most conservative estimate.

## 12.3 SELLING PRICE

The total cost of doing business is the sum of the total development cost and the cost of making the product. Over time, the product gets less expensive to produce, which means that the cost is the highest in the beginning and will drop a significant amount over a very short time to a certain point, where it will remain fairly constant for the rest of production. The cost analysis is performed for one, three, five, and ten years of selling Tempo and Encore. Five years was chosen as the time for Avem Dynamics to make a 10% profit (from the RFP), which is where the cost breaks even.

It is assumed that four aircraft will be sold every month which is a total of 240 aircraft over five years. The total cost of doing business is calculated to be \$26.3 million plus \$6.5 million development cost. In order to make a 10% profit in 5 years Avem Dynamics must sell each aircraft for \$120,500. This number is calculated by multiplying total cost of doing business by 1.1 and determining the necessary selling price in order to meet the 10% profit at five years. Because of the high degree of commonality, this analysis was done for the heavier airplane and the cost of doing business will be nearly the same. The selling price of Tempo will remain the same as Encore. Because Tempo is a high performing aerobatic aircraft it will undercut the competition when it is sold for a lower

price compared to existing aerobatic aircraft. This reduced price in conjunction with the fact that Tempo is part of an aerobatic family, will create a market niche where Avem Dynamics hopes to live.

## 12.4 OPERATING COST

The cost of owning and operating an airplane is rather expensive and include insurance, registration, storage, fuel, tires, maintenance, and engine overhaul. These costs are based on Gudmundsson's<sup>44</sup> approximation and then compared through an interview<sup>49</sup> with Arthur Koral who is an aerobatic flight instructor for the Sunrise Aviation aerobatic flight school. Tempo is recommended to assume 200 flight hours while Encore is assumed to have 500 flight hours. Regardless of how much the aircraft is used, it must be registered, insured, and kept in storage. Registration is 1% of the cost of the aircraft at \$1,205 for each aircraft. An additional \$450/month is used for the insurance cost and storage costs is approximately \$100/month. Fuel for Tempo and Encore costs \$4.75/gallon.<sup>50</sup> The tires of the airplanes must be replaced approximately every 200 flight hours and cost \$166/tire. The tubes are \$60/tube and are replaced every 400 flight hours. Every 130 flight hours, the aircraft must be professionally inspected which costs \$1000 and includes maintenance to the brakes and refilling of fluids. \$10/ flight hour is set aside for an engine overhaul and another \$7/flight hour is set aside for miscellaneous maintenance. The total yearly operating cost of Tempo and Encore is \$16,800 and \$30,000 or \$84/flight hour and \$60/flight hour, respectively.

## 13 Conclusion

Entering the market in 2020, Tempo will set the rhythm of aerobatic light sport aircraft to come. With a gross takeoff weight of 1087lbs, this lightweight aircraft has some impressive performance statistics. Tempo has a roll rate of 360°/sec, which doubles the roll rate required by the RFP in order to allow Tempo to maneuver with the best of the intermediate category of aerobatics. Tempo is also capable of +6/-5g maneuvers and has a climb rate of nearly 2000fpm. Being a light sport aircraft, Tempo has a maximum speed of 120 KCAS achieved by matching engine and propeller performance to limit its speed capabilities to the required 120 KCAS. This low speed in combination with its 39 KCAS stall speed makes Tempo a safe and enjoyable aircraft to fly.

Encore will follow Tempo in 2021. With 92% commonality, this two seat variant makes for the perfect trainer. Due to their nearly identical design, the pilots will experience the same handling qualities as they transition from student to intermediate aerobatic competitor. Encore has a stall speed of 43 KCAS and a climb rate of nearly 1600fpm. Both the Tempo and Encore will be sold for the very affordable price of \$120,500.



Avem Dynamics is proud to present Tempo and Encore, a fully designed family of aerobatic aircraft that will fill a new niche in the LSA market. Through superior engineering and innovation Avem Dynamics ensures that this family of aerobatic LSA will be profitable, marketable, and appealing to pilots of any kind.

## 14 References

1. AIAA. *Aerobatic Light Sport Aircraft Family (LSA) – Request for Proposal*. N.p.: AIAA, n.d. PDF.
2. ASTM International. Standard F2245-14. *Standard Specification for Design and Performance of a Light Sport Airplane*. 21 Sep. 2015.
3. "2014 General Aviation Statistical Databook & 2015 Industry Outlook." *General Aviation Manufacturers Association* (n.d.): n. pag. Web.
4. Johnson, Dan. "LSA Market Shares — Fleet and Calendar 2014." *ByDanJohnson*. N.p., 22 Mar. 2015. Web.
5. Rihn, Dan. "Avem Dynamics Design Review." Personal Interview. 4 Mar. 2016.
6. "IAC Known Compulsory Sequences 2016." *International Aerobatic Club*. Experimental Aircraft Association, INC., n.d. Web Nov. 2015
7. "The Aerobatic Box." *International Aerobatic Club*. Experimental Aircraft Association, INC., n.d. Web Nov. 2015
8. Lan, C. Edward, and Jan Roskam. *Airplane Aerodynamics and Performance*. Ottawa, Kan.: Roskam Aviation and Engineering, 1981. Print.
9. Lawrence, James. "Renegade Falcon LS 2 Light Sport Aircraft Taildragger." *Renegade Light Sport Aircraft*. N.p., n.d. Web.
10. Cook, LeRoy. "Onex: 85% Scale Equals 100% Fun." *KITPLANES Magazine* June 2013: n. pag. *KITPLANES*. Kitplanes.com. Web. 11 Feb. 2016.
11. Raymer, Daniel P. *Aircraft Design: A Conceptual Approach*. 5th ed. Reston, VA: American Institute of Aeronautics and Astronautics, 2012. Print.
12. "Seatpack Softie Parachute." *Softie Parachute*. Para-Phernalia Inc., n.d. Web. 20 Apr. 2016.
13. "The RG-12LSA Aircraft Battery." *Concorde Aircraft Battery*. N.p., n.d. Web. 08 May 2016.
14. *Acceleration in Aviation*. Federal Aviation Administration. FAA TV, 5 Apr. 2012. Web. 11 May 2016.
15. Abbott, Ira H. A., and Albert Edward Von Doenhoff. *Theory of Wing Sections; including a Summary of Airfoil Data*. New York: McGraw-Hill, 1949. Print.
16. Sheldahl, R. E., and P. C. Klimas. "Aerodynamic Characteristics of Seven Symmetrical Airfoil Sections through 180-degree Angle of Attack for Use in Aerodynamic Analysis of Vertical Axis Wind Turbines." (1981). Web.
17. "Welcome To Erect-A-Tube/Tee Hanagers." *Welcome To Erect-A-Tube/Tee Hanagers*. N.p., n.d. Web. 09 May 2016.
18. Neihouse, Ansha I., Jacob H. Lichtenstein, and Philip W. Pepoon. "NACA Technical Report 1045: Tail Design Requirements For Satisfactory Spin Recovery." *NASA Technical Reports Server*. NASA, n.d. Web.
19. Finck, R. D., and D. E. Hoak. *USAF Stability and Control Datcom*. Irvine, CA: Global Engineering Documents, 1978. Print.
20. *OpenVSP*. Computer software. Vers. 3.5.2. N.p., 14 Feb. 2016. Web.
21. Roskam, Jan. *Airplane Design*. 2nd ed. Vol. 6. Ottawa, Kan.: Roskam Aviation and Engineering, 1985. Print.
22. Hoerner, Sighard F. *Fluid-dynamic Drag: Practical Information on Aerodynamic Drag and Hydrodynamic Resistance*. Albuquerque, NM: Db Hoerner Fluid Dynamics, 1965. Print.
23. Grove Aircraft Landing Gear Systems Inc. Web. 11 Feb. 2016.
24. Pfeiffer, Neal J., and David Lednicer. "A Study of Excrescence Drag." *AIAA.com*. AIAA, n.d. Web.
25. Harloff, Gary. "Light Sport and General Aviation Airplane Comparison and Harloff Performance Factor." *ResearchGate*. Harloff Inc, n.d. Web. 12 Feb. 2016.
26. Airworthiness Standards: Aircraft Engines. 14 C.F.R. § 33.
27. *Advanced General Aviation Propeller Study*. Rep. no. CR-114289. Windsor Locks, CN: Hamilton Standard, 1971. Print.

28. Wood, K. D. "Weight Data." *Aerospace Vehicle Design: Aircraft Design*. 3rd ed. Vol. I. Boulder: Johnson, 1968. A159-180. Print.
29. *Aerocrafter: The Complete Guide to Building and Flying Your Own Aircraft*. Oshkosh, WI: AeroCrafter, 2001. Print.
30. "Garmin G300 for Cessna Skycatcher." *Garmin.com*. N.p., n.d. Web.
31. "FAA Regulations." *FAA Regulations*. Web. 16 May 2016.
32. Roskam, Jan. "Method for Estimating Stability and Control Derivatives of Conventional Subsonic Airplanes." Lawrence, Dr. Jan Roskam 1971.
33. *Athena Vortex Lattice*. Computer software. Vers. 3.35. N.p., 20 March. 2016. Web.
34. Roskam, J. *Airplane Flight Dynamics and Automatic Flight Controls Part I*. Design Analysis & Research. N.p., 1982. Print.
35. Stough, H. P., D. J. Dicarolo, and J. M. Patton "Flight Investigation of Stall, Spin and Recovery Characteristics of a Low-Wing, Single-Engine, T-Tail Light Airplane." (1985). NASA. Web.
36. "RGL Home." *RGL Home*. Web. 09 May 2016. <<http://www.airweb.faa.gov/>>.
37. Neihouse, A. I. "NACA Technical Report 1045: Tail Design Requirements For Satisfactory Spin Recovery." *NASA Technical Reports Server*. NASA, n.d. Web.
38. Seidman, Oscar, and Charles Donlan. "NACA Technical Note 711: An Approximate Spin Design Criterion for Monoplanes." *NASA Technical Reports Server*. NASA, n.d. Web.
39. Neihouse, A. I. "NACA Technical Report 1329: Tail Design For Satisfactory Spin Recovery for Personal Owner Type Light Aircraft." *NASA Technical Reports Server*. NASA, n.d. Web Stinton, Darrol. *The Design of the Aeroplane*. Malden, MA: Blackwell Science, 2001. Print.
40. Garcia, D. *Empirical Formulae for Radii of Gyration of Aircraft: Revision "A."* Los Angeles, CA: SAWE, 1962. Print.
41. McAvoy, W. H. "NACA Technical Report 555: Piloting Technique for Recovery from Spins." *NASA Technical Reports Server*. NASA, n.d. Web.
42. Cassidy, Alan. *Better Aerobatics*. Maidenhead: Freestyle Aviation, 2003. Print.
43. Roskam, J. *Airplane Flight Dynamics and Automatic Flight Controls Part II*. Design Analysis & Research. N.p., 1982. Print.
44. Gudmundsson, Snorri. *General Aviation Aircraft Design: Applied Methods and Procedures*. 1st ed. Oxford: Butterworth-Heinemann, 2014. Print.
45. Airworthiness Standards: Normal, Utility, Acrobatic, and Commuter Category Airplanes. 14 C.F.R. § 23.
46. "Aerospace Engineers." *Bureau of Labor Statistics*. United States Department of Labor, 17 Dec. 2015. Web. 21 Apr. 2016.
47. "Aircraft Structure, Surfaces, Rigging, and Systems Assemblers." *Bureau of Labor Statistics*. United States Department of Labor, 30 Mar. 2016. Web. 21 Apr. 2016.
48. "233 Series LSA Engines." *Lycoming*. Avco Corporation. N.d. Web. 21 Apr. 2016.
49. Koral, Arthur. "Aerobatic Operating Costs." Personal Interview. 4 Apr. 2016.
50. "100LL - Aviation Fuel Prices." *100LL.com*. Aviation Fuel Data LLC, 21 Apr. 2016. Web. 21 Apr. 2016